Epithermal deposits in New Mexico

Compiled by Ted L. Eggleston

CIRCULAR 199 New Mexico Bureau of Mines & Mineral Resources 1985

A DIVISION OF
NEW MEXICO INSTITUTE OF MINING & TECHNOLOGY

COVER—Miners at work in the silver mines. Much of New Mexico's early-day precious-metal production was won from the ground the hard way: double-jacking with hand-held steel by candlelight, shot with black powder, and the day's production packed out on the miners' backs. The more fortunate could hand-tram the ore out in one-ton wooden ore cars or hoist it to surface with the bucket and hand windlass. Machinery was a luxury beyond the reach of most early miners.
Woodcut, courtesy of Engineering and Mining Journal, vol. 27, Feb. 1, 1879, p. 75.

Circular 199

New Mexico Bureau of Mines & Mineral Resources

A DIVISION OF
NEW MEXICO INSTITUTE OF MINING & TECHNOLOGY

Epithermal deposits in New Mexico

Compiled by Ted L. Eggleston

Geoscience Department, New Mexico Institute of Mining and Technology, Socorro, New Mexico 87801

Socorro 1985

NEW MEXICO INSTITUTE OF MINING & TECHNOLOGY
Laurence H. Lattman, *President*

NEW MEXICO BUREAU OF MINES & MINERAL RESOURCES
Frank E. Kottlowski, *Director*
George S. Austin, *Deputy Director*

BOARD OF REGENTS

Ex Officio
Toney Anaya, *Governor of New Mexico*
Alan Morgan, *Superintendent of Public Instruction*

Appointed
Steve Torres, President, 1967–1991, *Albuquerque*
Judy Floyd, Sec./Treas., 1977–1987, *Las Cruces*
Gilbert L. Cano, 1985–1991, *Albuquerque*
Lenton Malry, 1985–1989, *Albuquerque*
Donald W. Morris, 1983–1989, *Los Alamos*

BUREAU STAFF

Full Time

ORIN J. ANDERSON, *Geologist*
RUBEN ARCHULETA, *Technician I*
BRIAN W. ARKELL, *Coal Geologist*
AL BACA, *Crafts Technician*
JAMES M. BARKER, *Industrial Minerals Geologist*
ROBERT A. BIEBERMAN, *Senior Petrol. Geologist*
DANNY BOBROW, *Geologist*
MARK R. BOWIE, *Research Associate*
LYNN A. BRANDVOLD, *Senior Chemist*
RON BROADHEAD, *Petroleum Geologist*
BRENDA R. BROADWELL, *Assoc. Lab Geoscientist*
FRANK CAMPBELL, *Coal Geologist*
KATHRYN G. CAMPBELL, *Drafter*
RICHARD CHAMBERLIN, *Economic Geologist*
CHARLES E. CHAPIN, *Senior Geologist*
MARIE G. CHAVEZ, *Secretary/Receptionist*
RICHARD R. CHAVEZ, *Assistant Head, Petroleum*
KEVIN H. COOK, *Research Associate*
RUBEN A. CRESPIN, *Laboratory Technician II*
LOIS M. DEVLIN, *Director, Bus./Pub. Office*
ROBERT W. EVELETH, *Mining Engineer*
ROUSSEAU H. FLOWER, *Sr. Emeritus Paleontologist*
MICHAEL J. GOBLA, *Manager, Inf. Ctr.*
ANNETTE GONZALES, *Admin. Secretary I*
MICHAEL J. HARRIS, *Metallurgist*
JOHN W. HAWLEY, *Senior Env. Geologist*
CAROL A. HJELLMING, *Editorial Secretary*
GARY D. JOHNPETER, *Engineering Geologist*
ANNABELLE LOPEZ, *Staff Secretary*
DAVID W. LOVE, *Environmental Geologist*
JANE A. CALVERT LOVE, *Assistant Editor*
VIRGINIA MCLEMORE, *Geologist*
LYNNE MCNEIL, *Technical Secretary*
NORMA J. MEEKS, *Accounting Clerk–Bureau*
DIANE MURRAY, *Geologist*
ROBERT M. NORTH, *Mineralogist*
GLENN R. OSBURN, *Economic Geologist*
JOANNE CIMA OSBURN, *Geologist*
BONNIE PELLETIER, *Technician I*
CHERIE PELLETIER, *Drafter*
BARBARA R. POPP, *Biotechnologist*
IREAN L. RAE, *Drafter*
MARSHALL A. REITER, *Senior Geophysicist*
JACQUES R. RENAULT, *Senior Geologist*
JAMES M. ROBERTSON, *Senior Mining Geologist*
CECILIA ROSACKER, *Technician I*
GRETCHEN H. ROYBAL, *Coal Geologist*
DEBORAH A. SHAW, *Assistant Editor*
STELLA L. SMITH, *Drafter*
WILLIAM J. STONE, *Senior Hydrogeologist*
SAMUEL THOMPSON III, *Senior Petrol. Geologist*
MARK A. TUFF, *X-ray Technician*
JUDY M. VAIZA, *Executive Secretary*
MANUEL J. VASQUEZ, *Mechanic*
ROBERT H. WEBER, *Senior Geologist*
DONALD WOLBERG, *Vertebrate Paleontologist*
ZANA G. WOLF, *Staff Secretary*
MICHAEL W. WOOLDRIDGE, *Chief Sci. Illustrator*
JIRI ZIDEK, *Chief Editor–Geologist*

Research Associates

CHRISTINA L. BALK, *NMT*
WILLIAM L. CHENOWETH, *Grand Junction, CO*
PAIGE W. CHRISTIANSEN, *NMT*
RUSSELL E. CLEMONS, *NMSU*
WILLIAM A. COBBAN, *USGS*
AUREAL T. CROSS, *Mich. St. Univ.*
JOHN E. CUNNINGHAM, *WNMU*
MARIAN GALUSHA, *Amer. Mus. Nat. Hist.*
LELAND H. GILE, *Las Cruces*
JEFFREY A. GRAMBLING, *UNM*
JOSEPH HARTMAN, *Univ. Minn.*
DONALD E. HATTIN, *Ind. Univ.*
ALONZO D. JACKA, *Texas Tech. Univ.*
DAVID B. JOHNSON, *NMT*
WILLIAM E. KING, *NMSU*
EDWIN R. LANDIS, *USGS*
DAVID V. LEMONE, *UTEP*
A. BYRON LEONARD, *Kansas Univ.*
JOHN R. MACMILLAN, *NMT*
HOWARD B. NICKELSON, *Carlsbad*
LLOYD C. PRAY, *Univ. Wisc.*
ALLAN R. SANFORD, *NMT*
JOHN H. SCHILLING, *Nev. Bur. Mines & Geology*
WILLIAM R. SEAGER, *NMSU*
RICHARD H. TEDFORD, *Amer. Mus. Nat. Hist.*
JORGE C. TOVAR R., *Petroleos Mexicanos*

Graduate Students

MARGARET BARROLL
STEVEN M. CATHER
TED EGGLESTON
RICHARD HARRISON
RICHARD P. LOZINSKY
DANIEL MCGRATH
BRIAN E. MCGURK
WILLIAM MCINTOSH
JEFFREY MINIER
RICHARD REIMERS
STEWART SMITH

Plus about 50 undergraduate assistants

Original Printing 1985

Published by Authority of State of New Mexico, NMSA 1953 Sec. 63–1–4
Printed by University of New Mexico Printing Plant, September 1985

Available from New Mexico Bureau of Mines & Mineral Resources, Socorro, NM 87801

Contents

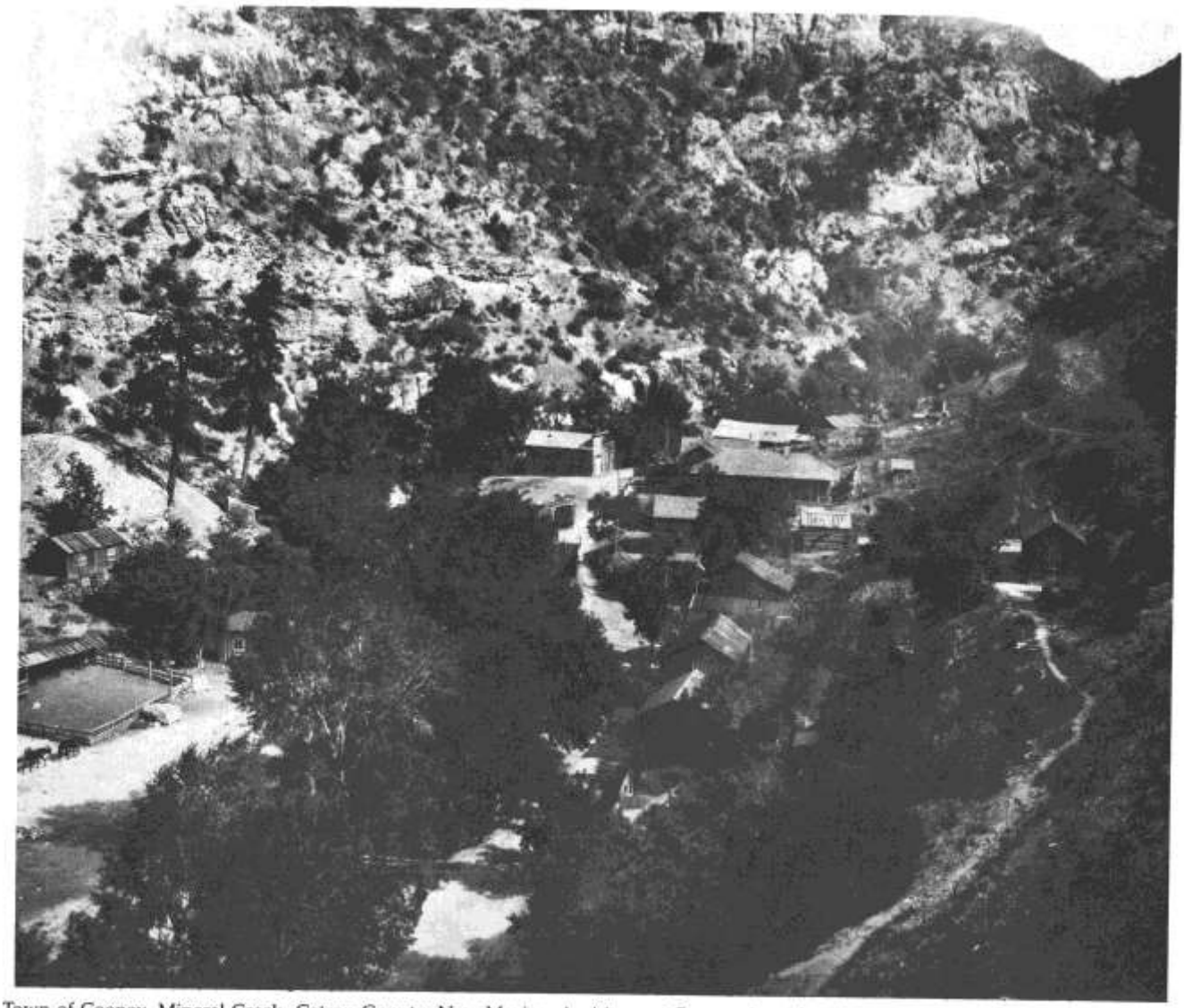

Town of Cooney, Mineral Creek, Catron County, New Mexico. An itinerant German is said to have discovered this district, but credit goes to James C. Cooney, a sergeant in the 8th cavalry at Fort Bayard in 1870, who took careful note of the prominent veins along Mineral Creek while in pursuit of Indians. The town which grew up about ½ mile west of the Cooney mine on the only nearby wide spot in the canyon was named in his honor. Cooney was a bustling little community in the early days, boasting a post office for 31 years, beginning 1884, and a population of nearly 400 in the 1890's. But it was soon eclipsed by its neighbor to the south, Mogollon; Cooney's population dropped below 200 in 1910 and the town was abandoned in the mid 1920's.
U.S. Geological Survey photo by L. C. Graton, ca 1905.

Preface

Mogollon, Kingston, White Oaks, Chloride, Pinos Altos, Hermosa—to the explorationist and student of New Mexico's mineral deposits these districts are but a few of the epithermal-vein systems found within the boundaries of the state. Since the first visit by Europeans, these high-grade, generally shallow deposits have been the focus of much attention; in recent years, both academicians and explorationists have been studying these deposits. This volume contains a number of papers and abstracts generated as a result of a symposium on epithermal-ore deposits in New Mexico held at the 1984 spring meeting of the New Mexico Geological Society. The symposium brought academicians and explorationists together for an exchange of data and ideas in hope that the exchange might stimulate the study and further discoveries of these important deposits. Abstracts of all the papers that were presented are published in this volume. Of the six papers presented here, two were not read at the symposium; they are included because they directly relate to the topic.

The response to the call for papers for this volume was less than expected, but the papers presented and the abstracts contain much information from company files that would otherwise remain unpublished. I would like to thank all the participants, the session chairmen, the speakers, and the New Mexico Geological Society for making the symposium a success; the authors for their patience during production of this volume; and Bob Eveleth, New Mexico Bureau of Mines and Mineral Resources, for captions to the historical photographs.

Ted Eggleston

Cooney mine and mill, Mineral Creek, Catron County, New Mexico. James C. Cooney located the Silver Bar lode soon after his discharge from the cavalry and began to develop the "Cooney" mine, by which name it is traditionally known, about ½ mile east of Cooney townsite (now abandoned). Indians (who killed Cooney just one year later) prevented any serious development work until 1879 when the first ore shipment was made. The first mill appears to have been one of five stamps and was gradually increased in capacity until 1905, when the Mogollon Gold and Copper Company was treating 100 tons per day. The mill burned shortly thereafter and little other than the dump now marks the spot. The Cooney was certainly one of the great early mines in New Mexico, producing a beautiful high-grade bornite-native silver (peacock) ore (only silver and gold were recovered initially; copper was lost) valued at over $1 million to 1904.

U.S. Geological Survey photo by L. C. Graton, ca 1905.

Geochemistry of host-rock alteration at the Eberle mine, Mogollon mining district, southwestern New Mexico

by Theodore **J.** Bornhorst and Gretchen R. Kent

Department of Geology and Geological Engineering, Michigan Technological University, Houghton, Michigan 49931

Abstract

The Eberle mine is located in the Mogollon mining district of southwestern New Mexico. Epithermal mineralization consists of a silver—gold—copper-bearing quartz—calcite—fluorite vein which is an open-space filling along a normal fault. At the 100-ft level of the Eberle mine the footwall is rhyolite and the hanging wall is andesite. The host rocks were hydrothermally altered during the process of vein emplacement. Both the rhyolite and the andesite were silicified and sericitized, and only the andesite was chloritized. Geochemical data and quantitative element-mobility calculations suggest that the rhyolite and andesite in close proximity to the Eberle vein had massive addition of Ag, Au, Rb, and K from the hydrothermal fluid, whereas Ca and Sr were largely removed. Na was depleted from both rhyolite and andesite. Si and Mn were added to rhyolite and andesite closest to the vein, but in less altered samples fall to background values or less. Zr, Y, Ti, and Sc were practically immobile during hydrothermal alteration. Fe, Mg, Al, Zn, and Ba exhibit different mobility within the rhyolite as compared to the andesite. The host rock alteration at the Eberle mine is an example of K-metasomatism.

Introduction

Throughout the western United States, Mexico, and Central America there are many moderate- to high-grade, low-tonnage Cenozoic deposits of precious metals in quartz—calcite veins associated with a volcanic environment (Buchanan, 1981). Pervasive propylitization is characteristic of Tertiary volcanic-hosted precious-metal districts (Buchanan, 1981; Boyle, 1979). Depending upon the depth of erosion and proximity to the veins, alunitization, silicification, and adularization may also be common (Buchanan, 1981). Most studies of these Tertiary deposits have concentrated on topics related to the veins themselves or to the mineralogy of the altered host rocks. Few, if any, have attempted to quantitatively evaluate element mobility resulting from hydrothermal processes. The purpose of this paper is to provide a quantitative analysis of element mobility during host-rock alteration associated with emplacement of an epithermal, preciousmetal-bearing vein in the Mogollon mining district of southwestern New Mexico.

The Mogollon mining district is located in the Mogollon—Datil volcanic field of southwestern New Mexico (Fig. 1). The district is situated on the ring-fracture zone of the Bursum caldera which was active 25-28 m.y. ago (Ratte, 1981). The structure of the area is complicated by the adjacent Glenwood graben and Mangas trench (Basin and Range grabens). Mineralization consists of silver—gold—copper-bearing quartz-calcite—fluorite veins which were open-space fillings along high-angle normal faults. The age of mineralization is believed to be 15-18 m.y. (Kent, 1983; Ratte et al., 1983; Ratte, 1981). The district was described by Lindgren, Graton, and Gordon (1910), and later Ferguson (1927) mapped the geology of the Mogollon quadrangle and provided a fairly detailed description of the mineralization. The Mogollon quadrangle was remapped by Ratte (1981). This study deals with one of the smaller mines within the district, the Eberle.

Although mining in the district is dormant, the Challenge Mining Company is attempting to reactivate the Eberle mine (Eveleth, 1979).

Acknowledgments

We thank the New Mexico Bureau of Mines and Mineral Resources for partial support of the field work involved in this project. The Center for Mining and Mineral Resources at Michigan Technological University also provided funds for this project. The Challenge Mining Company kindly gave us access to the Eberle mine and their other holdings. Doug McDowell, Michigan Technological University, provided helpful comments on this study and reviewed the manuscript. Ted Eggleston, New Mexico Institute of Mining and Technology, also reviewed the manuscript.

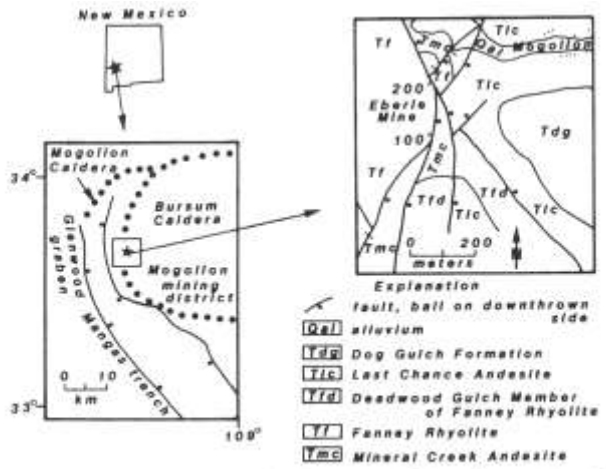

FIGURE 1—Location of the Eberle mine and Mogollon mining district, southwestern New Mexico. Detailed geology from Ratte (1981).

Geology at the Eberle mine

The vein at the Eberle mine is dominantly quartz and calcite. It dips steeply to the east and follows a north—south-trending normal fault (Fig. 1). Along most of the vein the footwall is Fanney Rhyolite and the hanging wall is Mineral Creek Andesite. There are minor branches of the vein which are bounded by only rhyolite or only andesite.

Vein mineralization

Vein mineralization at the Eberle mine consists of hypogene early quartz followed by calcite and then fluorite (Fig. 2). Hypogene mineralization was followed, after a distinct time break, by supergene enrichment. Early hypogene quartz is usually microcrystalline and is commonly banded or porcelaneous. It carries finely disseminated sulfide minerals (rarely more than 5 wt. %), which are often concentrated within chalcedonic bands. The sulfides are dominantly pyrite with lesser amounts of chalcopyrite, sphalerite, galena, argentite, stromeyerite, and chalcocite. Hypogene quartz and calcite are intergrown and the transition from Stage I to II is gradual. Banding is present in calcite due to changes in manganese content, relative crystallinity, and intergrowth with quartz or later fluorite (Ferguson, 1927; Scott, 1920). Hypogene sulfide minerals are larger and more coarsely crystalline in Stage II, but still form only a small percentage of the vein material. The final stage of hypogene mineralization is fluorite, which is usually barren with respect to precious metals. Fluorite occurs as thin crystalline veneers or banded with calcite.

After hypogene mineralization there was a period of supergene alteration. In the district the oxidized zones typically occur as small, irregular bodies composed of sulfides, iron, manganese and rare copper oxides, copper carbonates, silver halides, and occasional native gold and silver. At the Eberle mine, Ferguson (1927) reports cerargyrite and native silver in oxidized ore. At the Eberle 100-ft level, boxwork and iron-stained quartz are pseudomorphic after calcite or coating calcite. The iron-oxide coating on supergene quartz may be due to weathered sulfide minerals and contains 48 ppm Ag.

Study of fluid inclusions in hypogene gangue quartz, calcite, and fluorite suggests a drop in temperature during mineralization from 240 to 160°C (Bornhorst et al., 1984; Kent, 1983); fluids were not boiling. No fluid inclusions were found in the earliest variety of quartz at the Eberle mine. Quartz from the nearby Confidence mine was deposited at about 260°C (Bornhorst et al., 1984), but it is also not the earliest variety. The temperature for earliest quartz deposition probably exceeded 260°C. The salinity of mineralizing fluids apparently remained relatively constant at 3.2-3.5 wt. % equivalent NaCl. Bornhorst et al. (1984) suggest that if the Eberle vein was open to the surface, then during mineralization there was more than 500 m of cover over the Eberle 100-ft level.

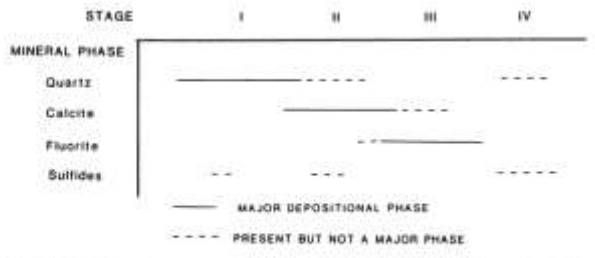

FIGURE 2—General paragenetic sequence at the Eberle mine. Stages I to III were hypogene deposition, Stage IV was supergene enrichment.

Host-rock alteration

There is a relatively sharp contact between the vein and host rocks at the Eberle mine. The mineralogy and geochemistry of altered host rocks were studied at the 100-ft level of the Eberle mine, where the footwall is rhyolite and the hanging wall is andesite. A suite of samples was collected at 10-ft intervals roughly perpendicular to the vein at the 100-ft level, to distances of 50 ft into the rhyolite and 100 ft into the andesite. Samples of rhyolite and andesite directly adjacent to the vein were also studied, but not from along the same profile.

Rhyolite alteration

The mineralogy of the rhyolite outside the district is characterized by approximately 5% phenocrysts of predominantly anhedral to subhedral sanidine, plagioclase (An20-25), quartz, and occasional biotite with minor opaques, apatite, zircon, and sphene (Bornhorst, 1980; Rhodes, 1976). The groundmass ranges from glassy to spherulitic containing microcrystalline intergrowths of quartz and feldspar with minor iron oxides, apatite, zircon, and sphene. Adjacent to the vein, the rhyolite contains only rare, skeletal feldspar altered to quartz and sericite. Iron oxides are the only evidence of ferromagnesian minerals. Identifiable quartz is anhedral to subhedral and appears to have formed in fractures, flow-laminations, and other voids during silicification. The groundmass consists of abundant, small, remnant spherulitic and axiolitic de-vitrification structures of quartz and sericite, and micro- to crypocrystalline quartz, sericite, and possible minor K-feldspar. Throughout the traverse, away from the vein, there is a gradual transition from cr yptocrystalline to more coarsely crystalline groundmass. Identifiable muscovite is present at 40 ft or more from the vein. All of the rhyolite samples have been silicified and sericitized to varying degrees. Sample TR-10, at 10 ft from the vein, contains minor secondary calcite.

Andesite alteration

Relatively unaltered Mineral Creek Andesite is difficult to find. The least altered samples within the area are composed of 5-7% ferromagnesian mineral phenocrysts, predominantly augite with some olivine altered to iddingsite, and 1-2% plagioclase phenocrysts. The groundmass consists of plagioclase laths with in-

terstitial magnetite and possible augite. Amygdule fillings are usually quartz and/or calcite. The mineralogy and degree of alteration of the Mineral Creek Andesite varies systematically in a 100-ft traverse taken perpendicular to the vein. Immediately adjacent to the vein and for approximately 14 ft the Mineral Creek Andesite is extremely brecciated. The pulverized breccia matrix consists of smectite clays and quartz. The only clearly identifiable clasts are angular quartz fragments. At distances greater than 14 ft from the vein, the andesite consists of an identifiable vesicular- to amygdaloidal-flow top and a dense-flow interior. The dip of the andesite-flow top is approximately 20°W. Fractures within the andesite are roughly parallel to the vein, which dips approximately 70°E. Phenocrysts of ferromagnesian minerals, probably augite and minor olivine, have been altered to chlorite with minor iron oxides and iddingsite. Some relict, altered ophitic phenocrysts are present. Skeletal-plagioclase phenocrysts are zoned, with anorthitic cores altered to sericite and with the more albitic rims relatively unaltered.

The predominant amygdule filling is a mixture of quartz and chlorite with possible epidote and albite. Calcite is also present and often displays crosscutting relationship with earlier amygdule-filling minerals (Fig. 3). Chloritization and sericitization are common throughout the 100 ft of andesite profile away from the vein. The abundance of calcite alteration tends to decrease away from the vein and no calcite was seen in thin section at 70 ft or more from the vein.

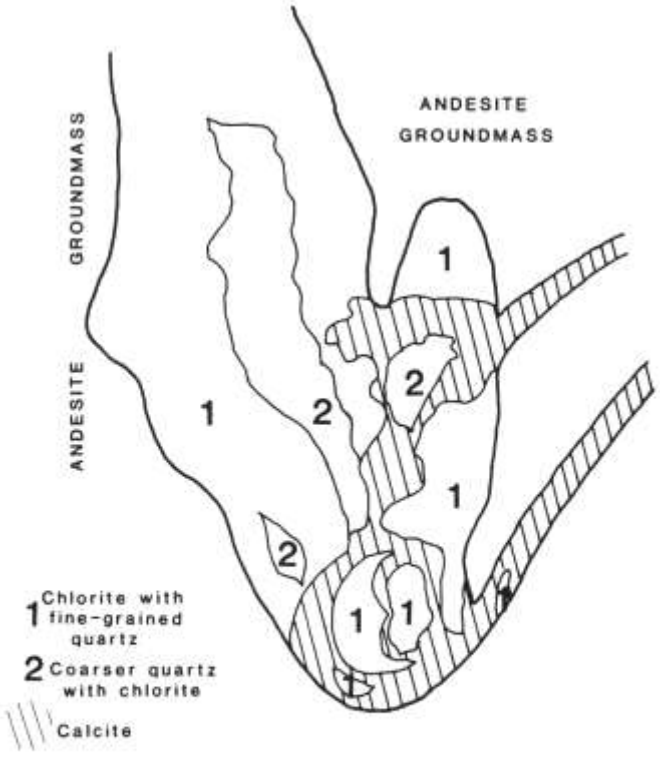

FIGURE 3—Relationship of amygdule-filling minerals in the andesite host rock adjacent to the vein (from sample TMA-30). The calcite crystallized later than the chlorite and quartz and displaced the previous filling. Calcite veinlets continue into a larger calcite vein.

Geochemistry of host-rock alteration

Analytical methods

Major- and trace-element compositions of eight samples of rhyolite and 11 samples of andesite from close proximity to the Eberle vein were determined for this study (Tables 1, 2). Most elements were analyzed using an automated Philips wavelength-dispersive x-ray fluorescence spectrometer at Michigan Technological University. The analytical technique used is a modification from that of Leake et al. (1969). Major and trace elements were determined on pressed powder pellets. The system was calibrated utilizing French and U.S. Geological Survey geochemical standards. The precision of the major elements is typically about 0.5% of the amount determined. The precision of the trace elements is better than 10% of the amount determined.

Analyses for Au, Ag, and Mo were done by Neutron Activation Services, Ltd. of Hamilton, Ontario, Canada. Au was determined by neutron-activation analysis using fire assay for separation of Au prior to irradiation (described by Hoffman et al., 1982; detection limit 1 ppb). Values for Ag and Mo were determined by D.C. Plasma emission spectrometry.

Geochemical-mobility calculations

Evaluation of element gains or losses during alteration requires that the altered rocks and the unaltered parent initially belonged to a chemically uniform population. The composition of unaltered parent for Fanney Rhyolite and for Mineral Creek Andesite was estimated through inspection of chemical data that were believed to be the freshest samples from these units. Data from Bornhorst (1980) and Ratte and Grotho (1979) were used, but interlaboratory bias was checked (unpublished data of Bornhorst) and appropriate corrections were made. There is certainly some primary compositional variation within these units as a whole, and as such the unaltered parent (Tables 1, 2) is our best estimate. However, we believe that within the close proximity of the Eberle mine the various samples of rhyolite and andesite had chemically uniform parents and, therefore, that chemical-mobility calculations are at least relatively correct.

Sometimes dramatic chemical changes caused by alteration can be correctly deduced from simple inspection of raw chemical data. However, in most cases simple inspection is not satisfactory. Kerrich and Fyfe (1981) point out that since the major component oxides must sum to 100%, then no individual component is independent of the others and there is no limit to the number of solutions. The volume changes that accompany metasomatism must be known in order to quantitatively calculate compositional changes (Gresens, 1967). Volume changes during alteration of a volcanic rock might occur, for example, by filling of

TABLE 1—Geochemical analyses of Fanney Rhyolite adjacent to the 100-ft level of the Eberle mine. TR sample numbers indicate number of feet from the vein. E1001 is a sample surrounded by vein, and 81T19C and 82T15 are adjacent to the vein where it pinches out. The unaltered parent represents a best estimate based on literature data. IR is described in the text. ' = unweighted mean. * = total Fe.

	TR-10	TR-20	TR-30	TR-40	TR-50	E1001	82T19C	82T15	Unaltered parent
SiO_2	75.4	77.07	79.78	76.00	75.71	78.5	74.87	72.71	74.7
Al_2O_3	11.46	13.00	11.34	12.42	12.89	11.32	13.71	14.42	12.7
Fe_2O_3*	1.88	1.95	1.36	0.77	1.85	1.96	0.60	0.86	1.1
MgO	0.16	0.20	0.15	0.07	0.23	0.25	0.40	0.22	0.4
CaO	0.13	0.06	0.06	0.09	0.07	0.16	0.08	0.08	0.5
Na_2O	0.19	0.19	0.18	0.20	0.17	0.08	0.26	0.19	4.1
K_2O	7.89	8.61	6.90	8.41	7.90	7.65	7.89	8.74	4.6
TiO_2	0.12	0.15	0.13	0.15	0.15	0.14	0.15	0.16	0.15
TOTAL	97.23	101.23	99.90	98.21	98.97	100.06	97.96	97.38	98.15
Mn	366.	275.	243.	225.	232.	186.	134.	125.	250.
Cu	34.	32.	32.	22.	37.	37.	41.	41.	30.
Zn	14.	16.	<10.	14.	16.	12.	<10.	18.	20.
Rb	310.	333.	283.	357.	310.	296.	334.	334.	250.
Sr	59.	77.	61.	86.	58.	91.	102.	49.	130.
Y	31.	38.	31.	42.	35.	30.	30.	36.	37.
Zr	114.	145.	125.	150.	144.	125.	159.	177.	150.
Ba	78.	134.	65.	69.	206.	156.	73.	283.	75.
Mo	1.	NA	NA	0.5	NA	NA	NA	NA	
Au	0.010	0.012	0.007	0.012	NA	0.011	NA	NA	0.001
Ag	<0.5	2.	<0.5	0.5	NA	6.	NA	NA	0.070
IR(Al)	1.11	0.98	1.12	1.02	0.99	1.12	0.93	0.88	
IR(Ti)	1.25	1.00	1.15	1.00	1.00	1.07	1.00	0.94	
IR(Zr)	1.32	1.03	1.20	1.00	1.04	1.20	0.94	0.85	
IR'	1.23	1.00	1.16	1.01	1.01	1.13	0.96	0.89	

TABLE 2—Geochemical analyses of Mineral Creek Andesite adjacent to the 100-ft level of the Eberle mine. TMA sample numbers indicate number of feet from the vein. EU-1A is a sample of andesite from the 200-ft level. The unaltered parent represents a best estimate based on literature data. IR is described in the text. ' = unweighted mean. * = total Fe.

	TMA-10	TMA-20	TMA-30	TMA-40	TMA-50	TMA-60	TMA-70	TMA-80	TMA-90	TMA-100	EU-1A	Unaltered parent
SiO_2	74.13	69.73	51.94	72.03	70.01	61.87	65.35	59.23	52.10	50.02	81.11	53.2
Al_2O_3	11.63	9.34	14.06	8.72	12.22	12.80	11.79	14.16	13.43	14.24	9.31	16.5
Fe_2O_3*	1.60	6.88	7.73	7.42	7.50	8.45	8.11	10.03	10.63	10.95	0.69	10.0
MgO	1.68	1.73	5.90	2.20	3.26	3.60	3.52	4.60	6.89	6.02	0.95	4.6
CaO	5.18	0.86	5.00	0.71	0.69	1.11	1.04	1.43	1.78	1.32	0.14	6.6
Na_2O	0.30	1.19	1.01	0.66	1.17	1.46	1.67	2.29	1.92	1.42	0.09	3.5
K_2O	4.17	4.47	8.91	3.79	4.92	5.60	4.63	5.48	4.88	6.72	3.98	2.2
TiO_2	0.32	1.13	1.37	0.84	1.29	1.37	1.38	1.62	1.72	1.98	0.15	2.0
TOTAL	99.01	95.33	95.95	96.37	101.02	96.27	97.49	98.84	93.35	92.67	96.42	98.6
Sc	7.	9.	17.	7.	11.	11.	12.	16.	16.	18.	<5.	18.
V	<15.	95.	49.	79.	66.	97.	43.	28.	<15.	123.	<15.	130.
Cr	<15.	141.	111.	240.	122.	147.	140.	140.	187.	189.	36.	190.
Mn	2802.	688.	854.	955.	730.	866.	843.	1049.	1221.	802.	161.	900.
Ni	36.	108.	82.	91.	105.	93.	90.	136.	145.	148.	<15.	150.
Cu	56.	39.	12.	44.	21.	11.	33.	13.	11.	13.	71.	45.
Zn	120.	68.	75.	63.	72.	75.	65.	91.	105.	109.	116.	100.
Rb	228.	209.	400.	167.	195.	220.	203.	223.	195.	300.	213.	50.
Sr	125.	71.	253.	36.	68.	78.	161.	215.	198.	247.	18.	750.
Y	70.	43.	81.	40.	44.	47.	46.	58.	54.	70.	27.	70.
Zr	124.	186.	258.	111.	166.	187.	186.	225.	241.	263.	127.	290.
Ba	158.	537.	1048.	366.	575.	715.	826.	1088.	1259.	1059.	74.	1100.
Mo	4.	NA	NA	NA	<0.5	NA	NA	NA	NA	<0.5	NA	
Au	1.7	NA	0.002	NA	0.017	NA	0.001	NA	0.003	0.001	NA	0.001
Ag	54.	NA	1.	12.	4.	NA	1.5	NA	2.	1.	NA	0.070
IR(Sc)	2.51	2.00	1.06	2.57	1.64	1.64	1.50	1.12	1.12	1.00	—	
IR(Zr)	2.34	1.56	1.12	2.61	1.75	1.55	1.56	1.29	1.20	1.10	2.30	
IR'	2.46	1.78	1.09	2.59	1.70	1.60	1.53	1.21	1.16	1.05	2.30	

vesicles (volume increase). The concentration of an immobile element would vary with volume change and gains or losses could be incorrectly deduced without knowledge of volume relations. Gresens (1967) presented a method for deducing volume changes and for calculation of the mass changes necessary to produce an alteration product from an assumed parent rock. His method has been successfully applied to evaluation of alteration associated with Archean lode-gold deposits in Canada (Kerrich, 1983; Kerrich and Fyfe, 1981) and the Mattagami Lake Archean volcanogenic massive sulfide deposit in Canada (Costa, Barnett, and Kerrich, 1983).

Gresens' (1967) method of element-mobility calculation requires that either the volume change is known or that at least one element can be assumed to be immobile. The method incorporates specific gravity, but manipulation of his formulae shows that knowledge of specific gravity is not necessary unless actual volume changes need to be calculated. The basic equation used in the method by Gresens (1967) is

$$X_N = [f_v(g_B/g_A)C_{NB} - C_{NA}]a \quad (1)$$

where X_N is the amount of material lost or gained from the parent rock; f_v is the volume factor; g_A and g_B are the specific gravities of the parent rock (A) and altered product (B), respectively; C_{NA} and C_{NB} are the concentrations of some element N in the parent rock (A) and altered product (B), respectively; and **a** is arbitrarily set to equal some specific amount. Since major-element chemical analyses sum to 100% by weight, **a** is set to 1 which results in calculated changes in grams per 100 g. When $f_v = 1$, metasomatism is constant volume and, for example, $f_v = 0.5$ and 1.5 represent a 50% volume reduction and 50% volume increase, respectively. For each element in a sample, f_v can be calculated by assuming the element is immobile, $X_N = 0$ (a = 1):

$$f_v = C_{NA}/C_{NB}(g_A/g_B) \quad (2)$$

A clustering of f_v's of several components empirically believed to be immobile (e.g., Zr, Sc, Al) provides a rational estimate of the volume change. Since the volume factor is calculated by a ratio of an immobile element in the parent rock (C_{IMMA}) to the same immobile element in the altered product(C_{IMMB}), then

$$f_v = (C_{IMMA}/C_{IMMB})\ (g_A/g_B) \quad (3)$$

Substitution of equation (3) into equation (1) with **a** = 1 gives

$$X_N = [(C_{IMMA}/C_{IMMB})C_{NB} - C_{NA}] \quad (4)$$

Thus, gains and losses can be quantitatively calculated without the need for specific-gravity data. A clustering of C_{NA}/C_{NB} ratios in an individual sample provides a means to estimate the "immobile element ratio":

$$IR = C_{IMMA}/C_{IMMB}$$

The percentage loss or gain of a component relative to the original amount in the parent can be calculated by

$$EF = (X_N/C_{NA}) * 100.0 \quad (5)$$

Substitution of equation (4) into equation (5) gives

$$EF = [IR(C_{NB}/C_{NA}) - 1] * 100.0$$

or

$$EF = [((C_{NB}/C_{IMMB})/(C_{NA}/C_{IMMA})) - 1] * 100.0$$

The latter ratio of ratios is often referred to as an enrichment factor.

Deduction of volume changes relies on the assumption of immobile elements (Kerrich, 1983). Immobile elements should maintain constant ratios relative to one another during alteration regardless of volume changes. Kerrich (1983) points out that if elements such as Ti, Al, Zr, and Sc, which do not covary in magmatic processes, maintain approximately constant ratios during variable degrees of alteration, then these elements can be presumed to be immobile. Otherwise, they would all have to be added or subtracted in the same proportion. Kerrich (1983), Costa, Barnett, and Kerrich (1983), and Kerrich and Fyfe (1981) have shown that Zr, Sr, Al, Ti, Y, and V are immobile to varying degrees during intense hydrothermal alteration. There is no element or a group of elements that can be considered to be always immobile because mobility depends on so many different factors, for example rock type and alteration conditions.

The chemical data listed in Tables 1 and 2 have been used to identify probable immobile elements and to evaluate IR for each sample . C_{NA}/C_{NB} was calculated for every element. Zr, Al, and Ti behaved coherently and were apparently immobile in the rhyolite. Zr and Sc were apparently immobile in the andesite. IR was calculated from the unweighted mean ratios (Tables 1, 2).

Rhyolite alteration

The rhyolite in close proximity to the Eberle vein underwent significant chemical changes during alteration (Fig. 4). There was massive addition of Ag, Au, Rb, and K in all analyzed samples. Na, Ca, Sr, and Mg were largely removed. Varying amounts of Fe, Ba, and Cu were added from the hydrothermal solutions, whereas Zn was removed. Si and Mn were added to the most intensely altered samples, which are generally close to the vein, and removed from the less altered samples. Y shows small and variable changes, and was nearly immobile during alteration. Zr, Al, and Ti were assumed to had been immobile during alteration of the rhyolite. Selected examples of the actual mass changes for the major elements are given in Table 3.

Andesite alteration

The chemical changes during alteration were more pronounced in the andesite than in the rhyolite (Fig. 5). On the basis of the IR's, probable volume changes within the andesite were also larger. Filling of vesicles and brecciation of the andesite support these observations. In the andesite there was pervasive and massive addition of Ag, Au, Rb, and K, and generally substantial removal of Sr and Ca. Na was depleted

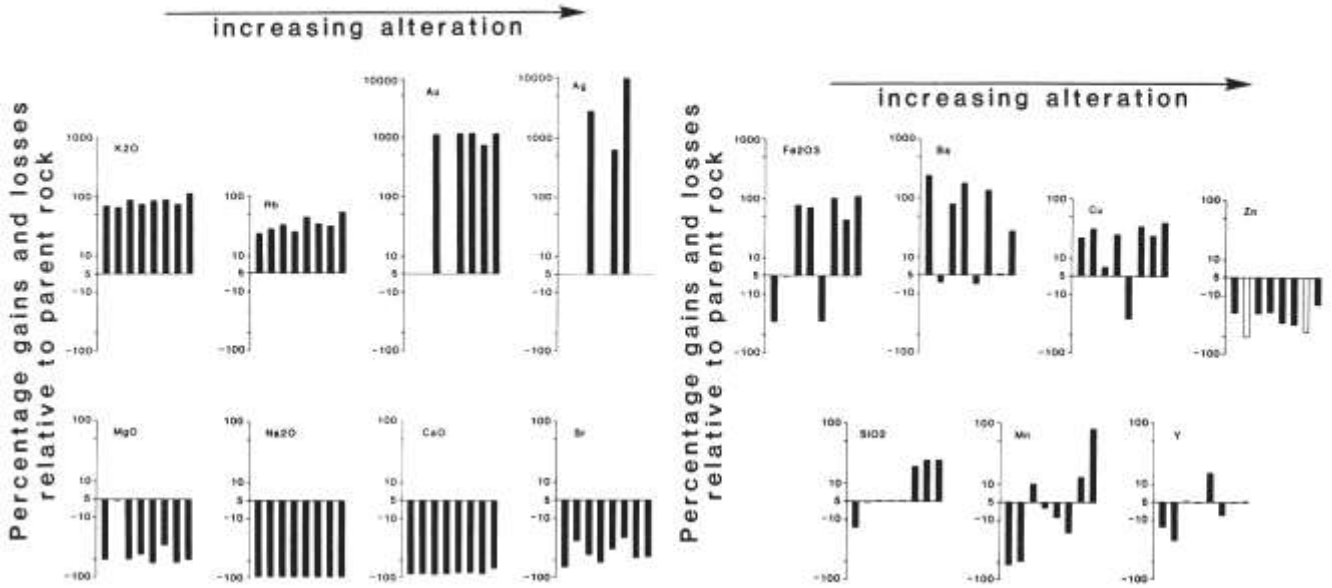

FIGURE 4—Gains or losses of major and trace elements from hydrothermally altered Fanney Rhyolite in proximity of the 100-ft level of the Eberle mine. Gains and losses expressed as percentage change relative to abundance in the best estimate of an unaltered parent. Samples ordered with increasing alteration on the basis of IR.

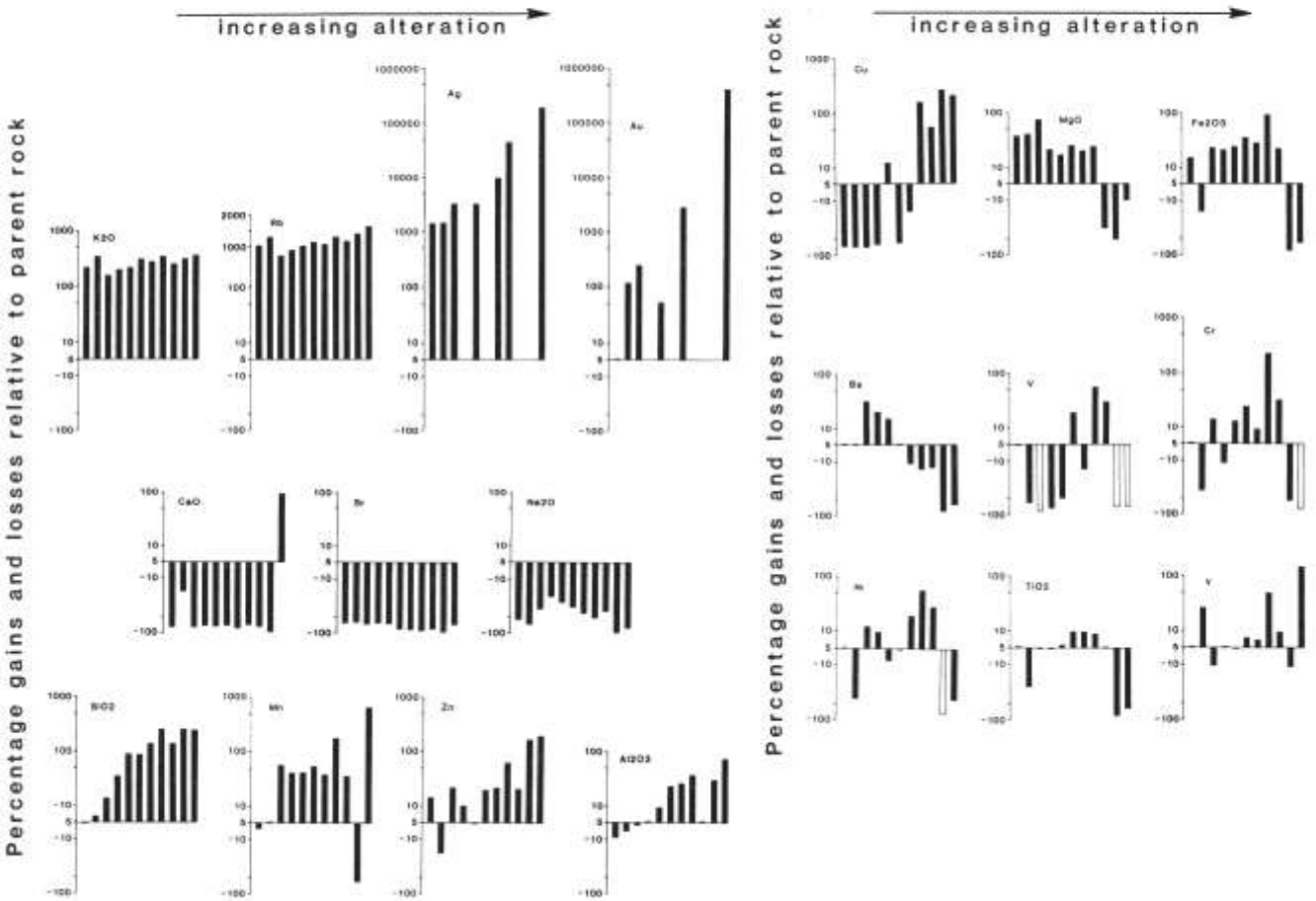

FIGURE 5—Gains or losses of major and trace elements from hydrothermally altered Mineral Creek Andesite in proximity of the 100-ft level of the Eberle mine. Gains and losses expressed as percentage change relative to abundance in the best estimate of an unaltered parent. Samples ordered with increasing alteration on the basis of IR.

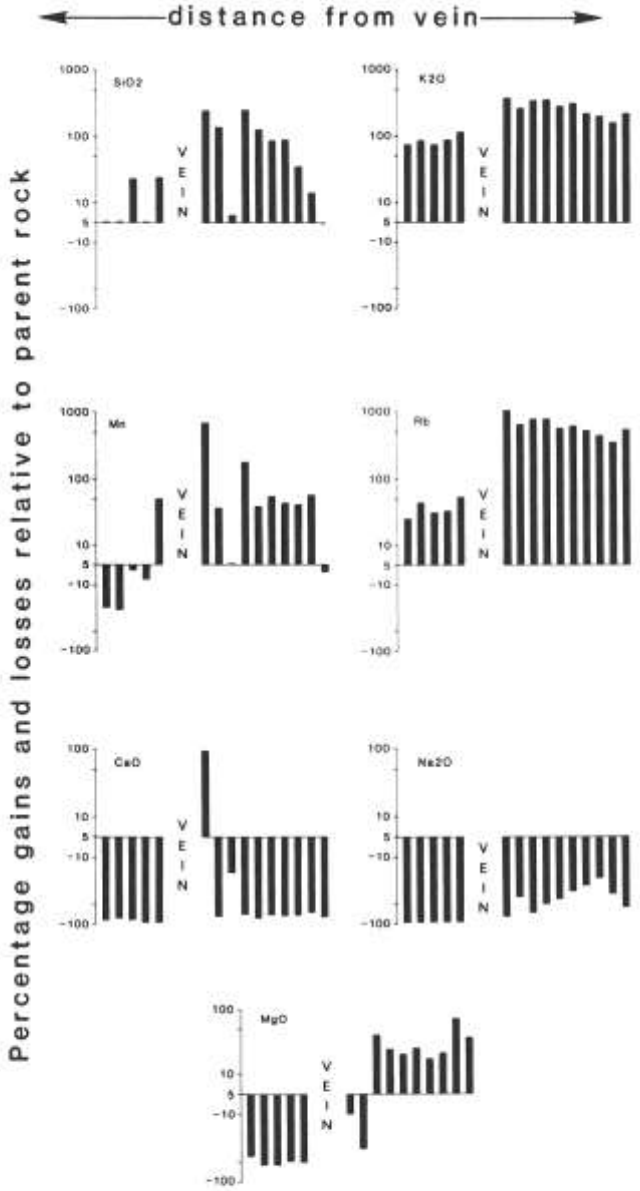

FIGURE 6—Gains or losses of selected elements from hydrothermally altered wallrock in proximity of the 100-ft level of the Eberle mine. Samples represent a profile at 10-ft intervals away from the vein beginning at 10 ft. Rhyolite is on the left, andesite is on the right. Gains and losses expressed as percentage change relative to abundance in the best estimate of an unaltered parent.

TABLE 3—Calculated chemical changes for the transformation of unaltered rhyolite and andesite to hydrothermally altered products in proximity of the Eberle mine. Calculations for selected samples are given and chemical changes are in grams gained or lost per 100 g of parent rock.

	Mineral Creek Andesite		Fanney Rhyolite	
	Less altered	More altered	Less altered	More altered
	TMA-90	TMA-20	TR-50	E1001
SiO_2	+7.24	+70.92	+1.77	+14.01
Al_2O_3	−0.92	+0.13	+0.32	+0.09
Fe_2O_3*	+2.33	+2.25	+0.77	+1.11
MgO	+3.39	−1.52	−0.17	−0.12
CaO	−4.54	−5.07	−0.43	−0.41
Na_2O	−1.27	−1.38	−3.93	−3.92
K_2O	+3.46	+5.76	+3.38	+4.04
TiO_2	−0.005	+0.01	+0.001	+0.008

from all samples, but the degree of removal varies from partial to almost complete. Si, Al, Mn, and Zn were strongly enriched in the most intensely altered samples (generally closer to the vein) and fall to background values in less altered samples. Cu was enriched in the most intensely altered samples and depleted in less altered samples. In contrast, Mg, Fe, and Ba were enriched in less altered samples, but are strongly depleted in the more altered ones. V has a mixed pattern, but is generally removed by hydrothermal solutions. Ni, Cr, Ti, and Y show variable enrichment and depletion, with Ti and Y being practically immobile in most samples. Sc and Zr were assumed to had been immobile during hydrothermal alteration. Selected examples of the actual mass changes for the major elements are given in Table 3.

A strict profile of chemical changes in samples taken perpendicular to the vein shows a clear correlation with distance for some elements in the rhyolite or andesite (Fig. 6). Chemical changes with distance such as those of Si and Mn in the rhyolite and Si, Mn, Rb, K, Mg, and Na in the andesite are positive evidence that alteration is directly related to the Eberle vein and not simply to more regional hydrothermal activity.

Discussion

The conduits for hydrothermal fluids in the Mogollon mining district were interconnecting faults and fractures within the ring-fracture zone of the Bursum caldera. These existing structures were probably opened or reactivated during Basin and Range tectonism. The mineralizing fluids followed this improved plumbing system. Local circulation patterns were undoubtedly influenced by primary textures and structures in the host rock, particularly by flow laminations in the rhyolite and vesicular-flow tops in the andesite. Fluid movement into the wallrock probably became restricted as hydrothermal precipitation occurred and as the outer margins of the fault channel become coated with gangue and ore minerals.

The composition of the hydrothermal fluids is poorly constrained. The salinity of mineralizing fluids was approximately 3.3 wt. % equivalent NaCl (Bornhorst et al., 1984). Inclusion fluids in four samples of fluorite from the vicinity, but outside of the Mogollon mining district, have Na/K ratios between 0.6 and 2.5, Na/ Mg ratios between 2 and 20, and Na/Mn ratios between 6 and 20. The composition of the hydrothermal fluids can also be inferred from the precipitated gangue and ore minerals, but only to the extent that a component is present.

The chemical-mobility calculations reveal that precious metals together with Rb and K were massively added to wallrocks from hydrothermal solutions. The

comparatively low Na/K ratios for the mineralizing solutions are consistent with massive K and Rb introduction. Hydrothermal fluids also contributed variable amounts of Si, Fe, Mg, Ba, and Cu to the altered wallrocks. The most significant and obvious elements added to the veins were Si, Ca, CO_2, F, Fe, Cu, S and precious metals. During alteration, Na, Sr, and Ca were largely removed from both andesite and rhyolite. The source for K, Rb, Si, Fe, Cu, and precious metals in the hydrothermal fluid had to be outside of the immediate vicinity of the veins, whereas some of the Ca and Na could have been leached from the wallrocks. The chemical changes in the andesite due to alteration are more pronounced than those in the rhyolite. This leads us to speculate that the hydrothermal fluids may have been in equilibrium with more silicic rock types prior to interaction at the 100-ft level of the Eberle mine.

During hydrothermal alteration, the Fanney Rhyolite adjacent to the Eberle 100-ft-level vein was sericitized and silicified. The rhyolite was probably devitrified prior to alteration and the microcrystalline groundmass had an enormous surface area available for reaction during alteration. The breakdown of phenocryst and groundmass feldspars during the formation of sericite would have released Na, Ca, and K:

$$\underset{\text{sanidine}}{6(K,Na)AlSi_3O_8} + 4H^+ =$$

$$\underset{\text{sericite}}{K_2Al_4(Si_6Al_2)O_{20}(OH_4)} + \underset{\text{quartz}}{12(SiO_2)} + 4(Na^+,K^+)$$

$$\underset{\text{plagioclase}}{(NaAlSi_3O_8)_4 \cdot (CaAl_2Si_2O_8)} + 4H^+ + 2K^+ =$$

$$\underset{\text{sericite}}{K_2Al_4(Si_6Al_2)O_{20}(OH)_4} + \underset{\text{quartz}}{8(SiO_2)} + 4Na^+ + Ca^{+2}$$

In both cases, H+ had to be contributed by the hydrothermal solution. The formation of large amounts of sericite would have stabilized K and geochemically similar Rb during alteration. In addition to SiO_2 released during sericite formation, some SiO_2 was also apparently precipitated, as quartz, from the hydrothermal fluids themselves. The hydrothermal solution probably cooled as it penetrated the rhyolite and the solubility of silica in solution should have decreased (Holland and Malinin, 1979), which would have promoted silica deposition. The liberated Na and Ca were removed by the hydrothermal fluids.

During hydrothermal alteration, the Mineral Creek Andesite adjacent to the Eberle 100-ft level was sericitized, silicified, chloritized, and carbonitized. The breakdown of plagioclase, pyroxene, minor olivine, and trace minerals during alteration would have made most elements available for either secondary-mineral formation or for removal by the hydrothermal solutions. Mg and Fe directly adjacent to the vein were removed, but further away the precipitation of chlorite caused the original contents of these elements to be retained. The enrichment of Mg and Fe over the unaltered-parent values suggests an additional contribution from the hydrothermal solutions. The formation of sericite captured K and probably H from the hydrothermal solutions. The high CaO gain in one sample (Fig. 5) was due to large quantities of calcite precipitated in vesicles. Significant quantities of silica were precipitated in vesicles, fractures, and matrix during hydrothermal alteration. Thus, for both the rhyolite and the andesite, chemical changes and secondary minerals formed during hydrothermal alteration are grossly consistent with one another.

Conclusion

Mineralization at the Eberle mine consists of Ag-Au—Cu-bearing quartz—calcite—fluorite veins. Para-genetically, in gradual succession, quartz is followed by calcite and then by fluorite. Mineralizing hydro-thermal solutions were low-salinity, K-rich, and carried precious metals and a wide variety of other elements. The mineralizing fluids permeated the adjacent rhyolite and andesite wallrocks, causing significant chemical modification of the original rocks and the formation of secondary minerals. Both the rhyolite and andesite were massively enriched in Ag, Au, K, and Rb and depleted in Ca, Sr, and Na. Sericitization and silicification were characteristic of alteration in both rhyolite and andesite, whereas chloritization was restricted to the andesite. The alteration at the Eberle mine is an excellent example of K-metasomatism. Massive introduction of K is also a common feature of altered wallrocks surrounding Canadian lode-Au deposits (Kerrich, 1983; Kerrich and Fyfe, 1981). Thus, K-fixation reactions may be a common feature of precious-metal deposits.

At the Eberle mine, the altered Mineral Creek Andesite is more strongly enriched in precious metals than the Fanney Rhyolite (Figs. 4, 5). Thus, reactions between the andesite and mineralizing hydrothermal solutions promoted precious-metal precipitation. Perhaps the andesite played a role in precious-metal localization in the vein. This idea is consistent with Scott's (1920) observation that economic mineralization within the district tends to be associated with the bimodal wallrock assemblage rhyolite—andesite.

Volume-corrected chemical-mass-balance calculations lead to accurate deductions about element mobility during hydrothermal alteration. This technique is readily applicable to other mines in other districts and is the only rigorous way of analyzing geochemical changes during metasomatic alteration. By analyzing rocks at and beneath epithermal mineralisation, it may be possible to identify the source bed(s) for precious metals.

References

Bomhorst, T. J., 1980, Major and trace element geochemistry and mineralogy of upper Eocene to Quaternary volcanic rocks of the Mogollon-Datil volcanic field, southwestern New Mexico: Ph.D. Dissertation, University of New Mexico, Albuquerque, 1108 pp.

Bornhorst, T. J., Kent, G. R., Mann, K. L., and Richey, S. R., 1984, Temperature of mineralization in Mogollon mining district, southwestern New Mexico: New Mexico Geology, v. 6, pp. 5355.

Boyle, R. W., 1979, The geochemistry of gold and its deposits: Geological Survey of Canada, Bulletin 280, 584 pp.

Buchanan, L. J., 1981, Precious metal deposits associated with volcanic environments in the Southwest: Arizona Geological Society Digest, v. 14, pp. 237-262.

Costa, V. R., Barnett, R. L., and Kerrich, R., 1983, The Mattagami Lake mine Archean Zn-Cu sulfide deposit, Quebec: hydrothermal coprecipitation of talc and sulfides in a sea-floor brine pool-evidence from geochemistry, $^{18}O/^{16}O$, and mineral chemistry: Economic Geology, v. 78, pp. 1144-1203.

Eveleth, D. W., 1979, New methods of working an old mine-case history of the Eberle group, Mogollon, New Mexico: New Mexico Geology, v. 1, pp. 7-10.

Ferguson, H. G., 1927, Geology and ore deposits of the Mogollon mining district, New Mexico: U.S. Geological Survey, Bulletin 787, 100 pp.

Gresens, R. L., 1967, Composition-volume relationships of metasomatism: Chemical Geology, v. 2, pp. 47-65.

Hoffman, E. L., and Brooker, E. J., 1982, The determination of gold by neutron activation analysis; *in* Precious metals in the northern Cordillera: Association of Exploration Geochemists, Proceedings of a symposium held April 13-15, 1981 in Vancouver, B.C., Canada, pp. 69-77.

Holland, H. D., and Malinin, S. D., 1979, The solubility and occurrence of non-ore minerals; *in* Barnes, H. L. (ed.), Geochemistry of hydrothermal ore deposits: John Wiley & Sons, New York, pp. 461-508.

Kent, G. R., 1983, Temperature and age of precious metal vein mineralization and geochemistry of host rock alteration at the Eberle mine, Mogollon mining district, southwestern New Mexico: M.S. Thesis, Michigan Technological University, Houghton, 84 pp.

Kerrich, R., 1983, Geochemistry of gold deposits in the Abitibi greenstone belt: Canadian Institute of Mining and Metallurgy, Special Volume 27, 75 pp.

Kerrich, R., and Fyfe, W. S., 1981, The gold-carbonate association: Source of CO_2 and CO_2 fixation reactions in Archaean lode deposits: Chemical Geology, v. 33, pp. 265-295.

Leake, B. E., Hendry, G. L., Kemp, A., Plant, A. G., Harvey, P. K., Wilson, J. R., Coats, J. S., Aucott, J. W., Lunel, T., and Howarth, R. J., 1969, The chemical analysis of rock powders by automatic x-ray fluorescence: Chemical Geology, v. 5, pp. 7-86.

Lindgren, W. A., Graton, L. C., and Gordon, C. H., 1910, Ore deposits of New Mexico: U.S. Geological Survey, Professional Paper 68, 361 pp.

Ratte, J. C., 1981, Geologic map of the Mogollon quadrangle, Catron County, New Mexico: U.S. Geological Survey, Geological Quadrangle Map GC-1557, 1:24,000.

Ratte, J. C., and Grotho, T., 1979, Chemical analysis and norms of 81 volcanic rocks from part of the Mogollon-Datil volcanic field, southwestern New Mexico: U.S. Geological Survey, Open-file Report 79-1435, 16 pp.

Ratte, J. C., Marvin, R. F., Naeser, C. W., Brooks, W. E., and Finnell, T. L., 1983, Volcanic history of southwestern MogollonDatil volcanic field as recorded along the Morenci lineament, New Mexico and Arizona: Geological Society of America, Abstracts with Programs, v. 15, p. 303.

Scott, D. B., 1920, Ore deposits of the Mogollon district: American Institute of Mining Engineering, Transactions, v. 63, pp. 289310.

Water carrier, Mogollon, 1903. Cool, clear water suitable for human consumption was, at times, as scarce as gold and silver in parts of the Mogollon Mountains, particularly during the hot summer months. The water boy and his desert canaries laden with H_2O were doubtless a welcomed sight to the thirsty miners.
Photo courtesy of Silver City Museum, Harlan collection.

Geology and mineralization of the Hermosa mining district, Sierra County, New Mexico

by Mark D. Shepard

Department of Geological Sciences, University of Texas at El Paso
(Present address: 2633B Granite NW, Albuquerque, New Mexico 87104)

Abstract

The old camp of Hermosa flourished during the period 1879-1893 and served as a support center for nearby mining activity in the eastern foothills of the Black Range, southwestern New Mexico. Since the initial discoveries, the mines in the district have produced over $1.5 million from small, high-grade deposits localized in Ordovician and Silurian dolomites.

Paleozoic sediments ranging from Ordovician through Pennsylvanian are exposed in a structurally elevated block at Hermosa and attain an aggregate thickness in excess of 610 m. The strata are flanked on the west by volcanic rocks of the Datil—Mogollon volcanic field and on the east by a major sediment-filled graben.

Detailed mapping has shown that the structural fabric is formed by normal faults of two dominant trends: north to northwest and east to northeast. Three major faults belonging to the first group are downthrown to the west 100 m or more and structurally control dikes and plugs of flow-banded rhyolite. They are interpreted as elements of a ring-fracture system along the northeast periphery of the Emory cauldron. Major areas of hydrothermal alteration and mineralization occur between ring fractures where complex fault and fracture systems have dislocated the Paleozoic sequence.

The majority of the ore deposits occur in two genetically related forms: (1) as irregularly distributed sulfide pods, stringers, and pipe-like bodies along steeply dipping fissure veins, and (2) as thin, concordant replacements just beneath the Silurian—Devonian unconformity. Both types show strong affinities for talc, with lesser amounts of calcite and quartz. Primary ore minerals include galena, sphalerite, and chalcopyrite, typically in coarse-grained aggregates, with finer concentrations of acanthite, tetrahedrite, polybasite, pyrargyrite, and stephanite.

Fluid-inclusion thermometry indicates that the ores precipitated between 240 and 350°C (pressure corrected) from weak to moderately saline solutions (2.1 to 11.4 equivalent wt. % NaCl). The ore deposits are prime examples of unconformity-controlled mineralization within the ring-fracture zone of a major mid-Tertiary cauldron.

Introduction

Hermosa once was a small settlement which supported nearby mining activity in the eastern foothills of the Black Range in southwestern New Mexico. Following the initial ore discoveries in 1879, the camp flourished for nearly 15 years until production was halted as the effect of silver demonetization became apparent. To date, the mines in the district have produced more than $1.5 million from deposits enriched in Pb, Zn, Ag, Cu, Sb, and Mo (Maxwell and Heyl, 1975). The principal ores are localized in Ordovician and Silurian dolomites.

Hermosa is situated about midway between the villages of Chloride and Kingston, approximately 45 km (72 mi) west—northwest of Truth or Consequences, in western Sierra County. The mining district encompasses more than 20 km^2 (7.7 mi^2) to the north, east, and south of the old townsite, and includes the principal mines at Palomas Camp, the Antelope—Ocean Wave area, the Flagstaff—American Flag claims, the Wolford group, the Silver Queen area, and numerous other small workings and prospects (Fig. 1).

This article is essentially a scaled-down version of the author's M.S. thesis which included district-wide surface mapping at a scale of 1:6,000, underground mapping of nine mines at a scale of 1:240, ore petrography, and fluid-inclusion thermometry of ore and gangue minerals. Field work began during July of 1982 and continued off and on until September of 1983. The project was completed in May 1984.

Acknowledgments

Key support for this study was provided by Triple S Development Corporation of Albuquerque, New Mexico. Additional funding was received in the form of grants from the William N. McAnulty Memorial Fund and the New Mexico Bureau of Mines and Mineral Resources, Dr. F. E. Kottlowski, Director.

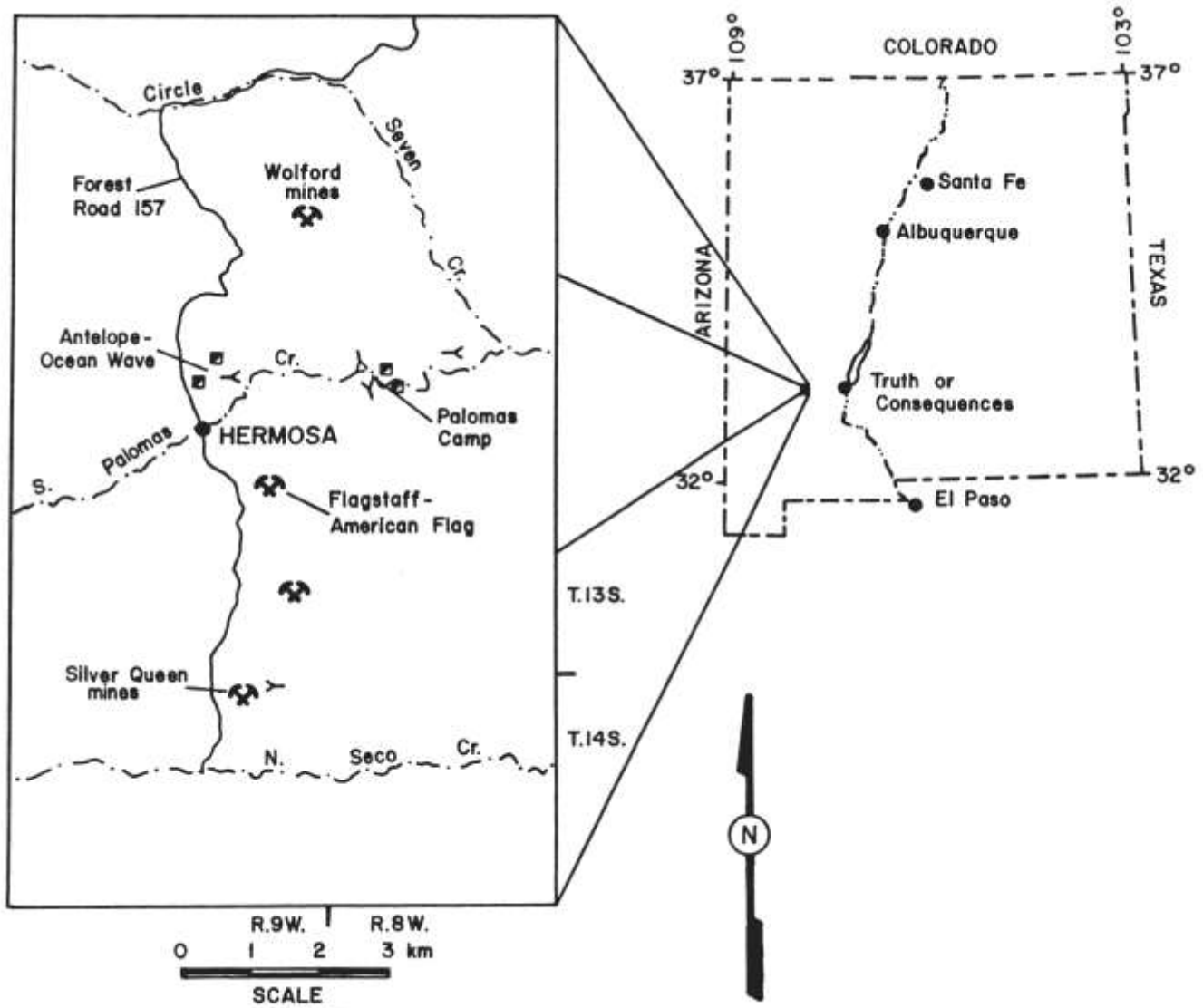

FIGURE 1—Index and location maps of the Hermosa mining district.

Geologic setting

The Hermosa district is situated in a block of Paleozoic strata which measures approximately 16 km north to south, and 4 km at its widest point, east to west. This block is located at the boundary between the Mogollon Plateau volcanic province and the Rio Grande rift system; consequently, it is flanked on the west by a series of mid-Tertiary volcanic rocks and on the east by a north-trending structural depression termed the Winston graben (Kelley, 1955). The outcrop relations of the Paleozoic sediments and surrounding lithologies are shown on the general geologic map of the mining district (Fig. 2).

The major drainages which transect the study area incised steep-walled canyons in the Paleozoic section and exposed marine strata from Ordovician through Pennsylvanian in age. The oldest rocks at the surface are dolomitic limestones of the El Paso Group which outcrop at the base of Circle Seven Canyon, as well as in a structurally high position near the Silver Queen mines. Recent core drilling within the Paleozoic block has confirmed the presence and character of Cambrian and Precambrian formations beneath the El Paso sediments.

To the west of Hermosa the terrane is primarily volcanic due to onlap of extrusive rocks from major mid-Tertiary eruptions and downthrown along the western sides of several north-trending faults. Flows, flow breccias, ash-flow tuffs, and epiclastic rocks dip gently westward toward the central core of the Black Range, where thick sequences (greater than 1,000 m) of Kneeling Nun Tuff occupy the northern portion of the Emory cauldron (Elston et al., 1975).

At the eastern edge of the district, the Winston graben comprises a subparallel offshoot of the Rio Grande rift system and is filled with an unknown thickness of Miocene through Pleistocene basin-fill deposits. These semiconsolidated sediments have been termed the Palomas Gravels, after exposures along Palomas Creek (Lindgren, Graton, and Gordon, 1910, p. 237), and are in juxtaposition with Paleozoic strata by virtue of considerable displacement along a range-boundary fault.

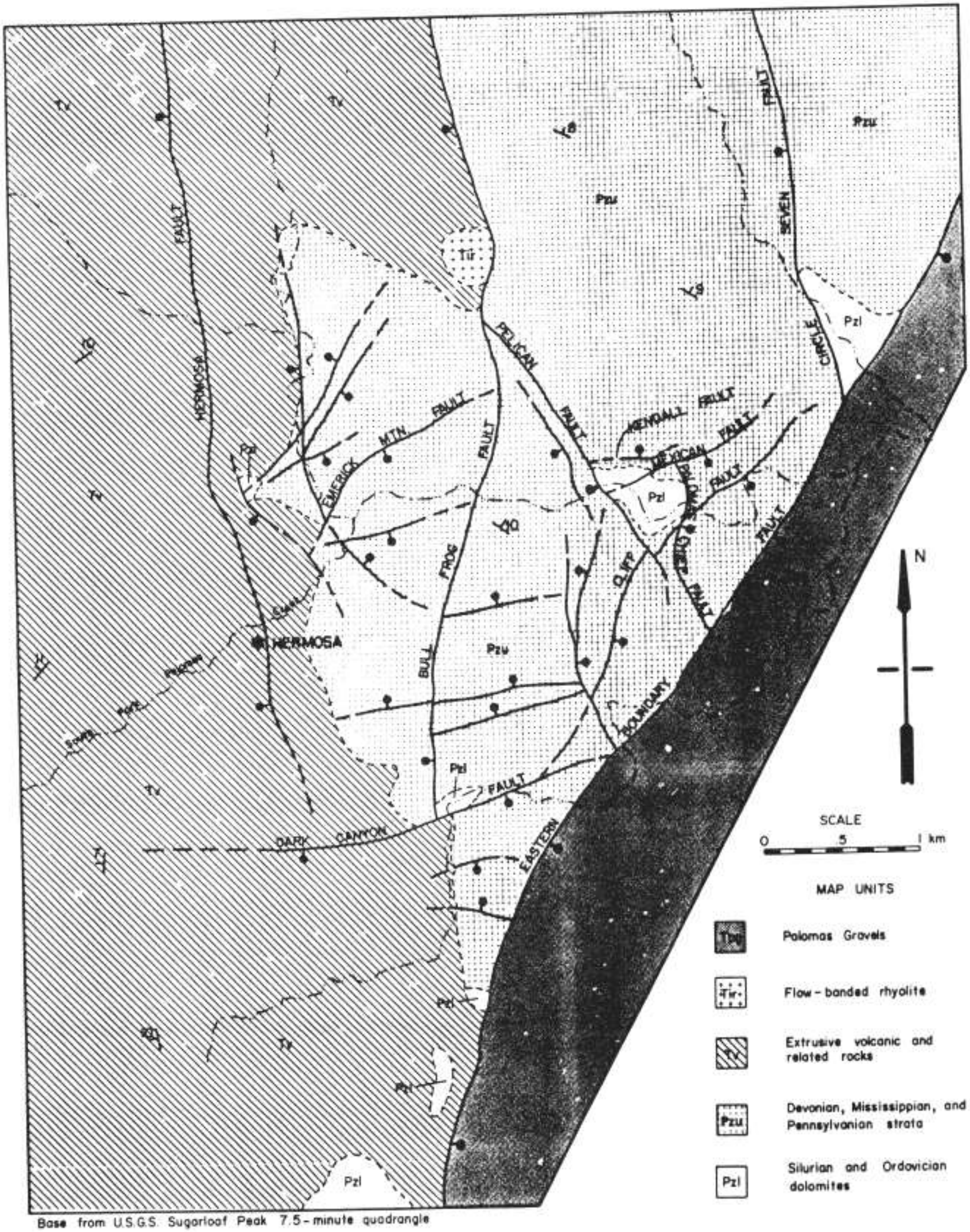

FIGURE 2—Generalized geologic map of the Hermosa mining district.

Stratigraphy

Paleozoic sediments ranging from Ordovician through Permian constitute the majority of rock exposures in the mining district and attain an aggregate thickness in excess of 610 m. General descriptions and thicknesses of these units are summarized in Table 1, which also includes subsurface formations. Much of the stratigraphic sequence was described and measured in the Palomas Camp area by Jahns (1957); other units appeared for the first time in Shepard (1984). It should be noted that outcrops of the Permian Abo Formation are not present in stratigraphic sequence. These red beds occur as detached, raft-like blocks "floating" in and around the oldest sequence of volcanic rocks.

Mid-Tertiary breccia flows and lahars, lava flows, epiclastic rocks, and ash-flow tuffs are exposed along the western edge of the district; their outcrop areas extend well beyond the limits of mapping. The units, which reach a combined thickness greater than 550 m, were briefly described by Ericksen et al. (1970) and included in the calc-alkalic andesite to rhyolite and coeval basalt—basaltic andesite suites of Elston et al. (1976). Summary descriptions of Cenozoic volcanic and sedimentary rocks within the study area are listed in Table 2.

Intrusive rocks are not particularly abundant in the mining district, although they do occur in two structurally controlled forms: (1) as altered latite(?) dikes and small plugs along east—northeast-trending faults, and (2) as domes and irregular dikes of flow-banded rhyolite controlled by north-trending faults.

The Palomas Gravels are primarily composed of volcanic-rock fragments derived from the Black Range and further distant sources in the Mogollon Plateau. They have been roughly correlated with the Santa Fe Formation, Gila Conglomerate, and the informally used "Winston and Cuchillo beds" (Jahns et al., 1978).

TABLE 1—Sequence, general character, and thicknesses of pre-Mesozoic rocks in the Hermosa mining district; [1]presence, general character, and thickness of units determined from diamond-drill core.

	Thickness (m)
Abo Formation (Permian) Siltstone, shale, and sandstone, red to maroon; occurs as detached, "rafted" blocks in oldest series of flow breccias.	highly variable
Unconformity	
Magdalena Group (Pennsylvanian)	
Madera Formation Limestone, medium-gray, medium- to very thick-bedded, locally fossiliferous; interbedded shale in upper part; weathers brown where chert is abundant; prominent cliff-former in steep canyon walls.	>296
Sandia Formation Siltstone, sandstone, and local lenses of pebble conglomerate; interbedded with limestone, medium- to dark-gray and cherty; 2–3 m of chert conglomerate at base.	46
Unconformity	
Kelly Limestone (Mississippian) Limestone, light-gray, coarsely crystalline, massive, and crinoidal; locally cherty; forms rounded cliff faces.	20
Lake Valley Formation (Mississippian) Upper part: limestone, light-gray, massive, crinoidal, cherty throughout. Lower part: limestone, gray to dark-gray, thin- to medium-bedded, and fossiliferous; locally cherty, nodular, and silty.	44
Unconformity	
Percha Shale (Devonian) Shale and siltstone, dark greenish-gray, fissile; weathers into thin chips.	43
Onate Formation (Devonian) Dolomitic siltstone, medium- to dark-gray, with thin dolomite interbeds; 5–8 cm of black shale at base.	21
Unconformity	
Fusselman Dolomite (Silurian) Dolomite, medium- to dark-gray, thick-bedded, finely crystalline.	9–15
Unconformity	
Montoya Group (Ordovician)	
Cutter (Valmont) Formation Dolomite, light-gray, medium- to thick-bedded, finely crystalline; becoming cherty near base.	6–15
Aleman Formation Dolomite, medium-gray, thin- to thick-bedded; abundant gray-chert seams and nodules.	26
Upham Dolomite Dolomite, medium- to dark brownish-gray, thick-bedded to massive, medium crystalline; becoming arenaceous near base.	16
Cable Canyon Sandstone Calcareous quartz sandstone, white, coarse-grained; contains local lenses of pebble conglomerate.	9
Unconformity	
El Paso Group (Ordovician) Dolomitic limestone, light- to medium-gray, fine-grained, irregular bedding; abundant flaser laminae in lower part; transitional with Bliss Sandstone; only upper 30–46 m exposed.	107
Bliss Sandstone[1] (Cambrian and Ordovician) Interbedded sandstone, siltstone, and minor dolomite, light-gray, olive-green, and reddish-gray; many layers rich in glauconite and hematite; oolitic-hematite beds in lower part.	29
Unconformity	
Metadiabase[1] (Precambrian) Dark-green, fine-grained; abundant chloritic alteration of hornblende; intrudes metasedimentary rocks.	>183
Metasiltstones and fine-grained metasandstones[1] (Precambrian) Dark greenish-gray to reddish-orange, arkosic, moderately to well sorted.	

TABLE 2—Sequence and generalized descriptions of Cenozoic volcanic and sedimentary rocks in the Hermosa district and flanking areas.

Palomas Gravels [Miocene to Pleistocene (?)]
Sands and gravels, fine- to coarse-grained, poorly sorted, well consolidated; clasts correspond to older rock units in adjacent source areas.

Intrusive rocks [Oligocene (?)]

Flow-banded rhyolite
Pale yellowish-orange, aphanitic to porphyritic, with delicate fluidal banding; occurs as domes and irregular dikes.

Latite (?)
Grayish-green, mostly aphanitic, well altered; locally contains subhedral pyrite; occurs as small plugs and dikes.

Latite and quartz-latite ash-flow tuffs (Oligocene)
Light greenish-gray, white, and grayish-pink, crystal-poor to crystal-rich, incipient to moderate welding; multiple cooling units interbedded with air-fall tuffs and volcaniclastic sandstones.

Unconformity

Sandstone of the Hermosa area (Oligocene)
Volcaniclastic sandstone, siltstone, and lacustrine shale, pale-purple, grayish-orange, and buff, crossbedded and ripple-marked; contains interbedded flows and breccias of basaltic andesite and basalt.

Unconformity

Rubio Peak Formation (Oligocene)

Latite porphyry
Lava flow, pale-purple, porphyritic; locally displays flow-foliation; intertongues with lower sandstone of the Hermosa area.

Breccia flows and lahars
Various shades of purple, poorly sorted, compact to partially friable; contains angular to rounded clasts of andesite, Paleozoic limestone, and Abo Formation; clasts locally exhibit reaction rims.

Structure

General features

The Paleozoic strata which host the principal deposits of the district form an intensely fractured block that has maintained its stability between two major tectonic features. The older of the two, the Emory cauldron, is a 55 by 25 km (34 x 15.5 mi) mid-Tertiary structure to the southwest of Hermosa; the younger Winston graben along the eastern edge of the district owes its origin to the inception of Basin and Range faulting. The positions of these features with respect to the Hermosa area and the tectonic framework of the surrounding region are shown in Fig. 3.

Detailed mapping of the mining district has shown that faulting conforms to two general trends: north to northwest and east to northeast. Major areas of hydrothermal alteration and mineralization tend to occur along zones of complex breakup in the Ordovician and Silurian dolomites. Such zones are only sporadically displayed in overlying limestone sequences and the pre- and post-ore volcanic cover.

The Paleozoic rocks dip to the northeast at angles less than 15°, although local variations are considerable, especially in the vicinity of the major faults. The volcanics dip to the southwest, west, and northwest at low angles, forming a gentle arc away from the older strata.

North to northwest-trending faults

The Hermosa, Bull Frog, and Circle Seven faults comprise the major features of the north to northwest-trending group. They are high-angle normal faults with down-to-the-west separations in excess of 100 m, and are interpreted to represent part of the ring-fracture zone associated with the northeast periphery of the Emory cauldron (Shepard, 1984). Two of the structures, the Hermosa and Bull Frog faults, have rotational displacements; i.e., stratigraphic separation increases northward along their fault traces. A small plug of flow-banded rhyolite has been emplaced along the Bull Frog fault in the northern part of the district (Fig. 2).

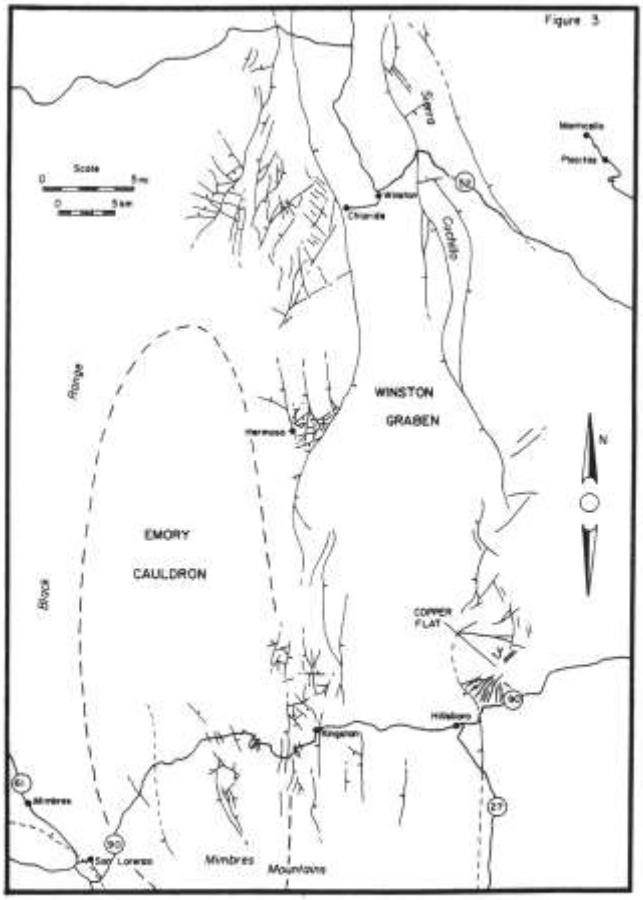

FIGURE 3—Tectonic framework of the Black Range and adjacent areas compiled from Alminas et al. (1975), Ericksen et al. (1970), Hedlund (1977), Jahns (1955), Maxwell and Heyl (1976), Shepard (1984), and Woodard (1982). Details of vein systems in the Copper Flat area from Harley (1934).

Lesser elements of the ring-fracture system include the Pelican and Palomas Chief faults, two structures that evidently developed in conjunction with the mineralizing event. In the Day mine scattered accumulations of ore minerals are found along the Pelican fault, but most of the displacement appears to postdate mineralization. These two faults collectively bound a north-trending horst which contains all of the previously discovered ore deposits at Palomas Camp.

East to northeast-trending faults

Faults with east to northeast trends are widespread in the mining district and include some of the oldest as well as youngest structures. The most prominent elements of this group are the Emerick Mountain and Dark Canyon faults, both with down-to-the-southeast separations greater than 100 m (see Fig. 2). Whereas the Emerick Mountain fault offsets Paleozoic sediments and is buried by younger volcanic rocks, the Dark Canyon fault offsets both rock types and is either a younger structure, or has experienced later reactivation.

The Mexican, Cliff, and Kendall breaks are part of a pronounced structural zone which crosscuts the Palomas Camp area bearing N 50° E and measuring over 366 m in width. Offsets along these faults are well displayed in the bluffs overlooking Palomas Canyon and in many of the underground workings, although only the latter two structures are known to be mineralized.

From the available evidence it is apparent that many faults of this group pre-date the mineralization epoch; however, the trend has been active for extended periods of time. Some of these structures may have developed as radial fractures related to the development of the Emory cauldron.

Mineralized structures

Major loci of hydrothermal activity seem to occur where faults of the two dominant trends intersect; to date, three areas have been identified: (1) the Palomas Camp area, (2) the Antelope—Ocean Wave area, and (3) the Flagstaff—American Flag area (still unexplored in favorable dolomite horizons). Within each of these areas mineralization occurs throughout a group of closely spaced subparallel faults with displacements that range from about 6 m to as little as 10 cm. The most productive structures trend north to northwest, dip steeply, and terminate at, or just above, the contact. The largest ore bodies are localized at structural intersections.

At Palomas Camp the mineralized zone is elongated north to northwest, has a known strike length of 700 m, and measures about 550 m across at its widest point. Unfortunately, at least 50% of this zone has been eroded away by the steady downcutting of Palomas Creek. A similar, though less extensive, structural pattern is present at the Antelope—Ocean Wave mines where mineralization occurs along strike for at least 213 m.

Some of the mineralized structures are generally simple faults that persist both laterally and vertically; other mineralization occurs in areas characterized by a complex array of fractures, but these are usually of local extent. Either of these types may occur within a short distance of the other. Bedding-plane faults, more typical of complex structural sites, are also known to be mineralized.

Ore deposits

General relations and character

Throughout the mining district, the ore deposits are confined to three stratigraphic intervals: (1) the Upper Ordovician and Silurian units; i.e., the Upham, Aleman, Cutter, and Fusselman Dolomites; (2) the Lake Valley and Kelly Limestones; and (3) a massive limestone bed in the Madera Formation. Almost all of the previous production has come from the dolomite sequence.

The ore deposits occur in a variety of different forms. Most are found along steeply dipping fissure veins as stringers, small pockets and pods, pipe-like bodies, and disseminations wholly encased in talc. Lesser amounts of ore have been mined from thin, concordant deposits at or near the contact between the Fusselman Dolomite and the (Mate Formation. In many of the old workings, the manto-like ores overlie, and are often connected to, the fissure veins.

At the Antelope—Ocean Wave mines a larger percentage of the ores consists of vuggy, silicified breccia containing disseminated sulfide minerals. These siliceous ores typically occupy the central portions of the veins and are surrounded by mixed sulfides and talc. Early miners confined their efforts to the talcose envelope as it was amenable to hand-sorting techniques, and much of the siliceous ore was discarded; today it remains scattered throughout the mine dumps. The siliceous material averages between 3 and 6 ounces of silver per ton and has a higher silver/base metal ratio than the talcose ores.

Mineralization

Over 35 mineral species were identified in the district by Jicha (1954), including a wide assortment of both primary and secondary occurrences. The hypogene ores are composed mainly of galena, sphalerite, and chalcopyrite, with lesser but economically significant amounts of acanthite, tetrahedrite, polybasite, pyrargyrite, and stephanite. Native silver and silver halides (cerargyrite, bromyrite, and embolite) evidently accounted for some of the bonanzas discovered in the early mining history of the district.

The chief sulfides occur in various ratios throughout the deposits. In general, ores of high sphalerite

content are low in silver value, whereas galena and chalcopyrite tend to be the major components of high-silver ores. Within individual deposits the sulfide minerals are often found as coarse-grained aggregates, which suggests unrestricted growth in open spaces or in a soft talc matrix.

Hydrothermal alteration is evidenced by two main types of occurrence: (1) talc, with associated calcite and lesser silicification in Ordovician and Silurian dolomites; and (2) irregular silicification, including the development of jasperoid bodies in Mississippian and Pennsylvanian limestones. In several areas these types of alteration appear to be manifestations of different levels within the same hydrothermal system. Talc replaces dolomite and dolomitic fault gouge in, and adjacent to, mineralized veins and commonly extends perpendicular to the structures along bedding planes. Many of the original cher t nodules in the Cutter and Aleman Dolomites have also been replaced by mixtures of talc and calcite at some distance from known veins. This type of alteration is widespread in areas that have experienced increased heat flow and can be used as a general guide to mineralization.

Natural solution cavities, caves, and other open watercourses have developed along throughgoing faults and fractures, and are prominent in many of the underground workings. The oxidized ores are typically composed of cerussite—silica boxworks encrusted by one or more of the following minerals: smithsonite, descloizite, anglesite, vanadinite, pyromorphite, mimetite, or wulfenite.

Fluid-inclusion studies

Introduction

Fluid-inclusion thermometry was undertaken to ascertain the prevailing temperatures of ore deposition and the salinities of parent hydrothermal fluids. In many respects, both ore and gangue minerals from the mining district are ideally suited for this type of study. Sphalerite, quartz, and calcite are sufficiently transparent and coarse-grained to provide excellent working material, and they can be separated from other minerals with relative ease. The data presented in this section represent an investigation of these three mineral species from six mines in the district.

Methods of study

With an R. CHAIXMECA heating and freezing stage, visual fluid-inclusion thermometry was conducted on doubly polished mineral plates whose thicknesses ranged between 0.5 and 1 mm. Above room temperature, the apparatus is calibrated by comparing known micro-melting points of standard compounds with their observed melting points during heating runs. These data are plotted to form a calibration curve which is then used as a correction factor for all subsequent homogenization measurements. Calibration of the freezing stage with deionized water showed it to be in equilibrium with the stage thermocouple; i.e., the thermal lag at or near 0°C was negligible. In light of the slight freezing-temperature depressions encountered, no further calibration was considered necessary.

Character of inclusions

Because fluid inclusions form at various stages during the history of a particular grain or crystal, distinction between types of inclusions must be made (i. e. , primary, secondary, or pseudosecondary). For a discussion of the various criteria used to make this distinction the reader is directed to articles by Roedder (1972, 1979). All three kinds of inclusions were encountered during the study, although secondary and pseudosecondary types prevailed.

With the exception of one large inclusion which contained a small group of unidentified daughter crystals, all other inclusions were simple two-phase varieties with estimated gas volumes from 5 to 15%, and all homogenized in the liquid phase. Strong evidence of fluid entrapment at or near boiling conditions was observed in a small group of inclusions in quartz from the Drake workings. These pseudo-secondary inclusions contained varied gas/liquid ratios, but homogenized within a fairly narrow temperature range; the homogenization occurred by the expansion of the dominant phase. They were the only inclusions which exhibited this behavior; it was thus assumed that boiling conditions were not widespread during precipitation of the ores.

Samples of sphalerite and quartz from the various mines in the district typically contained countless numbers of inclusions, but most of them were too small and opaque to study. Most temperature measurements were conducted on inclusions which ranged from 0.15 mm to less than 40 microns in size. These included a variety of negatively faceted, rounded to columnar shapes, as well as numerous indusions with irregular outlines.

Homogenization and freezing data

The fluid-inclusion study included over 80 homogenization and 15 freezing-point determinations. The results of these measurements are summarized in Fig. 4.

One of the more interesting aspects of the homogenization data is the limited variation in temperatures between the two mining centers of the district. Sphalerite in ore samples from the Lewandowski (H-15) shaft (Antelope—Ocean Wave area) and the Day mine (Palomas Camp) are located about 2 km (1.2 mi) apart, yet they show strikingly similar ranges [If (filling temperature) 265-301°C and 250-307°C, respectively]. This fact suggests that mineralization in both areas occurred from similar, although probably separate, hydrothermal systems. Eight primary and pseudosecondary inclusions measured from the Palomas Chief mine (eastern Palomas Camp) show a range of homogenization temperatures in general accordance with sphalerite from the other two workings. However, they include some of the lowest readings observed in

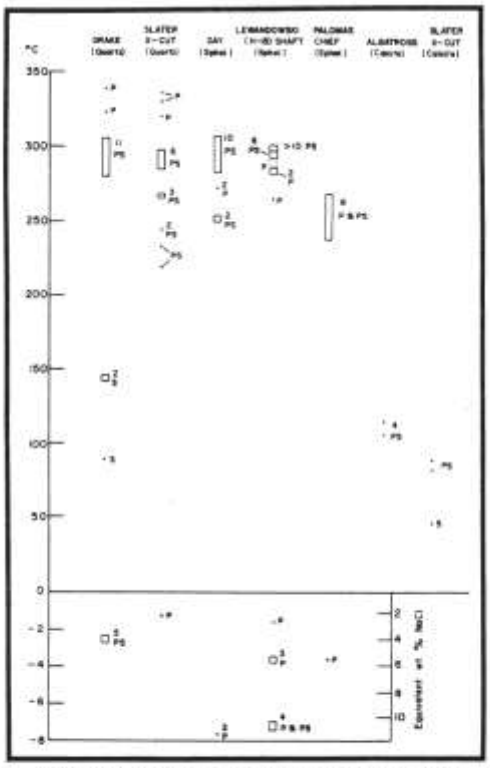

FIGURE 4—Homogenization and freezing temperatures of fluid inclusions plotted against sample location and host mineral. Equivalent wt. % NaCl from Potter et al. (1978). Style of presentation after Roedder et al. (1968). P = primary, PS = pseudosecondary, S = secondary; numbers indicate amount of inclusions observed; dots indicate individual inclusions.

this mineral (note filling temperature range of 238-269°C).

Quartz inclusions from the Antelope—Ocean Wave mines (Slater crosscut; Tf 219-336°C) and the Palomas Camp area (Drake workings; Tf 280-338°C) also show similar temperature characteristics. The highest homogenization temperatures recorded are in direct agreement, although the Slater crosscut samples showed the widest range of values.

Clear, coarse-grained calcite, which typically occurs as vug and cavity fillings, was probably deposited during the waning stages of hydrothermal activity. Pseudosecondary inclusions from both the Albatross drift and Slater crosscut showed low homogenization temperatures (82-115°C). Many of the inclusions observed in calcite samples did not contain a vapor phase.

Freezing-point determinations indicate that parent hydrothermal solutions were weakly to moderately saline brines whose compositions varied between 2.1 and 11.4 equivalent wt. % NaCI. Inclusion fluids in quartz, which generally precedes sphalerite in the paragenetic sequence, show lower salinity ranges (2.1-4.5 as compared with 2.6-11.4 for sphalerite). However, clear-cut salinity trends cannot be established from such widely spaced sampling and small data base. It should be noted that sphalerite samples from a single deposit in the Lewandowski (H-15) shaft showed a wide range of salinity values (2.6-11.1 equivalent wt. % NaCl). This variation may have resulted from dilution, or mixing, of hydrothermal solutions with fresher ground waters.

References

Alminas, H. V., Watts, K.C., Griffitts, W. R., Siems, D. L., Kraxberger, V. E., and Curry, K. J., 1975, Map showing anomalous distribution of tungsten, fluorite, and silver in stream-sediment concentrates from the Sierra Cuchillo–Animas uplifts and adjacent areas, southwestern New Mexico: U.S. Geological Survey, Miscellaneous Inventory Map 1-880.

Elston, W. E., Rhodes, R. C., Coney, P. J., and Deal, E. G., 1976, Progress report on the Mogollon Plateau volcanic field, southwestern New Mexico, No. 3—surface expression of a pluton; *in* Cenozoic volcanism in southwestern New Mexico: New Mexico Geological Society, Special Publication no. 5, pp. 3-28.

Elston, W. E., Seager, W. R., and Clemons, R. E., 1975, Emory cauldron, Black Range, New Mexico: source of the Kneeling Nun Tuff: New Mexico Geological Society, Guidebook 26, pp. 283292.

Ericksen, G. E., Wedow, Helmuth, Jr., Eaton, G. P., and Leland, G. R., 1970, Mineral resources of the Black Range primitive area, Grant, Sierra, and Catron Counties, New Mexico: U.S. Geological Survey, Bulletin 1319-E, 162 pp.

Harley, G. T., 1934, The geology and ore deposits of Sierra County, New Mexico: New Mexico Bureau of Mines and Mineral Resources, Bulletin 10, 220 pp.

Hedlund, D. C., 1977, Geologic map of the Hillsboro and San Lorenzo quadrangles, Sierra and Grant Counties, New Mexico: U.S. Geological Survey, Miscellaneous Field Studies Map MF 900-A.

Jahns, R. H., 1955, Geology of the Sierra Cuchillo: New Mexico Geological Society, Guidebook 6, pp. 158-174.

Jahns, R. H., 1957, The Pelican area, Palomas (Hermosa) district, Sierra County, New Mexico: New Mexico Bureau of Mines and Mineral Resources, Bulletin 55, 5 pp.

Jahns, R. H., McMillan, D. K., O'Brient, J. D., and Fisher, D. L., 1978, Geologic section in the Sierra Cuchillo and flanking areas, Sierra and Socorro Counties, New Mexico; *in* Field guide to selected cauldrons and mining districts of the Datil–Mogollon volcanic field, New Mexico: New Mexico Geological Society, Special Publication no. 7, pp. 131-138.

Jicha, H. L., Jr., 1954, Paragenesis of the ores of the Palomas (Hermosa) district, southwestern New Mexico: New Mexico Bureau of Mines and Mineral Resources, Circular 27, 20 pp.; Economic Geology, v. 49, pp. 759-778.

Kelley, V. C., 1955, Regional tectonics of south-central New Mexico: New Mexico Geological Society, Guidebook 6, pp. 96-104. Lindgren, W., Graton, L. C., and Gordon, C. H., 1910, The ore deposits of New Mexico: U.S. Geological Survey, Professional Paper 68, p. 237.

Maxwell, C. H., and Heyl, A. V., 1975, Mineralization and structure of mineral deposits in the Hermosa, Chloride, and Phillipsburg areas, New Mexico (abstract): New Mexico Geological Society, Guidebook 26, pp. 341-342.

Maxwell, C. H., and Heyl, A. V., 1976, Geology of the Winston quadrangle, New Mexico: U.S. Geological Survey, Open-file Map 76-858.

Potter, R. W., Clynne, M. A., and Brown, D. L., 1978, Freezing point depression of aqueous sodium chloride solutions: Economic Geology, v. 73, pp. 284-285.

Roedder, E., 1972, Composition of fluid inclusions: U.S. Geological Survey, Professional Paper 440-JJ, 164 pp.

Roedder, E., 1979, Fluid inclusions as samples of ore fluids; *in* Barnes, H. L. (ed.), Geochemistry of hydrothermal ore deposits, 2nd edition: Wiley-Interscience, New York, pp. 684-737. Roedder, E., Heyl, A. V., and Creel, J. P., 1968, Environment of ore deposition at the Mex-Tex deposits, Hansonburg district, New Mexico, from studies of fluid inclusions: Economic Geology, v. 63, pp. 336-348.

Shepard, M. D., 1984, Geology and ore deposits of the Hermosa mining district, Sierra County, New Mexico: M.S. thesis, University of Texas at El Paso, 215 pp.

Woodard, T. W., 1982, Geology of the Lookout Mountain area, northern Black Range, Sierra County, New Mexico: M.S. thesis, University of New Mexico, 95 pp.

Geology, character, and controls of epithermal silver mineralization in the Carbonate Creek area, Kingston, New Mexico

by Vertrees McNeil Canby[1] and Rex **L.** Evatt[2]

[1]*Department of Geoscience, New Mexico Institute of Mining and Technology, Socorro, New Mexico 87801*
[2]*Department of Geology, Western New Mexico University, Silver City, New Mexico 88061*

Abstract

The silver—gold deposits of the Carbonate Creek area are entirely within Paleozoic sedimentary rocks. The Fusselman Dolomite, limestones of the El Paso Group, and Lake Valley Limestone were extensively replaced by fine-grained silica (jasperoid) along a series of NW-trending faults prior to silver—gold mineralization. These faults are the major ore control in the area.

Silicification took place in three stages, with ore mineralization during the latest stage. In the first stage solutions flowed along the faults, jasperoidizing the wall rocks. The carbonate rocks, mostly the Lake Valley Limestone, Fusselman Dolomite, and Lower Montoya Group, which were in contact with the faults, were largely replaced, forming jasperoid bodies. In the second and third stages, reactivation of faults in the area brecciated the jasperoid zones. Solutions then flowed along the faults silicifying and mineralizing the breccia zones. The peculiar alteration that preceded, or coincided with, mineralization rendered limestone to a powdery, soft, calcite—clay mixture which, along with fault gouge, may have clogged faults where they traversed limestone, resulting in reduced permeability.

Ore minerals present are acanthite, ruby silver, and polybasite, with some native silver, native gold, chalcocite, and small amounts of azurite, malachite, and chlorargyrite. Gangue mineralization is mostly silica, with some calcite, limonite, hematite, and small amounts of manganese oxides, pyrite, fluorite, dickite, and adularia.

Introduction

The study area is located in the Kingston mining district on the west side of Carbonate Creek, which is on the east slope of the Black Range approximately 3 mi due north of Kingston, New Mexico (sections 25 and 36, T. 1 S., R. 9 W.—Fig. 1). Silver was discovered in the area in 1882 by two prospectors named Shedd and Henry. While prospecting their claim on the southwestern slope of what is now called Silver Gulch, they discovered acanthite float ranging from marble size to 250-lb masses (Fig 2). Downhill from the claim staked by Shedd and Henry was a claim owned by Governor Tabor of Leadville, Colorado. It is reported that a crew of men working for Tabor collected over $80,000 worth of silver within a few weeks.

Despite numerous workings, the source of the acanthite float was never discovered. The workings in the area are shallow and most explore silica and calcite pods, some of which contain acanthite mineralization.

Acknowledgments

We are indebted to Robert North, mineralogist at the New Mexico Bureau of Mines and Mineral Resources, for the use of x-ray-diffraction equipment, rock saws, atomic-absorption equipment, and assay facilities. Mr. North also provided excellent advice and discussions on the project and reviewed the manuscript. We are also indebted to Phillip Fields, a New Mexico Tech student, for spending many hours with us collecting samples, and to Thomas Keller for some assistance in the field.

FIGURE 1—Location of study area.

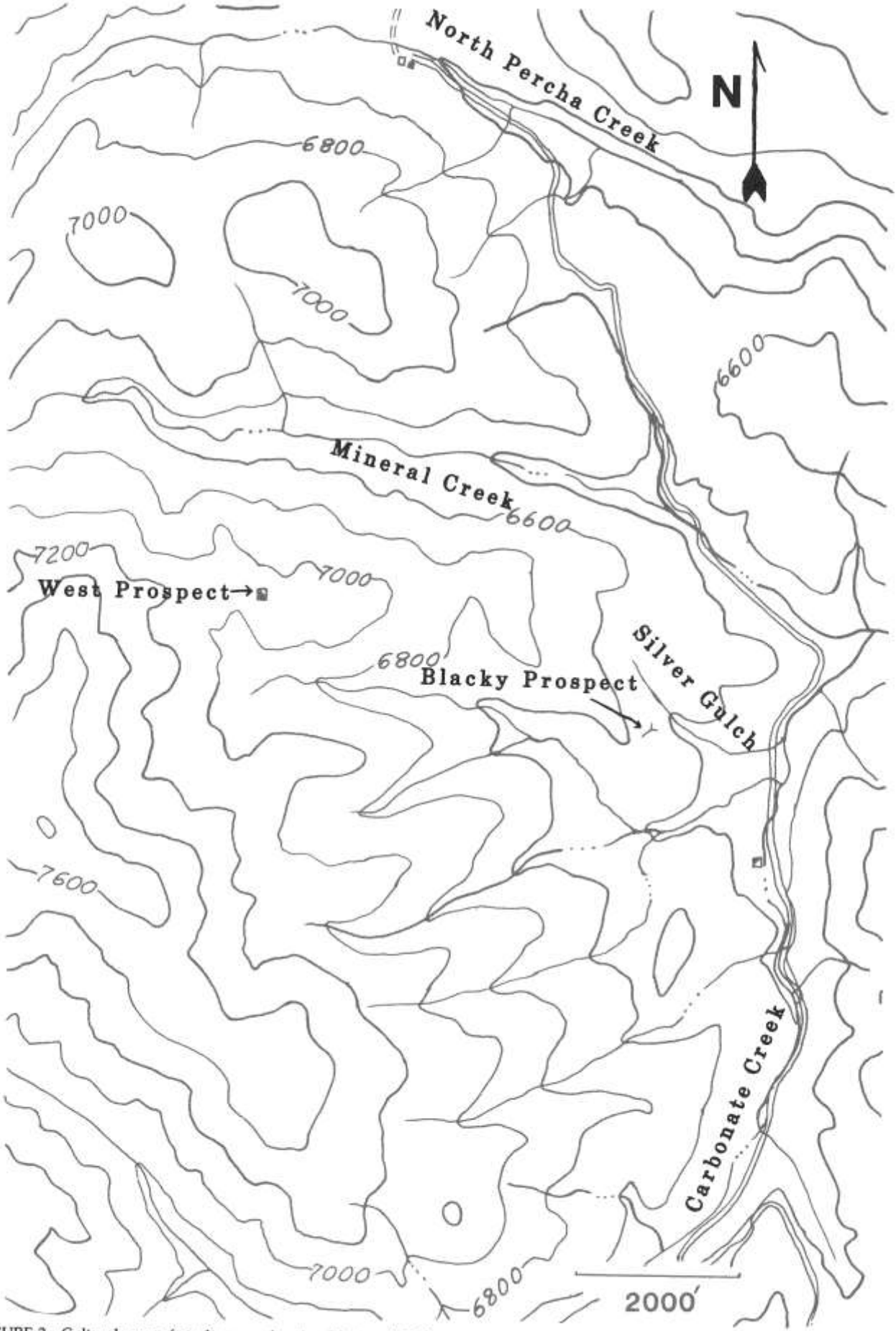

FIGURE 2—Cultural map of study area, showing West and Blacky prospects. Topographic base is Hillsboro NW 7.5 min. preliminary topo.

Geology

To the west of the study area are exposed Precambrian rocks consisting of granite and schist. Overlying the Precambrian rocks are Paleozoic sediments, mostly carbonates, which are host rocks for ore deposits in the area. The Paleozoic sediments dip to the east and are cut by N—NW-trending normal faults of small displacement. These faults parallel the large Carbonate fault which has a displacement of approximately 600 ft (Fig. 3).

Rubio Peak andesite lies unconformably on the Magdalena Group north of Silver Gulch and is displaced by some of the normal faults. Faults are generally harder to recognize in the andesite due to its homogeneity, but are marked in some places by slight argillic alteration. To the west, some of the Precambrian basement rocks are overlain by the Kneeling Nun Tuff.

Precambrian rocks

The Precambrian rocks consist of granite and hornblende—chlorite schist cut by metadiabase dikes. The granite is fine- to medium-grained, light red to tan, and contains perthite, quartz, plagioclase, biotite, and minor amounts of magnetite, ilmenite, zircon, fluorite, and chlorite. The metadiabase is dark green to black and contains hornblende and chlorite with small amounts of biotite, magnetite, ilmenite, plagioclase, and epidote (Kuellmer, 1954, pp. 6-10).

Paleozoic rocks

Paleozoic rocks consist of the Pennsylvanian Magdalena Group, Mississippian Lake Valley Limestone, Devonian Percha Shale, Ordovician Montoya Limestone and El Paso Group, and Cambrian Bliss Sandstone. The Magdalena Group is approximately 900-ft thick and consists of gray to black, thick- to thin-bedded fossiliferous limestone with interbedded shale; fossils are chiefly brachiopods and fusulinids. The Magdalena Group in this area has a basal unit 50-ft thick. The Lake Valley Limestone is approximately 100-ft thick and consists of gray to black thick- to thin-bedded cherty limestone which is in part shaly and fossiliferous, with brachiopods, crinoids, trilobites, and bryozoans common.

The Percha Shale is approximately 150-ft thick and consists of a lower member of black fissile, fossiliferous shale and an upper member of green, highly fossiliferous calcareous shale. The upper member contains nodules and thin beds of fossiliferous limestone with brachiopods, crinoid columnals, and bryozoans.

The Fusselman Dolomite is approximately 50-ft thick. It consists of gray- to brownish-gray and black fine-grained massive dolomite with thin beds of limestone and sparse nodules and lenses of gray chert.

The Montoya Limestone is approximately 150-ft thick and consists of gray to black, thick- to thin-bedded cherty limestone and dolomite with interbedded calcareous siltstone. The Montoya has a basal unit of white coarse-grained sandstone and locally contains a distinctive chert layer 25 to 35-ft thick, which is probably of secondary origin.

The El Paso Limestone is approximately 950-ft thick and consists of gray, fine-grained, slabby to massive-bedded limestone with abundant yellow—brown siltstone partings.

The Bliss Sandstone is approximately 75-ft thick and consists of glauconitic and hematitic sandstone, siltstone, and shale, with a few thin layers of limestone, pebble conglomerate, and quartzite (Kuellmer 1954, pp. 11-27).

Tertiary volcanic rocks

Tertiary volcanic rocks in the study area consist of the Rubio Peak Formation and the Kneeling Nun Tuff. The Rubio Peak Formation is a series of andesitic flows and autobreccias consisting of silicic amphibole latites and pyroxene andesites. Their colors range from pinkish gray to various shades of red, lavender, purple, brown, and black. Phenocrysts may be large or small, and the rock may be glassy or almost entirely crystalline.

The Kneeling Nun Tuff is a pinkish-gray to reddish-brown, medium-grained, highly porphyritic, welded rhyolite tuff. Phenocrysts consist of quartz as much as 3 mm in diameter, with lesser amounts of sanidine and plagioclase of similar size and minor biotite in a fine-grained glassy matrix (Jicha 1954, pp. 40, 44).

Ore deposits

Mineralization in the Carbonate Creek area was discovered in 1882 by prospectors who found large masses of acanthite float in what is now called Silver Gulch. Mining consisted of hand-collecting the float; it is reported that 80,000 ounces of silver were recovered. However, despite numerous later workings, the source of the large masses was never found.

At least two stages of mineralization have been recognized in the Carbonate Creek area: an early barren stage of fine-grained jasperoid as replacement of carbonates, shales, and sandstones, and at least one later stage of fine- to coarse-grained quartz that was widespread, but contains ore minerals only locally.

Jasperoid occurs throughout the Kingston district, but is most abundant in the study area, north of the historic mining area. It is concentrated in several specific stratigraphic horizons: the Fusselman Dolomite-Percha Shale contact, where it replaces both shale and dolomite; the lower sandstone member of the Montoya Group, where it replaces carbonates on both sides of the contact as well as the sandstone; the upper Magdalena Group; and the "blue crinoidal" member

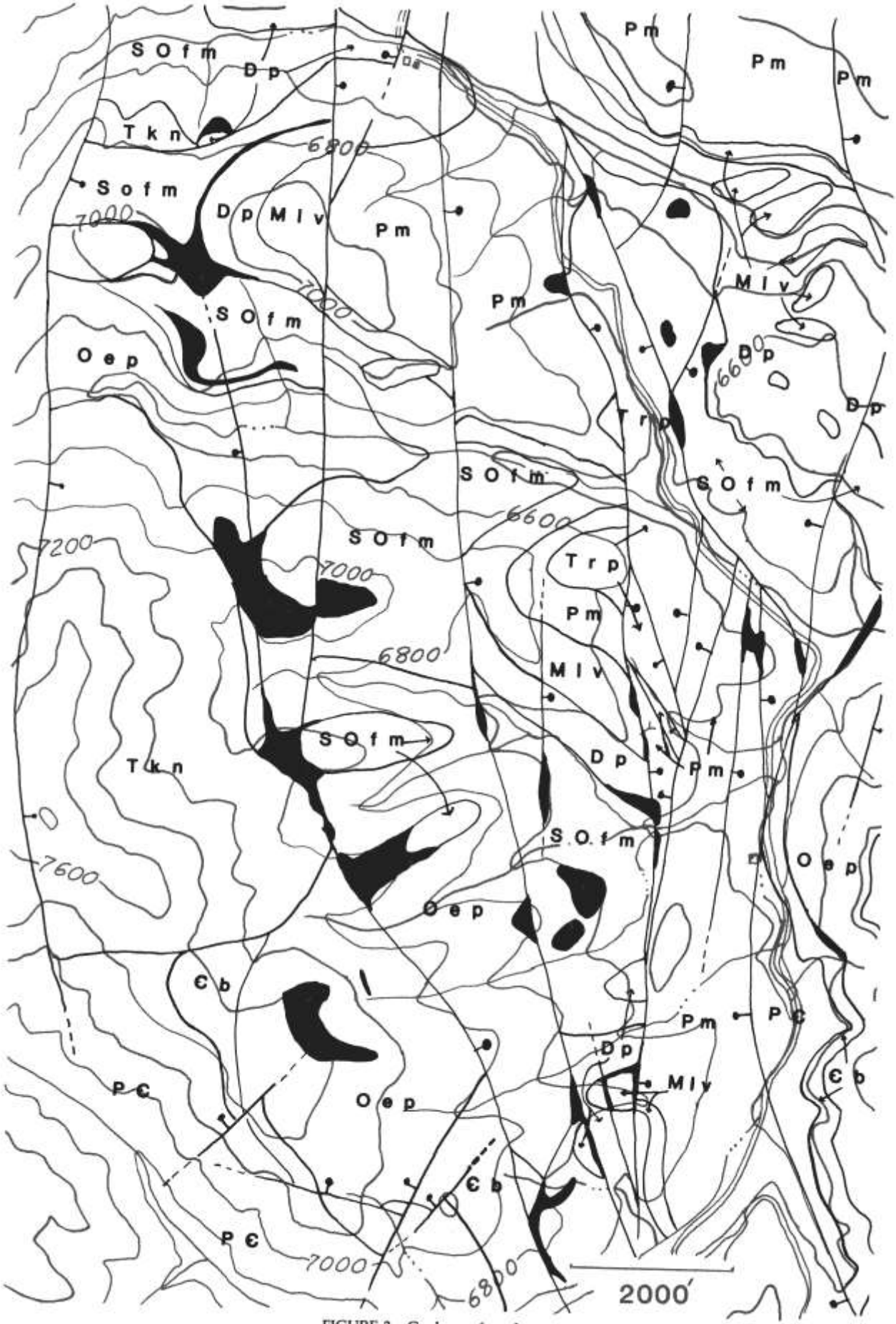

FIGURE 3—Geology of study area.

of the Lake Valley Formation. It also occurs along faults, which suggests that solutions depositing jasperoid followed permeable structures (i.e., the lower sandstone member of the Montoya Group, as well as breccia zones along faults), or were channeled under impermeable horizons such as the Percha Shale, an ore-capping horizon that has been productive throughout much of southwestern New Mexico. Jasperoids in the Montoya-El Paso contact average about 5 m in thickness and are more abundant and laterally extensive than those in other horizons; some can be followed for over 300 m along strike. Jasperoids in the other horizons average about 3 m in thickness and are generally less extensive along strike. The jasperoid is composed of very fine-grained quartz with no other megascopic minerals, and is tan, gray, yellow, or red-brown. Original structures in the host rocks are completely replaced and jasperoid/hostrock contacts are sharp. Although it contains no contemporaneous ore minerals, jasperoid is important because of its competence which allowed open space to form when faults were reactivated. In places, tuffs of the Kneeling Nun Tuff have been deposited on eroded jasperoid surfaces, indicating an age of early or middle Oligocene for jasperoid formation.

Vertical movement again occurred along old faults as well as on new ones, resulting in formation of both jasperoid and carbonate breccias. Shearing also occurred along bedding planes, especially in competent jasperoid beds, resulting in breccias composed of flat slabs oriented parallel to bedding; this is so extensive that few jasperoids can be found in the field that have not been brecciated either by vertical faulting or bedding-plane slippage. A second stage of fine- to coarse-grained quartz cements these breccias. The quartz

LEGEND

Tkn	Kneeling Nun Formation (Tertiary)
Trp	Rubio Peak Formation (Tertiary)
Pm	Magdalena Group (Permian)
Mlv	Lake Valley Formation (Mississippian)
Dp	Percha Formation (Devonian)
SOfm	Fusselman Formation (Silurian)
Oep	El Paso Group (Ordovician)
Cb	Bliss Formation (Cambrian)
PC	Precambrian
	Jasperoid
	Fault, ball on downthrown side
	Contact

commonly occurs as comb growths around vugs and fractures, the crystals frequently having multiple growth terminations. Locally, this second stage of quartz contains pyrite and minor fluorite, dickite, chalcopyrite, and adularia. Samples of this material rich in pyrite contain up to 0.15 oz Au/ton and 2.5 oz Ag/ton; the few average samples available of large, iron-stained jasperoids with this type of quartz veining contain about 0.01-0.03 oz Au/ton and about 1.5 oz Ag/ton.

Thirty fluid inclusions from second-stage quartz of this type were analyzed for homogenization temperatures and salinities. The samples came from a small jasperoid along a north-trending fault, north of the Blacky prospect. Pyrite-rich samples from this locality contain up to 0.15 oz Au/ton, with little Ag. The inclusions measured all were two-phase primary or pseudosecondary types with similar phase ratios; many had negative crystal shapes. Mean homogenization temperature for these inclusions is 224°C, uncorrected for pressure, with a range of 220-231°C. Salinities were very low (< 1%) and all inclusions were homogenized to a liquid.

Silver mineralization occurred after a third movement along the faults. It appears, however, that only a few of the faults were reactivated and displacements were very small. Ore minerals—small grains of acanthite, gold, polybasite, cinnabar, and realgar—were deposited in open space. Two prospects containing rich silver mineralization were examined: the Blacky claim and a prospect about 800 m west of the study area, referred to as the "West prospect."

The West prospect affords an excellent example of the sequence of mineralization in the area. Brecciated gray jasperoid (replacing the lower sandstone member of the Montoya Group) had been cemented by pyrite and quartz, which were in turn shattered and cemented by quartz containing polybasite, realgar, and native silver. Although the structure at the prospect is not completely clear, it does lie in a small north-trending fault that appears to have had at least three periods of movement.

On the Blacky claim, late silver mineralization occurs in faulted jasperoid that replaces the Tierra Blanca Member of the Lake Valley Formation. As can be seen on the map (Fig. 3), a normal fault of small displacement cuts down-slope and down-dip of the silver-bearing jasperoids, both of which lie along the strike of this fault. The down-dip extension of the jasperoid in both cases has been eroded or displaced by faulting and its contact with the fault has been erased. Ore-generation quartz varies from finely banded chalcedony to coarse and granular, and fills vugs containing earlier quartz crystals. It is commonly white, but the richest silver values are found in bright yellow or purple quartz. In some places sharp jasperoid fragments are cemented with acanthite-bearing quartz, but most often the contact of silver-bearing quartz and jasperoid is gradational, and it appears that some replacement has taken place. Although the earlier, second-stage quartz is present, there is no pyrite. Acanthite is abundant in many specimens as grains up to 2 mm in diameter. Native gold and silver are relatively common, often being intergrown with the

acanthite. Cinnabar has been found in one polished section as tiny grains frozen in quartz with acanthite, as well as in placer grains.

Twenty-four fluid inclusions from Blacky ore samples were analyzed for homogenization temperature and salinity. Unfortunately, only relatively large crystals were amenable to measurement and no inclusions were measured in the banded, chalcedony-type quartz that appears to be associated with ore minerals. Mean homogenization temperature for these inclusions was 214°C, uncorrected for pressure, with a range of 200-231°C. Like the samples discussed above, salinities were below 1%.

Alteration

Two types of altered rock are found in the study area, but their relation to silver mineralization is uncertain. The most apparent is a large area on the south side of Silver Gulch. Here limestones of the middle Lake Valley Formation and lower Magdalena Group have been altered to a powdery white clay-like material that is composed of calcite and montmorillonite. All texture of the original limestones is erased and approximately 10% of the original calcite has been removed. Altered and unaltered limestones were compared by x-ray-diffraction analysis and no mineralogical change has been found. The montmorillonite was present in both samples; it is probably detrital. Montmorillonite has been enriched relative to calcite in the altered samples due to its resistance to leaching. This type of alteration covers at least 10,000 m^2 as now exposed, and has been found over an even larger area under soil cover. Its contact with unaltered limestones is gradational and fragments of unaltered limestone are found surrounded by alteration. The relation of this material to structures is not clear, although it roughly follows bedding planes in some places. Where explored by old workings, the small faults in the altered area are filled with gouge that ends abruptly at the slickensided walls. No conclusions can be made relating faults and alteration in the study area.

This type of alteration occurs elsewhere in the district, although nowhere is it as strong as in the study area. In these cases it forms along, or in, faults of varying displacement, and is always associated with irregular quartz pods. No rich silver mineralization occurs at any of these other localities, although some contain minor gold and silver anomalies (up to 0.02 oz Au/ton and 0.5 oz Ag/ton). Quartz in these pods is granular and bears no resemblance to either jasperoid or second-generation quartz.

Alteration of a different type occurs on the north side of Silver Gulch in the Rubio Peak andesite and Magdalena Group. Here, along its contact with the Rubio Peak andesite, Magdalena limestone has been irregularly replaced by bright-red, hematite-rich silica. This replacement is most intense along the contact and the altered beds are up to 3-m thick. The overlying andesite has been bleached from its typical bluish color to a bright-white, hard rock stained red by limonite on fracture surfaces. Mineralogically, the original andesite (composed of andesine, amphiboles, and quartz) has been enriched in quartz, K-feldspar, muscovite (probably as sericite), and depleted of andesine and dark minerals. Pyrite occurs sparingly in the altered andesite.

The white, strongly altered andesite clearly occurs along fractures; away from the fractures, the andesite is weakly altered to a light-yellow color. Irregular areas of this strong alteration also occur. Wide breccia zones are not common in the andesite, but some occur along projections of small faults mapped in sediments south of Silver Gulch. As one proceeds further inside the andesite (away from the contact), alteration diminishes and faults become hard to trace. A large proportion of the andesite on the hill north of Silver Gulch is altered to varying degrees.

Conclusions

The silver deposits in the Carbonate Creek area occur in an unusual setting for epithermal deposits. No mineralized veins occur in volcanics, and, thus far, ore-grade mineralization has been found only in roughly pipe-like bodies following shattered jasperoid beds. No replacement ores have been found. Metallic mineralization appears to have occurred in two stages, with silver deposition restricted to the second stage. The relation of ore deposits to faulting is difficult to determine due to the reactivation of faults throughout time; some of the faults have been active since ore formation. However, the ore seen does occur as open-space filling in either fault or bedding-slip breccias. Faults explored in unsilicified limestones are largely gouge-filled, with restricted open space.

The fluid-inclusion data available are too limited to permit conclusions on the nature of solutions corresponding to different stages in paragenesis. However, the similarity of homogenization temperatures and salinities of quartz from the two sample areas suggests that the second-stage-quartz mineralization occurred under similar conditions in these two places, and that the homogeneity of this type of quartz throughout the study area may be true over a larger area. The banded texture of quartz and ore minerals as a filling around coarse quartz crystals (from which the Blacky inclusion measurements were taken), and the occurrence of ore minerals cementing second-stage quartz and pyrite at the West prospect both imply that silver mineralization began after coarse quartz

was deposited. Deposition of ore minerals could be due to physical or chemical changes in the same solution that deposited coarse quartz (such as boiling), or due to mixing of a new solution. Ore mineralization probably occurred in the waning stages of a hydrothermal system that had largely sealed itself, and thus was restricted to places where open space allowed access of the solutions and physical and chemical conditions were right for deposition.

The deposits lack the classic epithermal-alteration types, but it must be remembered that there are few volcanics here and a solution moving in the carbonate-dominated stratigraphic column would be quickly buffered. Thus, another facet is added to the problem of ore deposition. Further fluid-inclusion studies are expected to reveal more about the evolution of the hydrothermal system and factors which controlled ore deposition. In light of the assay data obtained thus far, the extensive jasperoids in the area deserve examination for bulk-tonnage low-grade deposits that are being reassessed throughout the Southwest. Further geologic work on the small, bonanza deposits may define the ore environment well enough to warrant search for these higher-risk orebodies.

References

Jicha, H. L., Jr., 1954, Geology and mineral deposits of Lake Valley quadrangle, Grant, Luna and Sierra Counties, New Mexico: New Mexico Bureau of Mines and Mineral Resources, Bulletin 37, 93 PP.

Kuellmer, F. V., 1954, Geologic section of the Black Range at Kingston, New Mexico: New Mexico Bureau of Mines and Mineral Resources, Bulletin 33, 100 pp.

Freight team on Whitewater Mesa, 1905. Mogollon, located at the end of the long road winding into the distance above the wagons, never enjoyed the service of a railroad, although at least three such lines were proposed: two from Silver City and one from Magdalena. Until heavy trucks became practical about WW 1, every pound of ore and concentrate, as well as nut, bolt, pick, shovel, and boiler, had to be packed or freighted in and out of these mountains either by burros or 6–10 mule or horse teams. Given this fact, it is astounding that Mogollon's mines were economically productive for so long a period. Here a matched team of 10 trotters owned by W. A. Tenney, a prominent teamster and general freighter of the time, has paused momentarily for a photo on the way to Silver City—the nearest railhead 85 miles by primitive road to the south.
Photo courtesy of Silver City Museum, Harlan Collection.

Geology of the Dripping Gold Prospect, Mogollon mining district

by Charles A. Wolfe

Western New Mexico University, Silver City, New Mexico 88061

Abstract

The Dripping Gold lode claim is an example of an epithermal precious-metal deposit of volcanogenic origin. It is located in sections 3 and 4, T. 11 S., R. 19 W., on the north wall of Whitewater Creek canyon.

The claim, formerly known as the Iron Bar, has been sporadically worked for gold and silver since the early 1900's. The ore was crushed and the concentrates recovered by sluicing.

The mineralization occurs along a southern extension of the Queen vein, at the contact between the Fanney Rhyolite and Last Chance Andesite, and is further localized by junction with a prominent east—west fault. The ore occurs in a hematitic gouge which encloses mineralized fragments of wall rock.

Wall-rock alteration is present and shows zonation. Quartz is the primary gangue mineral, and has been deposited in three stages. The second stage includes the granular type associated with gold and sulfide deposition. Secondary ore mineralization is localized and may include native silver.

Future development of the site includes detailed surface and underground mapping and delineation of possible low-grade ore reserves.

Introduction

The study area is located at the southern edge of the famed Mogollon mining district (Fig. 1), within the Gila National Forest, Catron County, New Mexico. It is about 12 km (7.5 mi) northeast of Glenwood and 2.5 km (1.5 mi) southwest of Mogollon, on the north face of Whitewater Creek canyon. At the center of the study area is a group of workings near Dripping Gold Spring, near the boundary between sections 3 ($SW^1/4$) and 4 (SE 1/4), T. 11 S., R. 19 W., New Mexico Principal Meridian.

Early miners followed a vein of auriferous and argentiferous quartz along the Queen fault for 87 m and mined out several other mineralized ore shoots. Fluids from depth encountered a relatively impermeable host in the dense ring-fracture flow of the Fanney Rhyolite, and were localized along an area of intense cross-faulting where the Last Chance Andesite hanging wall was readily altered, thus permitting the solutions to permeate it.

The site is quite remote and accessible only on foot or horseback. There has been little mechanization at the mine, and the author feels that possibilities may exist for discovery of new ore at depth.

The topography is very rugged (but beautiful), and some places are inaccessible or covered with talus.

Topography

The area lies within the Mogollon Mountains, which are characterized by a steep western escarpment and deep-cut canyons such as Whitewater Creek. The general topography is that of a fault-block range in an early stage of erosion (Ferguson, 1927). The eastern side of the mountains has a much gentler slope and impressive conifer forests.

The study area is at the southern edge of the Mogollon mining district, along the ring-fracture zone of the Bursum cauldron. Faulting of the Fanney Rhyolite has resulted in an imposing cliff which walls in the area adjacent to the mine workings. Elevations range between 1950 and 2300 m (5944 and 7010 ft). In general, slopes in the study area are extremely steep, including large areas of almost impassable Quaternary landslide deposits (Ratté and Gaskill, 1975).

Acknowledgments

I wish to thank Mr. R. C. Richards of Glenwood, Mr. R. Fabres of Mogollon, Mr. Robert Atwood of Reserve, Mr. John Baumberger of the U.S. Forest Service, the staff of the Random House bookstore in Silver City, and Dr. John E. Cunningham of Western New Mexico University. Dr. Cunningham and Mr. William VanDran reviewed the manuscript.

FIGURE 1—Location of study area (from F.S. map no. NM-337, U.S. Department of Agriculture, 1978).

Lithology

Measured stratigraphic thicknesses in this paper are those of Ferguson (1927), with the exception of the Last Chance Andesite (Elston, 1976). Description and chronology of the units are by Ferguson (1927) and Elston (1976), except where noted. Local descriptions are by the author.

Sequence and description of units

Whitewater Creek Rhyolite

This is the oldest member of the Mogollon volcanic sequence; it is found where Whitewater Creek has cut the deepest, and consists of light-purple flows, with beds of light tuff indicating periods of explosive activity. It shows flow banding and glassy texture, and contains cavities filled with quartz crystals.

Cooney Quartz Latite

This unit is thought to be the ash-flow-tuff sheet of the mostly covered Mogollon cauldron (Ratté et al., 1979), and is dated at 32 m.y. (Bikerman, 1972). It is cut off by an extensive north—south fault contact (with the Fanney Rhyolite) which shows little mineralization and extends roughly from the ridge crest above the north wall of Whitewater Creek canyon southeast along the old powerhouse road down to Pine Flat. The Cooney Quartz Latite has been placed within the calc-alkaline volcanic suite of Elston (Elston et al., 1976). Measured thickness at Whitewater Creek is 425 m. It consists of alternating flows of latite and ash-flow tuff with interbedded lenses of red to purple volcaniclastic andesine-rich sandstone. These flows are mostly brick-red, porphyritic, and crystal-rich. Phenocrysts include orthoclase, andesine (Ab_7An_3), magnetite, and biotite altered to chlorite. The author has also identified an ash-flow-tuff facies which outcrops northwest of Pine Flat. It is later than the red latite, and due to talus cover its extent could not be determined. The tuff is light gray and contains conspicuous biotite phenocrysts.

Some of the area previously mapped as Cooney Quartz Latite (Ratté and Gaskill, 1975) could be considered landslide deposits. The actual surface consists of Fanney Rhyolite talus slopes and the contact between the two units is in some places at best inferred.

Jointing, sometimes also exhibiting subconchoidal fracture, is common. Two intersections were measured. The first intersection consists of a joint set striking N 5° W and dipping 78° NE, and one striking N 75° W and dipping 81° SW. The second contains a set striking N 30° W and dipping 79° SW, and one striking N 52° E and dipping 84° SE.

At the dumps at Pine Flat, the Cooney is pink and contains phenocrysts of calcite, orthoclase, biotite, magnetite, pyrite, chalcopyrite, and bornite(?). The presence of these latter sulfides indicates some hydrothermal mineralization, but this may not have been accompanied by sufficient gold or silver values to be economic (see History and Production).

Mineral Creek Andesite

This unit lies uncomformably on the Cooney Quartz Latite and thins rapidly to the west. It ranges from 0 to 215 m in thickness, and flow-direction studies indicate an origin to the southwest. This unit can be distinguished from the Houston and Last Chance Andesites only by stratigraphic position, although material within the study area tends to be more amygdaloidal than the Last Chance. The Mineral Creek Andesite has not been dated, but is bracketed between the Apache Spring Quartz Latite (27.3 m.y.) and the quartz latite of Nabours Mountain (27.5 m.y.). It partly fills the moat of the Bursum cauldron. It is a dark-red to purple andesite with amygdules of quartz, calcite, and chlorite. Phenocrysts include ferromagnesian minerals that have been altered to aggregates of iron oxides and chlorite. The groundmass appears to be plagioclase of andesine composition.

This andesite outcrops along the trails between Pine Flat and the Dripping Gold mine, where it sometimes contains amygdules of malachite surrounding quartz. The contact with the overlying Fanney Rhyolite is irregular and trends to the northeast. Down-slope the andesite breaks off into landslide deposits.

Fanney Rhyolite

The Fanney is one of the major units that comprise the ring-fracture flows of the Bursum cauldron. It is dated at around 27.3 m.y. and consists of viscous intrusive and extrusive flows which have cooled in a mound-like form. This unit has been placed within Elston's high-silica rhyolite suite; it is thought to be a "framework" rhyolite, which may suggest a large subsurface pluton beneath the Bursum cauldron (Elston et al., 1976). It forms a spectacular east—west fault-block cliff in the study area and serves as a horizon marker between the Mineral Creek and Last Chance Andesites. At the junction of Whitewater Creek with the South Fork the measured thickness is 365 m.

This flow is distinguished by the presence of spherulites (especially near the Gold Dust mine) 0.65 to over 1.3 cm in diameter. Flow bands are common, and its viscous nature has resulted in many cavernous openings. The groundmass is light purple and varies in texture between glassy and spherulitic. Two generations of quartz are present. The first consists of crystals which have been intruded by the glassy groundmass, the second is a granular variety. Phenocrysts are uncommon and include orthoclase and rarely biotite.

The Fanney Rhyolite ring-fracture flows commonly show parting along flow bands. Later minerals present in the rhyolite include psilomelane (Ratté et al., 1979), pyrolusite, and hematite of the red-earth variety. These minerals may be found as disseminated grains or commonly as coating along joint and fault planes.

Last Chance Andesite

The unit is dated at about 25 m.y., and lies above the Fanney Rhyolite and below the Deadwood Gulch

Rhyolite Tuff. Both the Last Chance and Mineral Creek Andesites have been placed within Elston's basaltic suite (Elston et al., 1976). The Last Chance is about 95 m thick in the study area and borders the Fanney Rhyolite to the west. It may be less basic than the Mineral Creek Andesite. The name is derived from the Last Chance mine, where it forms the hanging wall of the vein.

The Last Chance Andesite consists of dark-red to purple andesite with phenocrysts of altered pyroxenes (to chlorite) and biotite. Flows are mostly thin, alternating with pyroclastics. Breccias and agglomerates present indicate explosive action accompanying the eruptions. The groundmass is composed primarily of andesine, but contains minor amounts of altered pyroxenes (augite?) and biotite.

This unit alters readily and served as a host rock for ore mineralization along fault contacts with the Fanney Rhyolite, as it fractured to permit entry of hydrothermal solutions. Fault scarps northeast of the mine adit show conspicuous quartz veining, and the contact with the Fanney is irregular and shows inter tonguing.

Deadwood Gulch Rhyolite Tuff

This distinctively white unit outcrops strikingly on the ridge north of the working, where it is in contact with the Fanney Rhyolite along the Queen fault. It consists of small fragments of white flow-banded rhyolite in a siliceous groundmass. Sandstone occurs as beds and lenses throughout the unit. It is relatively soft and may show weathering pockets.

Mogollon Andesite

This is the youngest unit in the study area, outcropping in the northeast corner near the Deadwood mine. It consists of dark-colored andesite with a nonoriented plagioclase groundmass and some dacite flows. The most numerous phenocryst is plagioclase of approximate composition Ab_5An_7.

History and production

The Dripping Gold lode claim was formerly known as the Iron Bar. In 1909, the Iron Bar group was being worked by Peterson, Lambert & Company, with principal development along the southern part of the Queen vein. A tunnel 52 m long connected with a shaft 21 m deep. Ore from the shaft was valued from $25.00 to as high as $71.60 per ton (1909 prices). Silver to gold ratio was estimated at 2:1. Some ore was also found on the adjacent Iron Cross, Iron Ring, and Iron Crown claims. The property was assessed as one of good potential, but requiring both a road and a mill site (Rackocy, 1981). However, a road was never built to the Iron Bar. The ore was pulverized with a small crusher, sluiced, and the concentrates recovered by the cyanide process. All drilling was done with hand steels. The main adit has rails, and a small ore cart was emptied into a hopper which fed the crusher. Miners lived in a cave above the workings, which is a natural pocket in the Fanney Rhyolite. There was also a telephone line to the site.

The mine entrance at Pine Flat has either caved or has been blasted shut, and there is no record of production for that mine. As the best ore at the Iron Bar was being depleted, the miners may have been induced by presence of primary sulfides in the Cooney Quartz Latite to tunnel in, hoping for a bonanza which did not exist.

The main adit (Fig. 2) is 87 m long and bears N 1° W along the Queen vein at the junction of the Last Chance hanging wall and the Fanney footwall. A vertical shaft of at least 21 m in depth appears to connect with a lower adit.

At a bearing from the main adit of N 19° W for 54 m is a drift which bears N 15° E for 18.5 m. A lower adit about 70 m south of the main tunnel strikes N 40° E. Length is not known because this working is caved shut as well as flooded.

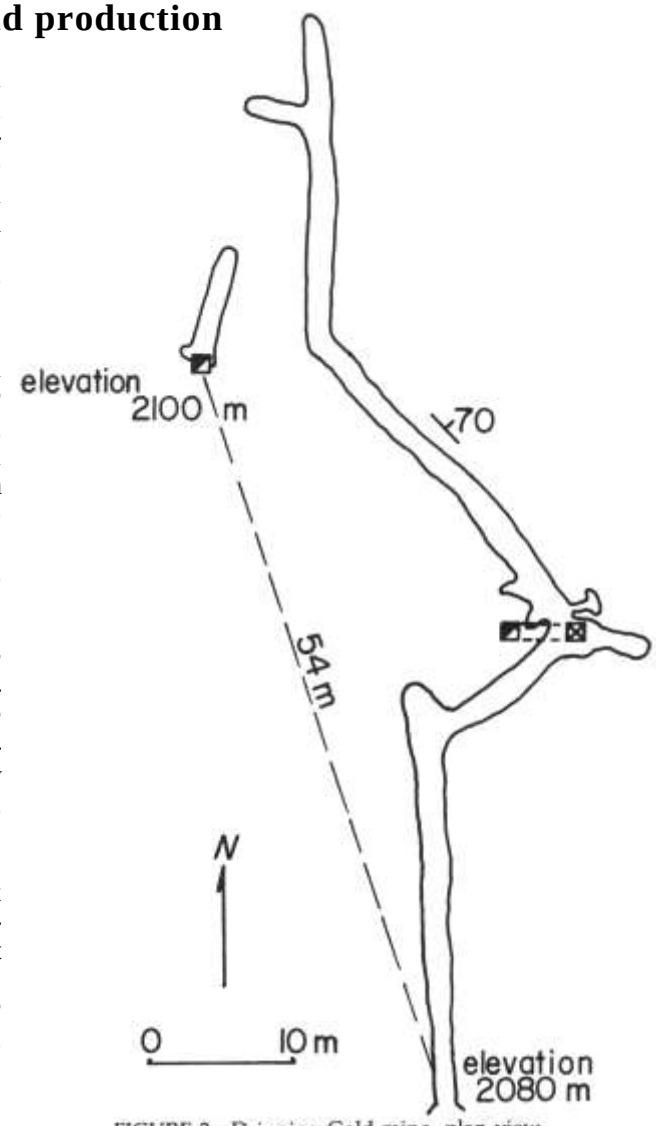

FIGURE 2—Dripping Gold mine, plan view.

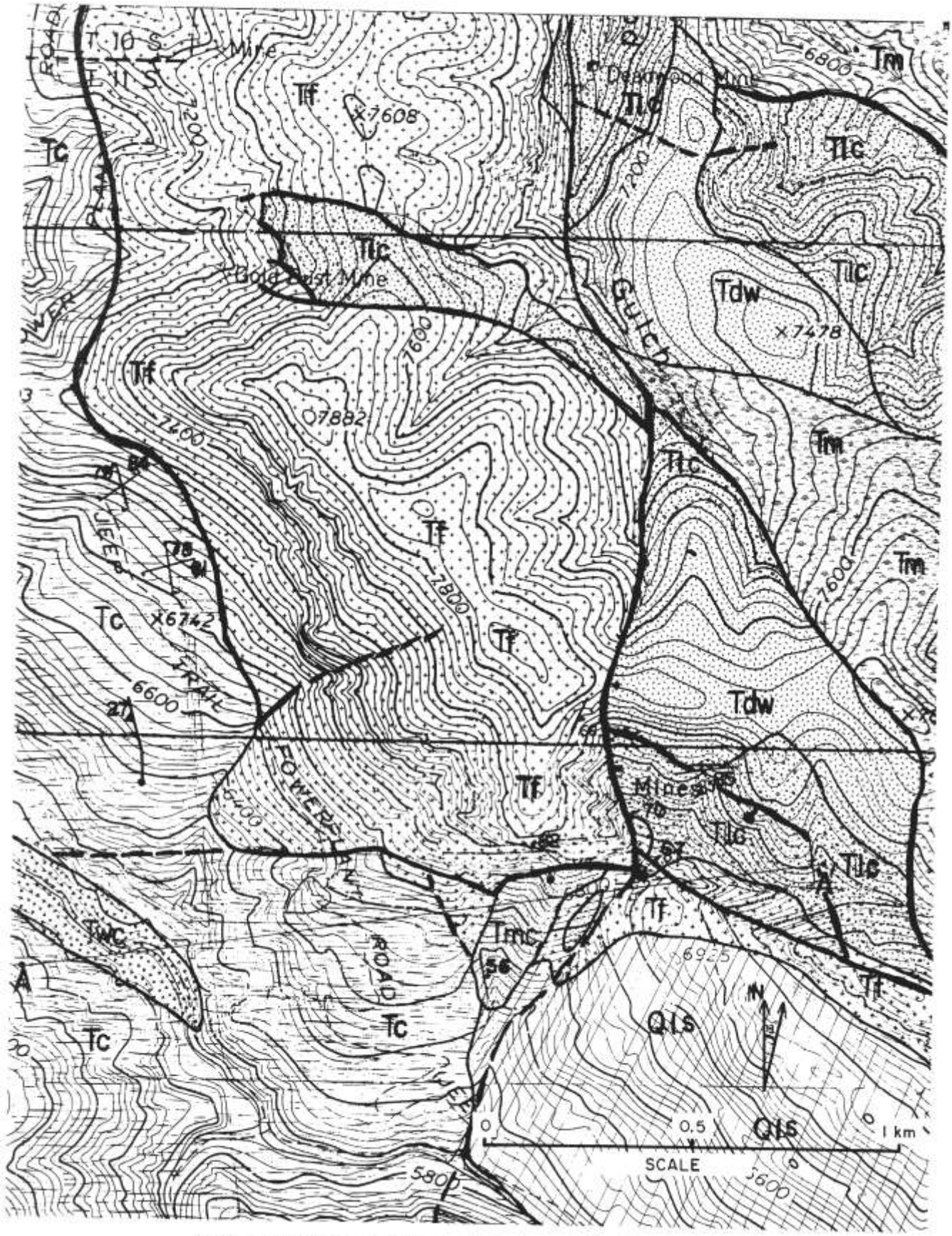

FIGURE 3—Geologic map of Dripping Gold mine area (after Ferguson, 1927).

Origin and structure

The structure of the Mogollon area was described by Coney (1976), who recognized three periods of deformation of the Mogollon Plateau. The earliest period coincides with the deposition of the Apache Spring and Fanney Formations.

The second period of deformation occurred penecontemporaneously with emplacement of the Mogollon—Dog Gulch Formation, before ore mineralization and before the eruption of the Bearwallow Mountain Formation. This period resulted in a downfaulted graben which includes the Mogollon mining district.

The third period of deformation occurred during and after emplacement of the Bearwallow Mountain Formation and Gila Conglomerate. This period resulted in the present western fault scarp along the Mogollon Range, which averages about 60°. The resultant horst was tilted eastward during this time.

The Mogollon district has the general form of an anticlinal structure, as evidenced by doming above a possible intrusive in the ring-fracture zone of the Bursum cauldron (Ratté et al., 1979). This doming along with localization of ore bodies at fault intersections (a cupola?) may suggest further evidence for the inferred Bursum pluton proposed by Elston (1976).

Ferguson (1927) recognized two periods of faulting in the Mogollon district, the latter producing the present-day fault scarp. The first period was later than the local andesites, perhaps late Miocene. These faults are the sites of quartz veins, which carry the sulfide mineralization. The gold and silver veins at Mogollon are younger than the Deadwood Gulch Rhyolite Tuff, but older than the Bearwallow Mountain Basaltic Andesite, probably around 21 m.y. (Elston, Rhodes, and Erb, 1976).

The Queen vein can be traced for nearly 11 km (6.8 mi) in a north—south direction and is the site of the first-formed and most extensive fissuring. The fault plane dips to the east, possibly suggesting a graben structure. Veins west of the Queen are characterized by a predominantly quartz gangue and have been the most productive. Very little ore has come from east of the Queen, where the gangue is primarily calcite, much of it manganiferous. Banding and sheeting of minerals parallel to the wall rock is common (Ferguson, 1927). The Dripping Gold workings are on a southern extension of the Queen vein. This extension may intersect with northwest-trending structures at Holt Gulch and Wilcox Peak (Ratté et al., 1979).

The ring-fracture zone of the Bursum cauldron may have created prominent channelways for hydrothermal solutions as well as sites for future fault activity. The resurgence of the cauldron resulted in tensional fractures, and veins in the Mogollon district follow the planes of subsequent normal faults. The lack of

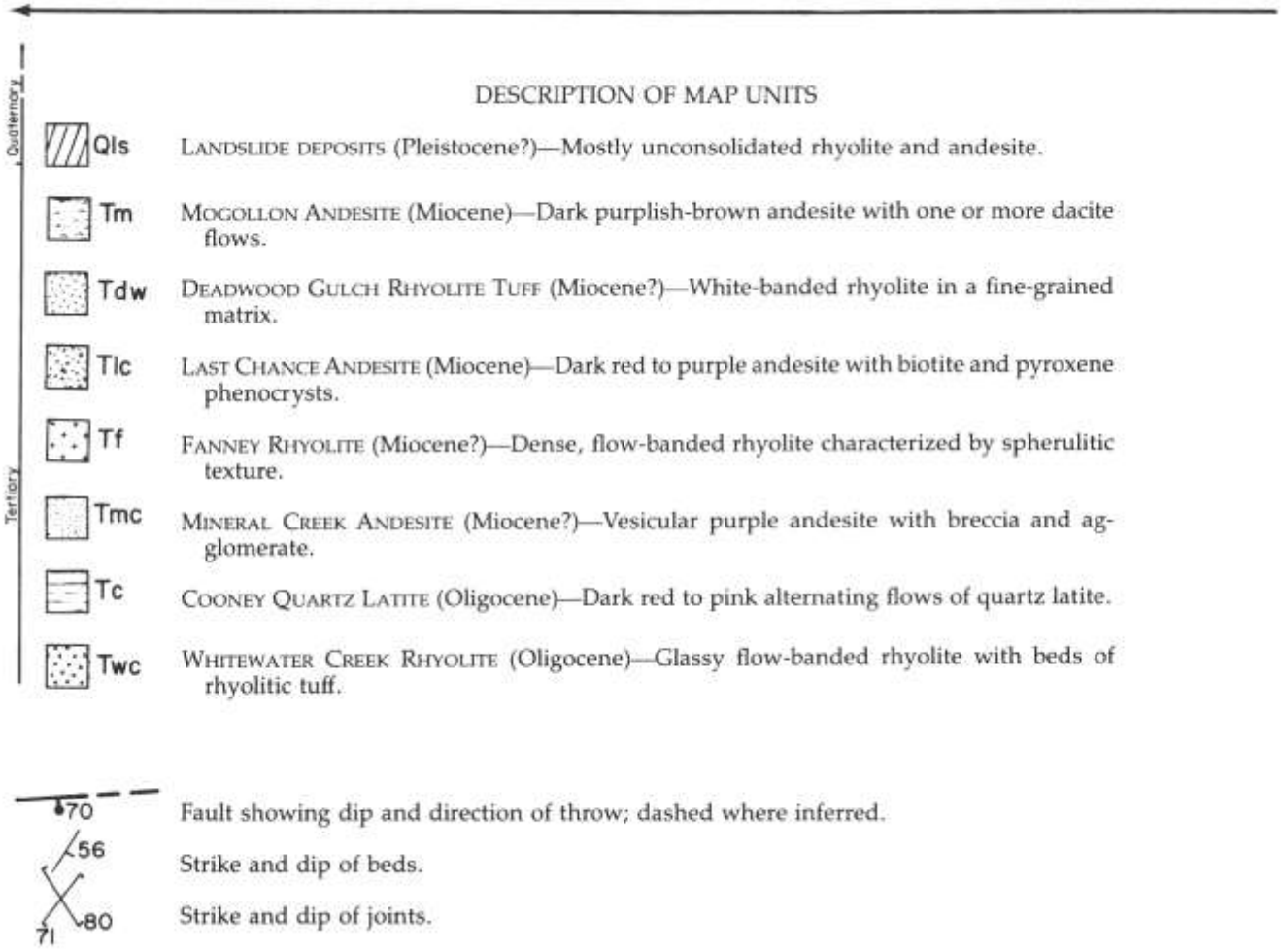

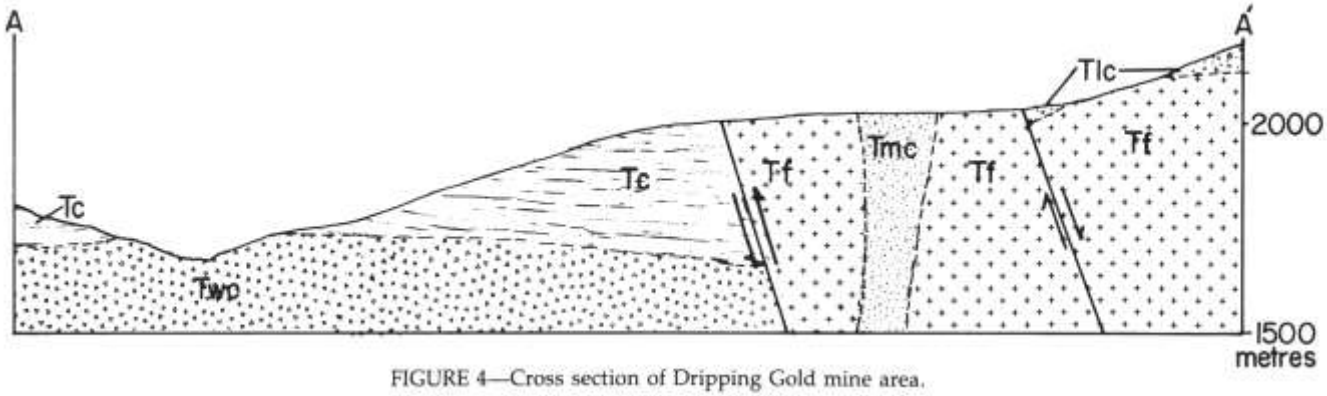

FIGURE 4—Cross section of Dripping Gold mine area.

timbering old workings may indicate tension relieved by faulting. Only basic shaft framing is present at the Dripping Gold.

Ore bodies within the district often occurred near points of intersection of the Queen with traverse veins, an example of which is the famed Last Chance—Confidence vein. These veins follow a series of east—west faults which are later than the Queen (Ferguson, 1927). Structural intersections are of basic importance in localizing ore deposits, and many mining districts occur at such "crossroads" (Ratté et al., 1979).

The Queen vein strikes N 1° W at the entrance to the Dripping Gold mine and may be traced directly along the fault contact between the Fanney Rhyolite and Last Chance Andesite northward to the Deadwood mine, where it intersects the Last Chance—Confidence vein. A prominent traverse fault at the Dripping Gold shaft (Fig. 4) created fissuring which enabled ore-bearing solution to localize at this intersection.

Earliest faulting produced a horst of Fanney Rhyolite, with downthrown blocks of Cooney Quartz Latite to the west and Last Chance Andesite to the east. Subsequent faulting produced the ridge of Deadwood Gulch Rhyolite Tuff to the north. Part of the Last Chance Andesite was also uplifted, but a block of the andesite downthrown to the southwest sheared along and thrust over the resistant rhyolite. This created a large fissure with a lateral component and thus a site for hydrothermal deposition. Along the Queen, the hanging wall of the andesite dips about 70° to the east, with the prominent rhyolite horst tilted toward the west.

The complex faulting at the Dripping Gold is at least in part post-mineral (Ferguson, 1927). Red hematitic gouge encloses crushed fragments of vein material. Considerable shearing has taken place along the strike of the Queen, evidenced by oriented argillic alteration, preferred orientation of wall-rock fragments, and slickenside striations.

Hydrothermal solutions rose through tensional post-cauldron fractures along the massive, relatively homogeneous flow dome of the Fanney Rhyolite, which proved too impermeable to localize the ore. The andesine groundmass of the Last Chance readily fractured, producing channelways for mineralization. Ferromagnesian minerals were altered to chlorite, with the groundmass undergoing intense alteration and brecciation. At this point the ore minerals, primarily native gold and argentite, were deposited in veins with silica that may have come from the adjacent rhyolite. This silicification appears to have cooled relatively slowly, producing a granular, sugary texture locally intergrown with masses of kaolin(?). Hematite and pyrolusite later followed fracture planes.

The main adit is the site of a prolific spring, and a similar situation exists at the lower adit, which is completely inaccessible due to caving. The intense shearing and brecciation at the site have allowed ground water to percolate into much of the mine workings.

Due to the rugged topography, little ground water exists in most of the Mogollon district. The Queen vein has acted as a ground-water dam, and very few of the workings near Mogollon have encountered any subsurface springs. A notable exception is the Deadwood mine north of the Dripping Gold adit along the strike of the Queen (Ferguson, 1927). This may suggest a structural intersection between the two areas.

Hydrothermal alteration

Rock alteration is present over the entire Mogollon district; the degree of alteration is dependent on the type of rock. Alteration of dense rhyolites is limited to silicification near the veins accompanied by sericitization of the feldspars and chloritization of the biotite.

The andesites have undergone extensive alteration due to a higher percentage of easily altered minerals and higher porosity. Ferromagnesian minerals have been altered to iron oxides and chlorite, often leaving crystal cavities. The iron oxides are at least in part derived from pyrite. Plagioclase phenocrysts may be replaced by calcite, quartz, kaolin, or sericite. The groundmass has altered readily, mostly to chlorite and calcite. This widespread alteration is attributed to hydrothermal action rather than weathering (Ferguson, 1927).

Hydrothermal alteration at the Dripping Gold mine is readily seen and shows zonation. The Last Chance Andesite of the hanging wall has been most affected,

while the Fanney Rhyolite has undergone silicification and possibly sericitization near the veins.

In the outermost zone, alteration has been propylitic. Ferromagnesian minerals and biotite have become aggregates of chlorite and in some cases iron oxide. The groundmass has been altered to chlorite or pulverized to a hematitic gouge. Primary pyrite has been replaced by hematite that locally shows cubic crystal outline.

In the middle zone (of varying thickness), argillic alteration is present, primarily in the form of kaolinite(?). This zone exhibits striations due to shearing movement and grades into an inner zone of intense silicification along the contact with the rhyolite. In some places crustification may be present. This silicified zone is associated with the deposition of precious-metal sulfides. Early formed fractures, probably mostly tensional, appear to control the alteration.

Wall-rock alteration at the mine may be categorized as advanced argillic. In this type of alteration, silicic alteration near the veins grades outward to argillization and propylitization. Such alteration is common in epithermal precious-metal deposits; Goldfield, Nevada, is a type locality (Meyer and Hemley, 1967).

Paragenesis and mineralization

The most common gangue mineral is quartz, which has been deposited in three stages. The earliest, often within hematitic gouge, is a white, chalcedony-like, "porcelain" variety containing few sulfides. Thin banding may be present. Primary pyrite, locally showing crystal outlines, has been replaced by hematite, often giving this quartz a pink coloration or spotted appearance.

The second-stage quartz has a coarsely crystalline, drusy to granular appearance and locally contains cavities resulting from the solution of calcite. This type is associated with sulfide deposition and comprises the bulk of the ore produced from the Dripping Gold. It is locally banded and may show a granitic texture.

The latest quartz may be intergrown with calcite; it has a hackly lamellar appearance where it has replaced the calcite. This type is only sparingly present at the Dripping Gold, but is abundant on the dumps at Pine Flat.

Calcite is less common in the gangue, and the early manganiferous variety found in other parts of the district is completely absent. It fills some of the later-formed veins, particularly in the andesite. Secondary calcite is found coating underground workings where flooding is encountered; it is deposited from solution in a semibotryoidal form or as stalactites up to 10 cm long. Calcite is quite common in the Cooney Quartz Latite in the dumps at Pine Flat, where it is a primary gangue mineral. It is white and often shows good cleavage.

No fluorite has been observed in the study area. The Gold Dust mine to the northwest has some light-green fluorite that occurs as small bands between layers of granular quartz.

In the Mogollon district, fragments of wall rock often served as nuclei for sulfide deposition. The Last Chance Andesite was enclosed in many places by a hematitic gouge, with the sulfide-bearing granular quartz having been deposited in channelways. This intermediate granular silica is contemporaneous with ore mineralization. Ore minerals include native gold, argentite, and possibly stromeyerite. Historically, argentite in the district has been found in some places to border or replace older sulfides.

Secondary ore mineralization is localized, but can be readily seen at the dump near the upper workings. Here malachite and perhaps other minerals were deposited as thin crusts and small veins. This type of occurrence in other parts of the district is sometimes associated with native silver (Ferguson, 1927).

Hematite is formed over a considerable period of time, but fairly recent material is found as slickensides on many fault planes. All hematite present is of the red-earth variety. Pyrolusite is the last metallic mineral to form; it is black with an earthy texture. It occurs as a coating or filling of thin veins, and locally has a dendritic appearance.

Conclusion

It is the opinion of the author that possibilities for undiscovered ore, possibly at depth, may exist within the study area. Although gold values have not been high, two samples, both taken from dump material, assayed 14.38 and 9.14 oz Ag per ton. All mining has been by hand methods, as there has never been road access to the site. These factors certainly could have limited development at the mine workings. The possibility also exists of a structural intersection between the Dripping Gold mine, the Gold Dust mine to the northwest, and the Deadwood mine to the north.

Considerable portions of the mine workings are presently inaccessible or unsafe due to flooding, caving, or rotted timbering. Future plans include correcting these conditions, with special emphasis on gaining access to lower workings of the main shaft, as well as complete surface and underground mapping. A thorough sampling program will then be implemented.

Long-term plans may include a crusher, rebuilding of the rail system and hopper, and reconstruction of existing sluiceworks, with emphasis on producing concentrate for further refining.

References

Bikerman, M., 1972, New K—Ar ages on volcanic rocks from Catron and Grant Counties, New Mexico: Isochron/West, no. 3, pp. 912.

Coney, P. J., 1976, Structure, volcanic stratigraphy, and gravity anomaly across the Mogollon Plateau; in Elston, W. E., and Northrop, S. A. (eds.), Cenozoic volcanism in southwestern New Mexico: New Mexico Geological Society, Special Publication no. 5, pp. 29-41.

Elston, W. E., 1976, Glossary of stratigraphic terms of the Mogollon—Datil volcanic province; in Elston, W. E., and Northrop, S. A. (eds.), Cenozoic volcanism in southwestern New Mexico: New Mexico Geological Society, Special Publication no. 5, pp. 131144.

Elston, W. E., Coney, P. J., Rhodes, R. C., and Deal, E. G., 1976, Progress report on the Mogollon Plateau volcanic field, southwestern New Mexico; *in* Elston, W. E., and Northrop, S. A. (eds.), Cenozoic volcanism in southwestern New Mexico: New Mexico Geological Society, Special Publication no. 5, pp. 3-28.

Elston, W. E., Rhodes, R. C., and Erb, E. E., 1976, Control of mineralization by mid-Tertiary volcanic centers; *in* Elston, W. E., and Northrop, S. A. (eds.), Cenozoic volcanism in southwestern New Mexico: New Mexico Geological Society, Special Publication no. 5, pp. 125-130.

Ferguson, H. G., 1927, Geology and ore deposits of the Mogollon mining district, New Mexico: U.S. Geological Survey, Bulletin 787, pp. 3-87.

Meyer, C., and Hemley, J. J., 1967, Wall rock alteration; *in* Barnes, H. L. (ed.), Geochemistry of hydrothermal ore deposits: Holt, Rhinehart, and Winston, New York, pp. 166-232.

Rackocy, B., 1981, Mogollon mines (1909): Bravo Press, El Paso, 40 pp.

Raft& J. C., and Gaskill, D. L., 1975, Reconnaissance geologic map of the Gila Wilderness study area, southwestern New Mexico: U.S. Geological Survey, Miscellaneous Investigations Series Map 1-886.

Ratté, J. C., Gaskill, D. L., Eaton, G. P., Peterson, D. L., Stotelmeyer, R. B., and Meeves, H. C., 1979, Mineral resources of the Gila Primitive Area and Gila Wilderness, New Mexico: U.S. Geological Survey, Bulletin 1451, pp. 41, 106.

Abundance of silver in mid-Cenozoic volcanic rocks of the Mogollon—Datil volcanic field, southwestern New Mexico

by Theodore J. Bornhorst and Steven P. Wolfe

Department of Geology and Geological Engineering, Michigan Technological University, Houghton, Michigan 49931

Abstract

The abundance of Ag in 33 selected samples of mid-Cenozoic calc-alkalic volcanic rocks from the Mogollon—Datil volcanic field ranges from 13 to 174 ppb. The abundance and variability are comparable to unaltered rocks in other parts of the world. One propylitized sample of mid-Cenozoic rhyolite from the Mogollon mining district had a very low Ag abundance of 10 ppb. We suggest that the volcanic rocks are a logical source for Ag in veins of the district.

Introduction

The Mogollon—Datil volcanic field, southwestern New Mexico, contains over 50,000 km^3 of mid-Cenozoic volcanic rocks (Elston and Bornhorst, 1979; Bornhorst, 1980). These rocks range in composition from basalt to high-silica rhyolite and are broadly calc-alkalic in character. The mid-Cenozoic volcanic rocks host a wide variety of mineral deposits (Elston, 1978). Precious-metal mineralization occurs in a number of localities, particularly the Mogollon mining district on the west-central side of the Mogollon—Datil volcanic field.

The abundance and distribution of a wide variety of elements are known for least altered volcanic rocks from the Mogollon—Datil volcanic field (Bornhorst, 1980). Notable exceptions are the precious metals. Here we briefly report on the abundance of Ag in a selected suite of least altered volcanic rocks.

Acknowledgments

We thank Jim Paces, Michigan Technological University, for his comments on drafts of this manuscript. Anaconda Minerals Company provided support for development of the Ag analytical technique. Samples used in this study were collected by the senior author for a different study which was supported by NSF grant EAR-77-24501, and grants 76-350, 77-3104, and 78-2123 from the New Mexico Energy and Minerals Department and its predecessor organizations (W. E. Elston, P. I., University of New Mexico). Reviewed by W. I. Rose and S. D. McDowell, Michigan Technological University, and T. Eggleston, New Mexico Institute of Mining and Technology.

Analytical results

Thirty-three samples of mid-Cenozoic volcanic rocks were analyzed for Ag (Table 1) by flame atomic-absorption spectrometry utilizing a solid sampling, iron screw-rod technique modified after Govindaraju, Morel, and Hinel (1977). The technique involves coating a wetted iron screw-rod with a known amount of rock powder which is volatilized in an air-acetylene flame using a specially designed burner head. The errors and detection limit are minimized by integrating the peak rather than simply considering the peak height. All samples and standards were analyzed, at least in duplicate. Calibration for Ag is made against USGS and French geochemical reference samples. The accuracy of our Ag analyses is roughly ± 15% of the amount determined and precision is about ± 10% of the amount determined for values less than 350 ppb. The detection limit for Ag is about 8 ppb.

TABLE 1—Ag content of 33 selected mid-Cenozoic volcanic rocks from the Mogollon–Datil volcanic field. Sample numbers correspond to Bornhorst (1980); Ag from this study; other data from Bornhorst (1980), including alteration index described in the text.

Sample number	ppb Ag	wt.% SiO_2	Petrographic alteration index
325	33.	52	no data
247	63.	53	no data
594	58.	54	none
500	30.	56	none
572	30.	57	none
564	13.	57	none
533	47.	58	no data
283	71.	59	none
460	20.	62	none
282	27.	63	none

Discussion

TABLE 1—continued

Sample number	ppb Ag	wt.% SiO_2	Petrographic alteration index
41	33.	63	none
184	95.	64	none
399	40.	66	slight
398	100.	67	slight
137	47.	68	none
194	33.	69	none
155	68.	70	slight
200	123.	70	none
581	68.	70	none
402	68.	71	none
417	23.	72	slight
78	143.	72	none
419	30.	73	none
174	40.	74	none
353	137.	75	none
401	47.	75	none
444	91.	75	none
508	78.	75	none
400	174.	76	none
205	27.	76	none
445	20.	77	slight
504	85.	78	slight
379	54.	78	none

The samples that were analyzed for this study are the same as those referred to in Bornhorst (1980). For every sample major-element data are available and, for most, also a wide variety of trace elements. The Ag contents of 33 samples were determined for this study (Table 1). Boyle (1968, 1979), in a worldwide compilation, reports arithmetic mean silver content in intermediate and silicic igneous rocks to be 60 and 50 ppb, respectively. Boyle's compilation includes intrusive and extrusive rocks and data from a wide variety of localities, ages of rocks, and analytical techniques. Over 80% of the Ag contents reported for 157 fresh Quaternary calc-alkalic volcanic rocks from Central America, Indonesia, and Mt. St. Helens by Bornhorst, Rose, and Wolfe (1984) fall between 20 and 150 ppb, and most commonly between 40 to 90 ppb (same analytical technique as this study). Based on the literature, Ag assumes a log-normal distribution in igneous rocks. It seems reasonable to conclude that mid-Cenozoic calc-alkalic volcanic rocks of the Mogollon—Datil field have Ag contents that are similar to rocks elsewhere in the world.

Most rocks analyzed in this study exhibited crystalline textures; however, the data include some glassy samples. A number of samples showed signs of alteration in thin section. The samples analyzed have been subdivided by means of petrographic criteria (Table 1). The alteration index is given only if the senior author has viewed the sample in thin section, except if the sample collector specifically stated that a sample is of altered character. "None" is equivalent to fresh-looking feldspar, with possible biotite oxidation and iddingsite development. "Slight" is equivalent to slight feldspar alteration, usually sericite along cracks, and strong biotite oxidation. "Some" is equivalent to an altered rock with pervasive feldspar alteration and commonly secondary calcite, sericite, chlorite, and other alteration minerals; no Ag data are reported in Table 1 for samples with this degree of alteration. The Ag contents reported are believed to generally represent unaltered magmatic values. Simple inspection suggests that there might be a crude correlation of Ag with rock type. Those rocks with 63 or less wt. % SiO_2 (basalt and andesite) tend to have lower Ag than those with greater than 63 wt. % SiO_2 (dacite and rhyolite) (Fig. 1). The log-normalized mean Ag content is 35 ppb (N = 11) for the former group and 61 ppb (N = 22) for the latter group. Bornhorst, Rose, and Wolfe (1984) concluded that Ag abundance is highest in more silicic volcanic rocks with log-normalized means of 74 ppb Ag for basalt (less than 52 wt. % SiO_2), and 85 ppb for rhyolite (greater than 70 wt. % SiO_2). The limited data of this study support the idea that Ag abundance is, in general, greater in more silicic-rock types. The magnitude of Ag variability in volcanic rocks from Mogollon—Datil volcanic field is also comparable to variability observed elsewhere in the world. In a broad sense, the larger sample numbers correspond to younger rocks and within the silicic-rock group there is no apparent correlation of Ag content with time.

Here we report Ag abundance on a small number of volcanic rocks from the Mogollon—Datil volcanic field. Much more data will be necessary to understand Ag variability in these rocks. Additional data may allow identification of units with particularly high magmatic Ag abundance or correlation of Ag with alteration so that source beds might be identified. For example, is the Cooney Tuff a possible source bed for Ag in the Mogollon mining district of southwestern New Mexico? The thick (more than 500 m) caldera-filling Cooney Tuff, interbedded ash-flow tuffs and volcaniclastic sandstones, is projected to exist beneath

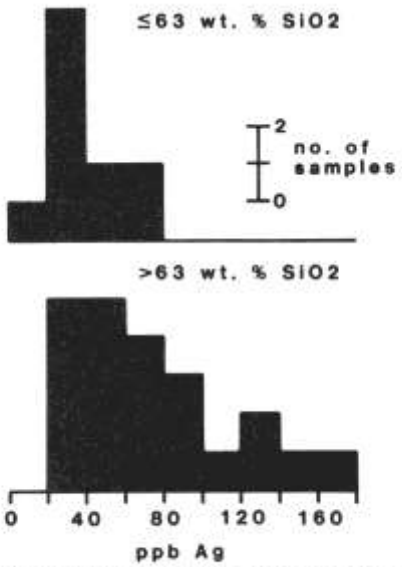

FIGURE 1—Histograms of Ag in two groups of mid-Cenozoic volcanic rocks from the Mogollon–Datil volcanic field.

the Mogollon mining district (Ratte, 1981). The base of the Cooney Tuff is today at a depth of 1,000 m or more (Ratte, 1981), and during mineralization was probably greater than 1,500 m (Bornhorst et al., 1984). The Cooney Tuff is pervasively propylitically altered in exposures on the flanks of the district. Thus, thickness, structural position, availability of permeable horizons, pervasive propylitic alteration, and analogy with modern geothermal systems (see Ellis, 1979) suggest that the Cooney Tuff could have been a hydro-thermal aquifer (Kent, 1983). We analyzed one strongly altered sample of Cooney Tuff from our collection of "fresh" samples (sample no. 156 of Bornhorst, 1980) and found that it contained 10 ppb Ag. Even with volume corrections, Ag was likely leached from this sample. Rough calculations suggest that tens of millions of oz Ag were probably present in the Cooney Tuff when it was emplaced (volume beneath the Mogollon mining district). The district production was about 13 million oz Ag (Ferguson, 1927). On the basis of one data point we speculate that the Cooney Tuff might have been the source bed for at least some of the Ag won from the veins. Clearly, additional studies are needed.

References

Bornhorst, T. J., 1980, Major and trace element geochemistry and mineralogy of upper Eocene to Quaternary volcanic rocks of the Mogollon—Datil volcanic field, southwestern New Mexico: Ph.D. dissertation, University of New Mexico, Albuquerque, New Mexico, 1108 pp.

Bornhorst, T. J., Rose, W. I., Jr., and Wolfe, S. P., 1984, Abundance of gold and silver in fresh calc-alkalic Quaternary volcanic rocks: Geological Society of America, Abstracts with Programs, v. 16, p. 450.

Bornhorst, T. J., Kent, G. R., Mann, K. L., and Richey, S. R., 1984, Temperature of mineralization in Mogollon mining district, southwestern New Mexico: New Mexico Geology, v. 6, pp. 5355.

Boyle, R. W., 1968, The geochemistry of silver and its deposits: Geological Survey of Canada, Bulletin 160, 264 pp.

Boyle, R. W., 1979, The geochemistry of gold and its deposits: Geological Survey of Canada, Bulletin 280, 584 pp.

Ellis, A. J., 1979, Explored geothermal systems; *in* Barnes, H. L. (ed.), Geochemistry of hydrothermal ore deposits: John Wiley & Sons, New York, pp. 632-683.

Elston, W. E., 1978, Mid-Tertiary cauldrons and their relationship to mineral resources: a brief review: New Mexico Geological Society, Special Publication 7, pp. 107-113.

Elston, W. E., and Bomhorst, **T. J., 1979, The Rio Grande rift** in context of regional post-40 m.y. volcanic and tectonic events; *in* Riecker, R. E. (ed.), Rio Grande rift: tectonics and magmatism: American Geophysical Union, pp. 416-438.

Ferguson, H. G., 1927, Geology and ore deposits of the Mogollon mining district, New Mexico: U.S. Geological Survey, Bulletin 787, 100 pp.

Govindaraju, K., Morel, J., and Hinel, N. L., 1977, Solid sampling atomic absorption determination of silver in silicate rock reference samples. Application to a homogeneity study of silver in a one-ton two mica granite reference sample: Geostandards Newsletter, v. 1, pp. 137-142.

Kent, G. R., 1983, Temperature and age of precious metal vein mineralization and geochemistry of host rock alteration at the Eberle mine, Mogollon mining district, southwestern New Mexico: M.S. Thesis, Michigan Technological University, Houghton, **84 pp.**

Ratte, J. C., 1981, Geologic map of the Mogollon quadrangle, Catron County, New Mexico: U.S. Geological Survey, Geologic Quadrangle Map GC-1557, 1:24,000.

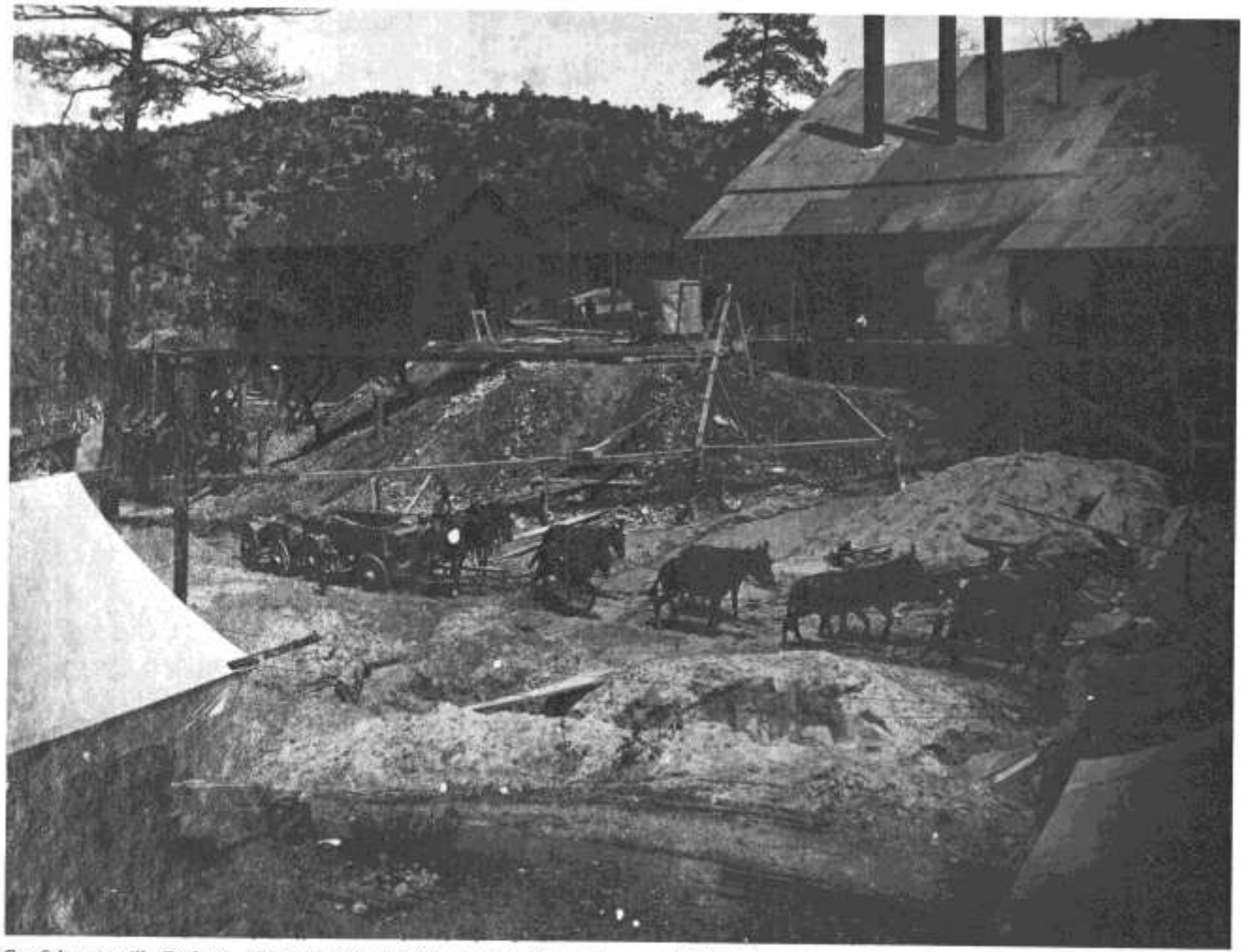

Confidence mill, Graham, New Mexico, ca 1895. Graham (sometimes called Whitewater) was located on Whitewater Creek some four miles from Helen Mining Company's Confidence mine. John T. Graham of Denver was the secretary/treasurer for the company and superintendent of the property. No less an illuminary than David Moffat, one-time governor of Colorado, was the president. Thus the mill was named after the mine and the town after the superintendent. Originally built as a 20-stamp mill in 1893, capacity was increased to 30 stamps in late 1895, handling about 80 tons per day. A three-mile pipeline was laid up Whitewater Creek to a large storage reservoir for water-power generation. The scaffolding and trestlework for the line was the forerunner of today's famed "catwalk." The Confidence mine and mill produced about $1,000,000 in silver and gold, but were idled suddenly in 1902 by Graham's accidental death.
Photo courtesy of Silver City Museum, Harlan Collection.

Geology and geochemistry of rhyolite-hosted tin deposits, northern Black Range and Sierra Cuchillo, southwestern New Mexico

by Ted L. Eggleston and David I. Norman

Geoscience Department, New Mexico Institute of Mining and Technology, Socorro, New Mexico 87801

Abstract

Tertiary (28 my) rhyolite lavas host a number of tin occurrences in southwestern New Mexico. These lavas are typically crystal-rich, white, flow-banded, high SiO_2, K_20, F, Cl, and low CaO, Fe_2O_3 Sr, Ba "topaz" rhyolites. Vapor-phase recrystallization, due to magmatic fluids exolved during ascent and cooling of the lavas, bleached and recrystallized the groundmass glass to a fine mosaic of quartz and feldspar. Tin was partitioned into this fluid from the melt and was deposited from it near the carapace of the rhyolite domes in response to the extreme thermal gradients there. Temperatures for tin mineralization range from >600 to <400°C, with salinities exceeding 50 eq. wt. % NaCI. Lower temperatures (400-130°C) and lower salinities (2-5 eq. wt. % NaCl) suggest that meteoric water was important late in the cooling of the dome.

Introduction

Placer tin was first discovered in the northern Black Range of southwestern New Mexico in 1908 (Harrington, 1943), and in 1918 hematite—cassiterite veinlets were discovered in Tertiary rhyolite domes and flows (Hill, 1921). These discoveries led to a short-lived boom in the area. Sporadic exploration continues today. Fig. 1 shows the location of part of the lode-tin occurrences in the region. No production has been reported from these lodes. Placer deposits which sit on the top and flanks of the rhyolite domes that host the lodes have had modest production. In the Black Range, the region encompassing the tin occurrences is known as the Taylor Creek tin district. A similar but unnamed district is located in the Sierra Cuchillo, a low mountain range east of the Black Range. These deposits are similar to the larger and more extensive deposits found in Durango, Mexico (Lee Moreno, 1972; Pan, 1974; Huspeni et al., 1984) and are frequently referred to as "Mexican type" tin deposits.

The origin of these deposits and their relationship to the rocks that host them has long been a subject of speculation (Hill, 1921; Fries, 1940; Lufkin, 1972; Correa, 1981; Goerold, 1981). Little work has been directed at a district-wide understanding of the tin occurrences and their relationship to the rocks that host them. This paper presents preliminary results of such a study with the aim of understanding the origin and controls of the tin mineralization.

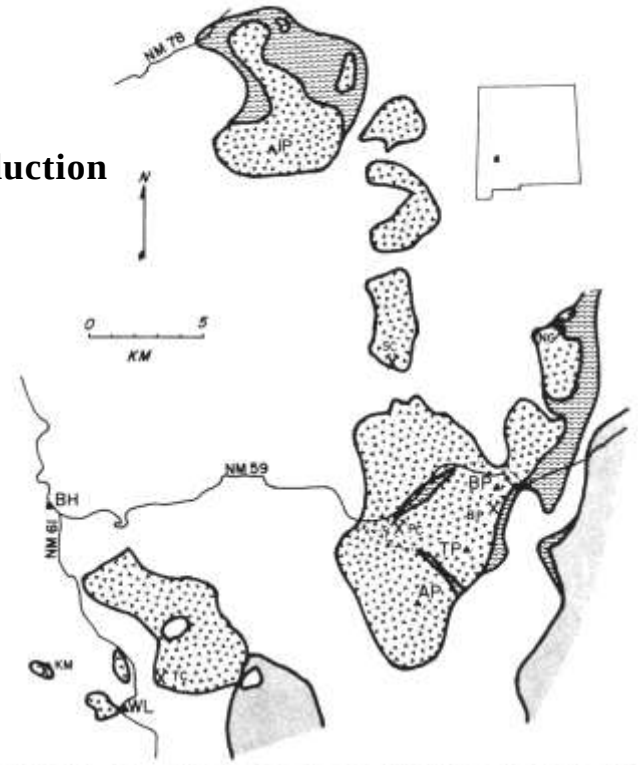

FIGURE 1—Generalized geologic map of the Taylor Creek tin district. Geologic-map patterns: *"v,"* Taylor Creek Rhyolite; *wave,* pyroclastic rocks associated with the Taylor Creek Rhyolite; *stiple,* older volcanic rocks; *white,* younger rocks. Locations of tin occurrences marked with pick and hammer; *SC,* Squaw Creek; *NG,* Nugget Gulch; *BP,* Boiler Peak; *PC,* Paramount Canyon; *TC,* Taylor Creek; *KM,* Kemp Mesa. Dotted lines near Paramount Canyon mark the boundaries between rhyolite effusive centers. Geographic reference points: *IP,* Indian Peaks; *BP,* Boiler Peak; *TP,* Taylor Peak; *AP,* Alexander Peak; *BH,* Beaverhead Ranger Station; *WL,* Wall Lake.

Geologic setting

The tin deposits in the Black Range and Sierra Cuchillo are located in the central part of the Mogollon—Datil volcanic field, a mid-Tertiary volcanic plateau consisting of mafic to felsic lavas, felsic pyroclastic rocks, and volcaniclastic sedimentary rocks (Chapin et al., 1978). The Taylor Creek district is on the Mogollon plateau west of the Winston graben, the westernmost structural feature in this area that is related to the Rio Grande rift. Dips in the region are 6-12° to the west. The Sierra Cuchillo is a strongly rotated structural block between the Winston graben and the Engle basin (Kelley, 1955; Chapin et al., 1978). Dips in this block are 10-30° to the east.

The tin occurrences in both districts are hosted by widely separated rhyolite eruptive centers, each of which may contain more than one rhyolite dome. In the Black Range, these tin-bearing rhyolites are collectively known as the Taylor Creek Rhyolite. In the Sierra Cuchillo, the host rhyolites are as yet unnamed. The stratigraphy in both areas is similar; for a detailed discussion of the Black Range stratigraphy see Eggleston and Norman (1982). The general stratigraphic sequence consists of (ascending) basaltic andesite, rhyolite tuffs and lavas, Taylor Creek Rhyolite, basaltic andesite, and volcaniclastic sedimentary rocks. The age of the Taylor Creek Rhyolite is poorly known, but the most recent radiometric dates place it at about 28 my, and stratigraphic information at between 29 and 28 my. It is possible, however, that significantly younger and older rhyolite domes are present in the region. The host-rock rhyolite in the Sierra Cuchillo has been dated by fission-track techniques at 27.8 my (Heyl, Maxwell, and Davis, 1983).

Though the uneroded tops and bottoms of the lavas are rarely seen, as much as 300 m of rhyolite is locally exposed. The rhyolites are white to reddish-brown, moderately crystal-rich to crystal-rich, flow-banded rocks with subequal quartz and sanidine as the dominant phenocryst phases. Plagioclase, biotite, and opaque oxides are present in trace amounts. The quartz and sanidine are subhedral to euhedral and range from 1 to 7 mm on the long axis. Many of the eruptive centers have characteristic phenocryst contents and sizes. Much of the sanidine in the rhyolites is irridescent "moonstone." Lithophysae are locally concentrated near the tops of many of the domes, immediately below the carapace.

Chemically, these rhyolites are typical "topaz" rhyolites in the sense of Burt et al. (1982). Table 1 compares a representative analysis of these rhyolites with those of A-type granites (White and Chappell, 1983) and average rhyolites (Cox, Bell, and Pankhurst, 1979). The table clearly shows the high SiO_2 and K_20 and low CaO and Fe_2O_3 nature of these rocks. The very high Rb/Sr ratios are quite distinctive. As much as 0.05% Cl and 0.6% F have been determined in these rocks along with moderate enrichments of Nb and Y and strong depletions of Ba and Sr when compared to the low Ca granites of Turekian and Wedepohl

TABLE 1—Representative analysis of the Taylor Creek Rhyolite and comparison with an average rhyolite (Cox et al., 1979) and with an A-type granitoid (White and Chappell, 1983).

	Rhyolite	A-type	Taylor Creek
SiO_2	72.82	73.6	77.35
TiO_2	0.28	0.33	0.1
Al_2O_3	13.27	12.69	12.44
Fe_2O_3T	2.65	2.75	1.16
MnO	0.06	0.06	0.05
MgO	0.39	0.33	0.01
CaO	1.14	1.09	0.19
Na_2O	3.55	3.34	3.70
K_2O	4.30	4.51	4.87
P_2O_5	0.07	0.09	0.02
$\delta^{18}O$	5–7	5–11	8
Rb/Sr	2/1	2/1	10/1–150/1

(1961). Chondrite-normalized rare-earth-element patterns (Fig. 2) are relatively flat, with deep Eu anomalies.

Carapace breccias form during growth of a dome by brecciation of a rapidly cooling rind on the margin of the dome. In the Taylor Creek district, these breccias are locally preserved and frequently mark the boundary between two juxtaposed domes. Much of the growth of the domes was endogenous, but a single pyroclastic block flow, possibly formed by spire collapse, suggests limited exogenous growth. Fine- to coarse-grained pyroclastic-flow and -fall deposits locally mantle the rhyolite domes. Bedding in these deposits generally conforms to the slope of the underlying rhyolite dome.

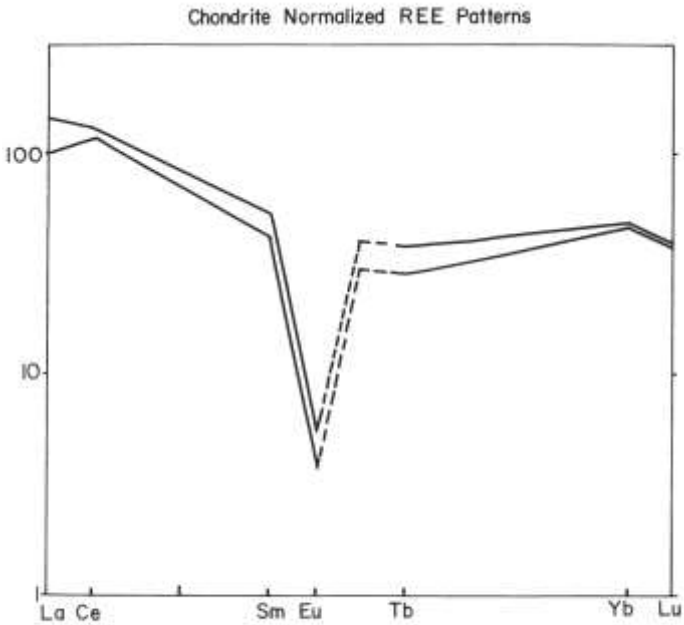

FIGURE 2—Chondrite-normalized rare-earth-element pattern for the Taylor Creek Rhyolite.

Vapor-phase recrystallization

Most of the Taylor Creek Rhyolite is white and quite porous. Locally, the rhyolites are punky and may resemble poorly welded pyroclastic rocks; however, the rare, very fresh rhyolite is generally red to brown, dense, and may exhibit spherulitic or granophyric devitrification textures. The white color and the porosity of the bulk of the rhyolite is due to bleaching and material removal during vapor-phase recrystallization (frequently known as vapor-phase alteration). The fluids responsible for the recrystallization are magmatic fluids evolved during ascent and cooling of the magma. The upward and outward migration of the fluid allows it to affect virtually all of the cooling rock body. Locally, intense zones of vapor-phase recrystallization have left behind a punky, friable rock resembling poorly welded pyroclastic material capped by mildly recrystallized rhyolite. The localization of these zones is believed to be due to channeling of fluids along flow banding or similar internal structures and entrapment by impermeable caprock. Since lithophysae are commonly found in the caprock, immediately below the carapace of the rhyolite domes, the caprock must have been fluid enough to expand due to gas pressure and must have cooled quickly to preserve the lithophysae. The zones of intense vapor-phase recrystallization may have formed at the same time as the lithophysae, and, therefore, the still-fluid outer rim of the dome may have trapped the ascending fluid. Fluid-inclusion and isotopic data from the lithophysae support this conclusion. Fluid-inclusion homogenization temperatures from quartz and topaz in lithophysae are >680°C. These temperatures are near the solidus temperature for rhyolites with about 1% F (Manning and Pichavant, 1983). The $8^{18}O$ of druse quartz in the lithophysae is about 7.5 per mil, identical to that of phenocrystic quartz in preserved vitric rhyolite. These data indicate that the fluids responsible for the lithophysae and possibly for the vapor-phase recrystallization are indeed magmatic fluids.

When the fluid is exolved from the melt, incompatible elements such as Be, Li, B, F, Cl, Sn, and W will be partitioned into the fluid and move with it. Evidence for this partitioning and migration is the presence of topaz and red beryl in lithophysae near the carapace of some of the rhyolite domes.

Tin occurrences

Two types of tin deposits are found in southwestern New Mexico. Placer deposits have been the most productive and consist of unconsolidated, arroyo-filling alluvial deposits with variable amounts of wood-tin and cassiterite admixed. These tin deposits are spatially related to the tin-bearing rhyolite domes and are the result of the erosion of those domes. Wood-tin, the botryoidal, cryptocrystalline form of SnO_2, is the dominant tin mineral in the placers. Coarsely crystalline cassiterite is the dominant mineral in the lode-tin deposits which are hosted by the rhyolite domes; wood-tin is rare and is known from only one isolated outcrop. The cassiterite in the lode deposits occurs with hematite as veinlets and fracture encrustations 1 mm to 5 cm wide. The vertical and horizontal dimensions of these deposits are less than 3 m. The veinlets consist of hematite with encrustations, intergrowths, and replacements of cassiterite. The ratio of hematite to cassiterite varies dramatically between occurrences and within a single occurrence. The lode-tin deposits are restricted to within 100 m of what was the carapace of the rhyolite dome (Fig. 3) and are always spatially related to zones of intense vapor-phase recrystallization.

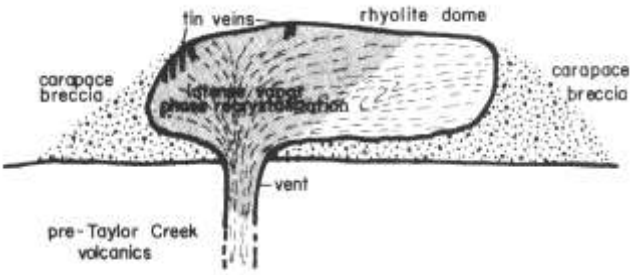

FIGURE 3—Schematic cross section across a typical tin-bearing rhyolite dome.

Fig. 4 graphically depicts the general paragenesis and approximate temperatures of formation for the various ore and gangue minerals. This paragenesis can easily be divided into three stages. The first stage is represented by quartz, topaz, pseudobrookite, bixbyite, hematite, and rare cassiterite. This stage of the paragenesis is restricted to lithophysae and thin selvages along some of the hematite—cassiterite veinlets. Fluid-inclusion homogenization temperatures are >670°C. The $d^{18}O$ of quartz in this stage is 7.5 per mil.

The second stage consists of hematite and cassiterite in veinlets. Fluids-inclusion homogenization temperatures in cassiterite range from >600 to <400°C. The salinity of the fluid inclusions in this stage is very high, probably >50 eq. wt. % NaCl. This salinity was calculated using the temperature at which daughter minerals dissolve (Roedder, 1984, p. 235).

The third stage in the paragenesis is represented by quartz, topaz, calcite, fluorite, durangite [NaAI (AsO_4)F], wood-tin, and possibly zeolites. Fluid-inclusion homogenization temperatures range from 400 to 130°C. Between 300 and 400°C the second and third stages may overlap. Salinities on a limited number of inclusions in calcite (130-295°C) are about 2-5 eq. wt. % NaCl.

Since it is rarely found outside the placer deposits, the position of wood-tin in the paragenesis and its temperature of formation are problematic. Where wood-tin is found in lode occurrences, it is generally associated with stage three of the paragenesis, suggesting that the temperature of formation was <400°C. Also, the fact that is is rarely found in lodes and is

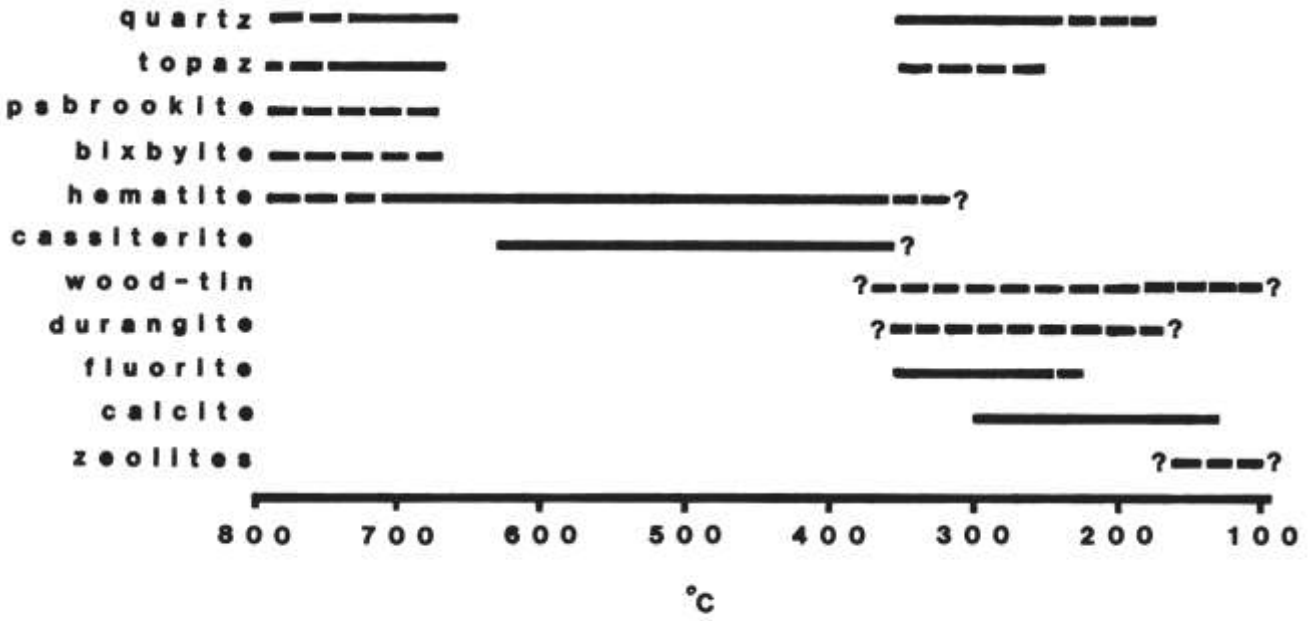

FIGURE 4—Generalized paragenesis of the Taylor Creek tin district. Temperature is from fluid-inclusion homogenization temperatures.

quite common in the placers suggests that it was deposited closer to the dome carapace than the cassiterite, implying lower temperatures of formation. Locally, however, tiny hematite and cassiterite crystals coat wood-tin nuggets. This suggests that there is an overlap between stages two and three.

The age of the mineralization is not directly ascertainable. The above temperature data suggest that mineralization began immediately upon extrusion of the rhyolites and continued until the dome cooled. Also, when two rhyolite domes are juxtaposed, vapor-phase recrystallization in the lower, presumably older, dome does not cross the contact, thus limiting the time allowable for mineralization. These two lines of evidence, as well as the spatial relationships of the tin deposits to the rhyolite domes, suggest that the tin mineralization was deposited immediately upon emplacement of the dome and was a very short-lived event, probably lasting only until the dome had cooled.

Model

In light of the data presented above, we propose that the tin deposits in the Black Range and Sierra Cuchillo were formed in three stages (Fig. 5): first, the rhyolite dome was emplaced. During ascent and cooling of the magma, a fluid phase containing high concentrations of incompatible elements was evolved. This fluid migrated upward and outward, recrystallizing and bleaching the rhyolite as it went. Temperatures in excess of 680°C indicate that the fluid was evolved from a lava at, or near, the solidus. Near the carapace of the dome lithophysae expanded and stage one of the paragenesis was deposited. The plastic nature of the rhyolite in which the lithophysae were growing retarded the upward ascent of the fluid, thus causing local zones of intense vapor-phase recrystallization.

The second stage began when this plastic zone had cooled sufficiently to crack. At this time the fluid escaped rapidly, depositing the hematite and cassiterite as it went. The salinity as well as temperature of the mineralising fluid decreased rapidly with time. Wood-tin probably began to form late in this stage.

The third stage began when cassiterite deposition stopped and deposition of the quartz, calcite, fluorite, durangite, and wood-tin assemblage began. The low

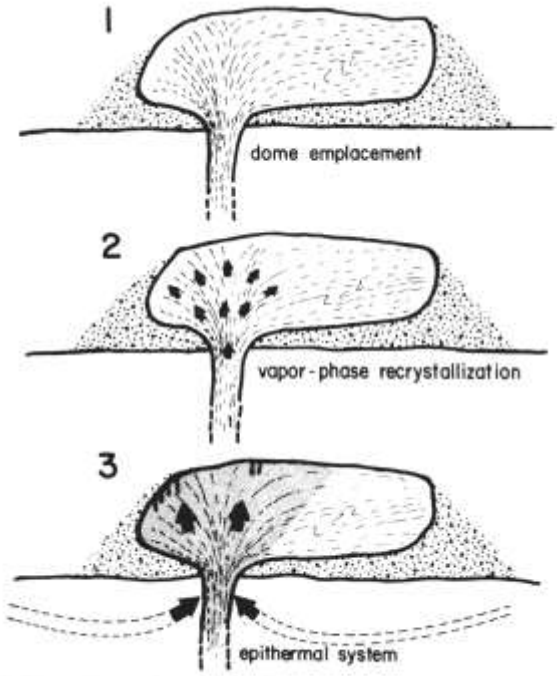

FIGURE 5—General model for the origin of the tin deposits in the Taylor Creek tin district.

salinities of the mineralizing fluids and the low $d^{18}O$ mixed and was replaced by meteoric water. The third suggest that the magmatic fluid responsible for the stage continued until the dome was too cold to sustain tin mineralization and vapor-phase recrystallization the hydrothermal system.

Conclusions

Preliminary conclusions from this study of the tin mineralization in southwestern New Mexico include:

1) The rhyolites that host the tin mineralization are effusive domes and flows mantled by carapace breccia and locally by pyroclastic material related to explosive eruptions during the dome-building process.

2) The rhyolites that host the tin mineralization are high SiO_2, **K2,** F, Cl and low CaO, Fe_2O_3, Sr, Ba "topaz" rhyolites.

3) The tin mineralization is spatially, temporally, and genetically related to the host rhyolites.

4) The process responsible for the tin mineralization is vapor-phase recrystallization. The fluid is a magmatic fluid evolved during the ascent and cooling of the rhyolite lava.

5) The tin was deposited within a few tens of meters of the carapace of the dome in an essentially fumarolic environment. Wood-tin was deposited closer to the dome carapace than cassiterite, and probably at somewhat lower temperatures.

6) As the rhyolite dome cooled, influx of meteoric water was in part responsible for the late-stage paragene sis .

References

Burt, D. M., Sheridan, M. F., Bikum, J. V., and Christiansen, E. H., 1982, Topaz rhyolites-distribution, origin, and significance for exploration: Economic Geology, v. 77, pp. 1818-1836. Correa, B. P., 1981, The Taylor Creek Rhyolite and associated tin deposits, southwestern New Mexico: M.S. Thesis, Arizona State University, 105 pp.

Cox, K. G., Bell, J. D., and Pankhurst, R. J., 1979, The interpretation of igneous rocks: George Allen and Unwin, London, 450 pp. Chapin, C. E., Jahns, R. H., Chamberlin, R. M., and Osburn, G. R., 1978, First day road log from Socorro to Truth or Consequences via Magdalena and Winston; *in* Chapin, C. E., and Elston, W. E. (eds.), Field guide to selected cauldrons and mining districts of the Datil-Mogollon volcanic field, New Mexico: New Mexico Geological Society, Special Publication 7, pp. 1-32. Eggleston, T. L., and Norman, D. I., 1983, Taylor Creek tin district-stratigraphy, structure, and timing of mineralization: New Mexico Geology, v. 5, pp. 1-4.

Fries, C., 1940, Tin deposits of the Black Range, Catron and Sierra Counties, New Mexico: U.S. Geological Survey, Bulletin 922-M, pp. 355-370.

Goerold, W. T., 1981, Geology and geochemistry of tin occurrences in southwestern New Mexico: M.S. thesis, Pennsylvania State University, 131 pp.

Harrington, E. R., 1943, Tin in New Mexico: Mines Magazine, v. 33, pp. 123, 130.

Heyl, A. V., Maxwell, C. H., and Davis, L. L., 1983, Geology and mineral deposits of the Priest Tank Quadrangle, Sierra County, New Mexico: U.S. Geological Survey, Map MF-1665.

Hill, J. M., 1921, The Taylor Creek tin deposits, New Mexico; *in* Ransome, F. L., and Burchard, E. F. (eds.), Contributions to economic geology-1921: U.S. Geological Survey, Bulletin 725, pp. 347-359.

Huspeni, I. R., Kesler, S. E., Ruiz, J., Tuta, Z., Sutter, J. F., and Jones, L. M., 1984, Petrology and geochemistry of rhyolites associated with tin mineralization in northern Mexico: Economic Geology, v. 79, pp. 87-105.

Kelley, V. C., 1955, Regional tectonics of south-central New Mexico: New Mexico Geological Society, Guidebook 6, pp. 96-104.

Lee Moreno, J. L., 1972, Geological and geochemical exploration characteristics of Mexican tin deposits in rhyolite rocks: University of Arizona, 108 pp.

Lufkin, J. L., 1972, Tin mineralization within rhyolite flow domes, Black Range, New Mexico: Ph.D. Dissertation, Stanford University, 149 pp.

Manning, D. A. C., and Pichavant, M., 1983, The role of fluorine and boron in the evolution of granitic melts; *in* Atherton, M. P., and Gribble, C. D. (eds.), Migmatites, melting, and metamorphism: Shiva Publishing Co., Cheshire, pp. 94-109.

Pan, Y. S., 1974, The genesis of the Mexican type tin deposits in acid volcanics: Ph.D. Dissertation, Columbia University, 286 pp.

Ratte, J. C., Marvin, R. F., and Naeser, C. W., 1984, Calderas and ash-flow tuffs of the Mogollon Mountains, southwestern New Mexico: Journal of Geophysical Research, v. 89, pp. 8713-8732.

Roedder, E., 1984, Fluid inclusions: Mineralogical Society of America, Reviews in Mineralogy, v. 12, 644 pp.

Turekian, K. K., and Wedepohl, K. H., 1961, The elements in some major units in the earth's crust: Geological Society of America, Bulletin, v. 72, pp. 175-192.

White, A. J. R., and Chappell, B. W., 1983, Granitoid types and their distribution in the Lachlan fold belt, southeastern Australia: Geological Society of America, Memoir 159, pp. 21-34.

New Mexico ore deposits have long been the subject of geological investigation by both federal and state geologists. Beginning with USGS Professional Paper 68, in which the now legendary geologists Waldemar Lindgren, Louis C. Graton, and Charles H. Gordon examined mineral deposits throughout the territory during 1905, detailed studies of districts such as Magdalena, Tyrone, Mogollon, Santa Rita, Lordsburg, and Pinos Altos soon followed. Here Gerald F. Loughlin has set up his plane table on a rhyolite spur south of South Camp in the Magdalena District during October 1916. This was Loughlin's second year of investigations in the district, which led to the publication of Professional Paper 200, on the geology and ore deposits of the Magdalena mining district.
Photo courtesy of U.S. Geological Survey.

Abstracts

CONODONT COLOR ALTERATION: A POSSIBLE EXPLORATION TOOL FOR ORE DEPOSITS

Kevin H. Cook, David Johnson, and David I. Norman, *Department of Geoscience, New Mexico Institute of Mining and Technology, Socorro, New Mexico 87801*

Conodont elements, which are microscopic toothlike hardparts of an unknown organism, irreversibly change in color in response to increasing temperature and time, and, therefore, these elements should record thermal events related to ore deposition. Three ore deposits representing different thermal environments were studied to test this concept; the Carthage Mississippi Valley-type deposit (70-120°C), the Hansonburg Mississippi Valley-type deposit (140-210°C), and the Continental Cu-skarn deposit (250-450°C). Samples of carbonate country rock were collected away from these deposits over vertical and horizontal intervals. Conodont elements, which are composed of francolite (a carbonate apatite), were extracted by dissolving the carbonate hosts in a 15% formic-acid solution. Conodont colors were defined by comparing the conodonts collected in the field to a set of conodont standards, as well as to the published conodont color-alteration index established by Epstein et al. Conodonts from the Carthage, Tennessee, deposit do not demonstrate any alteration, indicating either that the temperature of the deposit was insufficient to change conodont colors, or that the mineralizing event was too short-lived to imprint any thermal effects upon the conodont elements. The Hansonburg conodonts do show a progressive change in the color index away from the deposit, recording a thermal anomaly up to .4 km away from the deposit. The Continental Cu-skarn is located against a granodiorite intrusive stock. Conodonts extracted from the surrounding Paleozoic carbonates decrease in color away from the stock, and the conodont colors reflect the thermal anomaly associated with the intrusion rather than the later mineralizing event. From this study **I** have concluded that conodont color alteration may be used as a directional indicator towards sediment-hosted ore deposits which are >=140°C and spatially isolated from other heating sources.

THE STRUCTURAL CONTROL OF EPITHERMAL VEIN DEPOSITS IN WESTERN NORTH AMERICA

John Drier, *Sage Associates, Inc., 48 N. Tucson Blvd., Suite B, Tucson, Arizona 85716*

The epithermal vein deposits of western North America, which are found throughout a region of some 800,000 km', occur in structures produced by regional tectonism. Veins of the early Tertiary, including those of Paleocene through early Oligocene age, occur in generally east—west-trending, vertical to subvertical strike—slip faults of minor offset. The host structures of this age comprise swarms consisting of many short, discontinuous faults. Individual veins within these systems are less than 2 km in length and commonly are of greatest extent in the vertical direction. Fault-veins of the early Tertiary are apparently related to the Mesozoic through Laramide compressive deformation of western North America.

In the western U.S., vein deposits of mid- to late Oligocene age are rare, but those surviving examples are poorly developed. Typical mid—late Oligocene veins would be the sheeted lodes and fracture-intersection deposits at Cripple Creek, Colorado. These bodies are characterized by replacement textures, assay walls, and the absence of vein breccias. They appear to have been localized in fracture zones of local extent produced by tectonism of the gentlest degree. Epithermal veins of Miocene age in western North America are more widespread and have been much more productive than those of the early and mid-Tertiary. Miocene epithermal veins occur in a great variety of structures. Within an area encompassing southwestern and southern Nevada, the low-desert area of southeastern California and Arizona, and stretching down around the Gulf of California to about Mazatlan, epithermal vein deposits of Miocene age occur in left- and right-lateral strike—slip faults, low-angle normal faults, listric normal faults, and decollement zones. Peripheral to this area on the north and east, epithermal veins of Miocene age are localized in generally north-trending normal faults having dip angles of 65 to 70°. Throughout western North America, epithermal veins of Miocene age are distinguished by great horizontal length and continuity. They occur in the wide variety of structures that opened in response to the tensional deformation of western North America which has been ongoing since about 25 m.y. ago.

While it is currently fashionable to relate epithermal veins to caldera development, this study has shown little if any relationship between ore-controlling structures and fractures produced by caldera subsidence.

GEOLOGY OF THE RED RIVER MINING DISTRICT, TAOS COUNTY, NEW MEXICO

Karl M. Emanuel, Michael W. Selke, and Gary A. Parkison, *NICOR Mineral Ventures, Inc., Albuquerque, New Mexico*

The Red River mining district is centered on the town of Red River, nestled within the Sangre de Cristo Mountains of northern New Mexico. Past production from the district is minimal, with sporadic activity from 1890 to about 1940.

Precambrian crystalline rocks are overlain by a variable thickness of andesitic to rhyodacitic volcanic rocks of the Latir volcanic field, dated at 26 to 35 m.y. The south and southeast ring-fracture zone of the recently recognized Questa caldera has localized the intrusion of three extremely altered and mineralized granitic plutons along Red River that date at 22 to 23 m.y.

Precious-metal mineralization of the Red River district forms an arcuate pattern a few miles outside the ring-fracture zone peripheral to the late mineralized intrusives of the Questa caldera. Most mineralization is associated with quartz-cemented breccia zones or finely banded, massive or vuggy quartz veins. Many veins have argillically altered and weakly silicified and mineralized envelopes. Vein trends are generally east—west or north—south, are steeply dipping, and may be related to concentric ring-fracture zones and radial faults associated with the Questa caldera. Silver to gold ratios are typically 80:1 in mineralized zones. Known ore minerals are native gold, pyrargyrite, and chalcopyrite.

Fluid-inclusion studies indicate that boiling occurred. These studies also suggest a positive correlation between inclusion temperature and associated precious-metal grades. Precious-metal mineralization in the district may be related to the molybdenum deposits at Questa.

GEOLOGY OF THE PALM PARK BARITE DEPOSIT, SOUTHERN CABALLO MOUNTAINS, DONA ANA COUNTY, NEW MEXICO

Bradford E. Filsinger, *University of Texas at El Paso*

Jasperoid—barite—fluorite—quartz—calcite mineralization of the Palm Park deposit occurs at and just below the Silurian Fusselman Dolomite—Devonian Percha Shale contact along the crest of a N 34° W-trending asymmetrical anticline. The

deposit crops out over a 6,000 ft (1,800 m) by generally 200 to 600 ft (60 to 180 m) area. The ore zones average 12 ft (3.7 m) in thickness and contain approximately 25 to 30% barite and 3 to 4% fluorite. The Fusselman Dolomite and, to a lesser extent, the Percha Shale have been replaced by jasperoid and usually brecciated. Crustiform barite-fluoritequartz-calcite mineralization comprises the matrix of the brecciated jasperoid and fills vugs between beds that have been replaced by jasperoid.

Mineralization apparently occurred sometime during the Oligocene-Miocene time interval and was probably related to the early magmatic and/or hydrothermal activity of the Rio Grande rift. Fractures that formed due to rift deformation and perhaps the Laramide orogeny contain jasperoid and barite stratigraphically below the breccia and bedded ore and probably represent the conduits used by the ascending ore fluids. The combination of the Percha Shale and anticlinal fold acted to trap and concentrate the ascending fluids below the dolomite-shale contact, along the fold crest. Brecciation resulted from the solutioning and collapse of the host rocks as they were replaced by jasperoid. Subsequently, barite, fluorite, quartz, and calcite were precipitated predominantly in open spaces between breccia fragments and bedding planes, at temperatures ranging between 163.5 and 341.0°C.

There is excellent potential for extensions of the Palm Park deposit and for the presence of similar deposits in the surrounding region.

GEOLOGY AND PRECIOUS-METAL OCCURRENCES OF THE SAN JOSE DISTRICT, SOCORRO COUNTY, NEW MEXICO

Jon Foruria, *Colorado State University*

The San Jose district encompasses several silver-gold "fissure-type" vein occurrences hosted within the Oligocene Vicks Peak Tuff. The Vicks Peak rhyolite is a thick, densely to partially welded ash-flow tuff overlain by the Springtime Canyon Quartz-latite flow and constitutes the majority of the upper felsic volcanic sequence exposed in the southern San Mateo Mountains. The major veins infill and replace steeply dipping, northeast- and northwest-trending normal faults possibly related to the proposed Nogal Canyon cauldron.

Hydrothermal-alteration effects contemporaneous with precious-metal mineralization consist of quartz-alunite-replacement alteration, pervasive intermediate argillic alteration, and pervasive and veinlet silicification related to a single hydrothermal episode. Silicification is strongly localized along fracture and breccia zones, and is accompanied by the deposition of adularia, sericite, calcite, pyrolusite, and cryptomelane. Intermediate argillic alteration consists of montmorillonite, montmorillonite-illite mixed layer, illite, kaolinite, and pyrite systematically zoned as reaction aureoles about major structures. Argillization typically broadens beneath the Vicks Peak Tuff-Springtime Canyon Quartz-latite contact, which acted as a permeability barrier to ascending hydrothermal fluids. Supergene alteration resulting primarily from hypogene-pyrite oxidation locally complicates hypogene-alteration patterns.

Mineralization accompanies vein-related silicification consisting of pyrite, cerargyrite, native gold, and native silver. Trace-element studies indicate the low-grade mineralization lacks significant base-metal introduction at present exposure levels and exhibits very low arsenic and antimony signatures. Cursory fluid-inclusion examinations document the presence of local boiling confined to structures which led to the development of argillic and advanced argillic assemblages.

Ag-Ni-Co-U MINERALIZATION IN THE BLACK HAWK MINING DISTRICT, GRANT COUNTY, NEW MEXICO

J. E. **Gerwe and D. I. Norman,** *Department of Geoscience, NMIMT, Socorro, New Mexico 87801*

The Black Hawk mining district in the Burro Mountains near Silver City, New Mexico, was studied by field mapping, petrography, whole-rock major- and minor-element geochemistry, fluid-inclusion microthermometry, and K-Ar dating methods.

The predominant lithologies in the district are a Precambrian monzodiorite gneiss and a Late Cretaceous monzonite-porphyry stock (72.5 ± 4.7 m.y.) which intrudes the gneiss. The gneiss contains 35 ppm Co and 23 **ppm** Ni, while the monzonite contains 20 ppm Co and 11 ppm Ni. Ag-Ni-Co-U mineralization occurs in NE-trending fissure veins, dominantly in the monzodiorite gneiss. The major ore minerals are native silver, argentite, skutterudite, rammelsbergite, and uraninite within a carbonate gangue. Pyrite, quartz, clay, and carbonate are the most commonly occurring alteration minerals along the vein. Away from the vein, the maflc minerals are altered to chlorite, feldspars to sericite, and disseminated pyrite occurs along fractures. A whole-rock sample of the vein alteration assemblage yielded a date of 65.3 ± 1.2 m.y. There is a bimodal distribution of homogenization temperatures from the Black Hawk mine; one population with an average temperature of 357°C (299-404) and another with an average of 189°C (155-210). The salinities of the fluids were 0.0 to 2.6 eq. wt. % NaCl. Boiling occurred as evidenced by the coexistence of vapor- and liquid-filled inclusions.

The petrography, geochemistry, fluid-inclusion, and K-Ar-age data allow the following conclusions to be made. First, the source for the Ni and Co was probably the monzodiorite, since it has the largest areal distribution in the district and the highest Ni and Co concentrations of the predominant lithologies. Second, the low salinities of the fluids suggest that the water was meteoric in origin. Third, the high temperatures and the relatively similar ages of the intrusion and alteration suggest that the monzonite-porphyry intrusion was the heat source for the hydrothermal system. Finally, boiling and cooling of the fluids along the northeastern fractures were responsible for the Ag-Ni-Co-U mineralization.

GEOLOGY OF THE ST. CLOUD AND U.S. TREASURY MINES, SIERRA COUNTY, NEW MEXICO

Richard Harrison, *St. Cloud Mining Company, P.O. Box 1670, Truth or Consequences, New Mexico 87901*

The St. Cloud and U.S. Treasury mines are located within the Chloride mining district, situated along the eastern flank of the Black Range in Sierra County, New Mexico. The district consists of precious- and base-metal-bearing epithermal fissure veins hosted primarily by intermediate volcanic and volcaniclastic rocks of the mid-Tertiary DatilMogollon volcanic field. The St. Cloud-U.S. Treasury vein system has a mineralized strike length of approximately 7,700 feet, with trends from N 45° W to N 70° W and dips from 65° to 85° to the southwest. Ore-grade mineralization occurs in distinct shoots within the vein system, with low-grade to barren-vein material surrounding the ore shoots. Recognized ore controls are primarily structural. The mineralogy of the ore shoots consists of bornite, sphalerite, galena, chalcocite, betekhtinite $(Cu_{10}(Fe,Pb)_6S_6)$, and chalcopyrite, with minor hematite, covellite, malachite, native silver, and gold. Gangue mineralogy consists of quartz, calcite, and minor adularia (sericite).

OCCURRENCES AND GEOCHEMICAL CHARACTERIZATION OF CASSITERITE MINERALIZATION IN THE TAYLOR CREEK TIN DISTRICT

David B. **Harvey,** *University of Texas at El Paso*

Tin mineralization occurs within rhyolite and ash-flow tuff in the Taylor Creek tin district. The occurrences of vein and disseminated mineralization in ash-flow tuff are in conflict with the age and spatial restrictions to the Taylor Creek Rhyolite as inferred by several previous investigators. Numerous mineralized localities are typified by irregular networks of hematite—cassiterite—silica veins with replacement and open-space textures.

Semiquantitative spectrographic analyses of surface and drill-hole samples demonstrate that As, Pb, Sb, and Zn enrichment as great as 5000 ppm, 15,000 ppm, 1000 ppm, 10,000 ppm, respectively, is associated with tin mineralization. Fluorine is highly enriched in mineralized zones in the form of microcrystalline fluorite. Alteration of hosts is primarily characterized by the introduction of hematite and corresponding iron enrichment, although silicification is locally significant.

Preliminary fluid-inclusion studies of cassiterite exhibit homogenization temperatures ranging from 344 to 417°C. Relatively high formational temperatures of crystalline cassiterite and intergrown wood tin are in contrast to low-temperature inferences commonly made. Daughter crystals are commonly abundant in fluid inclusions and reflect the complexity of mineralizing solutions.

Mineralization is not restricted to the domes and flows of the Taylor Creek Rhyolite (25 m.y.), and the occurrences in overlying Railroad Canyon Tuff (23.5 m.y.) indicate tin introduction to be significantly younger than Taylor Creek time. The temperature and chemical and mineralogical associations of cassiterite mineralization in the Taylor Creek tin district are compatible with a hydrothermal origin.

THE MINERALOGY AND GEOCHEMISTRY OF THE SOUTHERN AMETHYST VEIN SYSTEM AT CREEDE, COLORADO

Mark P. Hemingway and David I. Norman, *Department of Geoscience, New Mexico Institute of Mining and Technology, Socorro, New Mexico 87801*

The Amethyst vein system is an epithermal, caldera-associated, Ag—base-metal deposit. Historically, the southern end of the system has been the most productive, with ores averaging 1300 ppm Ag.

A petrographic study was made on ore and country rock samples from over 300 m of vertical section at the southernmost end of the Amethyst. The paragenetic sequence observed is complex, dominated by multiple replacement episodes, and exhibiting some variations with height within the system.

Veins are primarily quartz, with up to three generations of colorless or white quartz preceding amethystine quartz. The bulk of the sulfide mineralization is within the colorless quartz, the amethyst being generally barren. Rhodochrosite with interstitial sulfides is the dominant Mn mineral in the stratigraphically lowest part of the system sampled, but disappears at higher levels in favor of Mn oxides of occasional Mn sulfides. The sulfide-replacement sequence may be summarized as sphalerite to galena to chalcopyrite to pyrite to argentiferous covellite to argentite to hematite, but any or most of these minerals may be minor or absent, and sequential variations appear as well.

Geochemical modeling of the mineralizing solutions indicates that the sequence of replacement observed could most simply be explained by a decrease in system temperature. This would result in thermodynamic instability of one mineral phase relative to another, causing replacement reactions. This explanation correlates well with previous work on Creede which postulated the mixing of hydrothermal solutions with cooler, less saline meteoric waters within the relatively shallow system.

ORGANIC COMPOUNDS IN EPITHERMAL ORE-DEPOSITING FLUIDS

G. Hodge and D. I. Norman, *Department of Geoscience, New Mexico Institute of Mining and Technology, Socorro, New Mexico 87801*

Fluid inclusions in samples from epithermal-ore veins were analyzed by mass spectrometry to determine the volatile compounds present and their relative amounts. Identification of the organic constituents was of primary concern. Epithermal-ore fluids were characterized by a combination of N_2 and organics. A typical gas analysis from the St. Cloud-U.S. Treasury mines yielded the following values (in weight percent): H_2O, 94.690; CO_2, 2.856; SO_2, 1.102; N_2, 0.869; organics, 0.481; and **H2,** 0.002. An analysis from the Cochiti—Bland mines contained: H_2O, 98.121; SO_2, 1.211; CO_2, 0.326; CO, 0.153; **N2,** 0.117; organics, 0.042; H_2S, 0.027; and CS_2, 0.002. Organic content ranged from 1.203 to 0.006 wt. %. Compounds up to **C6** were present and tentatively identified as short straight-chain alkanes (methane, propane, butane, pentane), cycloalkanes (possibly cyclopentane, methylcyclopentane, cyclohexane), and aromatics (benzene, toluene). These compounds correspond with literature reports of the types of organics present in subsurface brines. The significance of organic compounds and their role in ore deposition has not yet been determined.

TYPES OF EPITHERMAL DEPOSITS

David I. Norman, Khosrow Bazrafshan, and Ted L. Eggleston, *Department of Geoscience, New Mexico Institute of Mining and Technology, Socorro, New Mexico 87801*

Hydrothermal systems can vary from oxidizing to very reducing. Oxidizing systems deposit Mn—Fe—W—Sn—Pb—ZnAg oxides. Reduced systems deposit precious and base metals with Au mineralization associated with the most reduced mineralizing waters.

Study of the Luis Lopez Mn deposits indicates that oxidizing epithermal systems are short-lived and have a number of geothermal characteristics that differ from reduced systems.

Epithermal systems may start as oxidizing and evolve in time to reducing systems. Characteristics of these two types of geothermal systems are:

Oxidizing type (Luis Lopez Mn deposits)	Reducing type (precious- and base-metal deposits)
Similarities	
Temperature of mineralization: 200–350°C	same
Salinity of ore-forming fluids: 0.0–0.5 eq. wt. % NaCl	0.0–10 eq. wt. % NaCl
Boiling condition during mineralization	same
Shallow depth of mineralization	same
Association with intrusives	same
CO_2 content of ore-forming fluids: 1–2%	same
Differences	
No H_2S in ore-forming fluids	0.01–1.0% H_2S in ore-forming fluids
No organic materials in ore-forming fluids	0.01–1.0% organic materials in ore-forming fluids
Associated and/or hosted with volcanic rocks	Associated and/or hosted with volcanic rocks and sedimentary rocks
No alteration associated with the veins (pervasive alteration, hematization)	Low-pH alteration type
Ores are oxides of Mn–Fe–W–Sn–Pb–Zn–Ag	Ores are sulfides of Fe–Pb–Zn–Ag plus Au
High $\delta^{18}O$ fluids	Low $\delta^{18}O$ fluids
Low to medium water/rock ratio	High water/rock ratio
Fast moving ore-forming fluids	Slower moving ore-forming fluids
Fluids not in contact with sedimentary rocks	Fluids in most cases in contact with sedimentary rocks

GEOLOGY OF THE COCHITI MINING DISTRICT, SANDOVAL COUNTY, NEW MEXICO **Gary A. Parkison and Karl M. Emanuel,** *NICOR Mineral Ventures, Inc., Albuquerque, New Mexico;* **David J. Wronkiewicz and David I. Norman,** *New Mexico Tech, Socorro, New Mexico*

The Cochiti or Bland mining district is located about fifty miles north of Albuquerque on the southeast flank of the Jemez Mountains. The majority of mining activity was conducted from 1897 to 1903 and again from 1914 to 1916. A total of at least 185,000 tons of ore grading .20 oz/t gold and 4.0 oz/t silver has been produced.

Mid- to late Miocene andesitic volcanic and felsic hypabyssal intrusive rocks underlie the area. This sequence of rocks may reflect the early evolution of the adjacent Valles-Toledo caldera complex. Numerous north-south-trending, steeply dipping faults and fractures cut all rock types and may be related to extensional tectonism of the Rio Grande rift.

Veins and stockwork zones are generally associated with these north-south-trending structures and are composed primarily of sugary to chalcedonic quartz with only minor calcite. Multiple periods of vein filling and brecciation can be demonstrated. At least thirteen separate vein systems have been mapped, some extending for over two miles along strike. Veins locally exceed sixty feet and typically are at least ten feet in width. Ore shoots are localized at flexures and dilatant zones along veins, and ore grades generally increase with vein width. Vein sulfides are quite sparse and are primarily pyrite, gold, electrum, argentite, ruby silver, and minor base-metal sulfides. Alteration zoning towards veins grades from regional propylitization through advanced argillic to silicification.

Fluid-inclusion data suggest that precious-metal deposition occurred at or above the zone of boiling, typically at temperatures between 240 and 315°C, from dilute hydrothermal fluids with greater than 1% H_2S. Mineralization occurred between about 6.5 and 1.5 m.y.

GEOLOGY, STRUCTURE, AND MINERALIZATION IN THE STEEPLE ROCK MINING DISTRICT R. **W. Robinson,** *Pioneer Nuclear, Inc., P.O. Box 151, Amarillo, Texas 79189*

The Steeple Rock mining district is located in western New Mexico near Duncan, Arizona. More specifically, it occupies the southwestern portion of the Blue Creek basin, which contains the Schoolhouse Mountain cauldron. The district lies in a transition zone between the Datil-Mogollon volcanic field to the northeast and the Basin and Range Province to the west.

Tertiary volcanic rocks cover the majority of the Steeple Rock district, with only small exposures by hypabyssal rocks in the western portion of the area. The three main units are the Virden dacite (34.7 m.y.; host to most of the mineralization in the district), a younger amygdaloidal andesite, and the brown andesite porphyry.

The ore deposits of the district are veins which occupy northwest- to west-northwest-trending normal faults. The main structural pattern is linear, but there are numerous vein intersections, warped fault planes, bifurcations, and cymoid loops. All of these features occur at both large and small scales, and in horizontal as well as vertical planes.

Mineralization is in epithermal silica veins that contain gold, silver, copper, lead, and zinc. Production from the district to 1975 is as follows: gold-140,700 ounces; silver-3,140,500 ounces; and significant amounts of base metals.

The paragenesis consists of at least three stages, but has received limited attention district-wide. The precious metals were deposited in the third stage. Selected large areas of the district have been very intensely silicified and/or argillically altered. This alteration is interpreted to be the result of hydrothermal solutions flowing along open structures during the mineralizing event in the Steeple Rock mining district.

GEOLOGY OF THE KINGSTON MINING DISTRICT, WITH DETAILED WORK ON THE BLACK COLT MINE

Peter A. Sanders, *Redco Silver Inc., Enterprise, Utah;*
Thomas Giordano, *New Mexico State University, Las Cruces, New Mexico*

The Kingston mining district is located on the east flank of the Black Range, approximately 50 miles east of Silver City. The district produced more than six million oz. of Ag prior to 1904. The majority of the mineralization occurs between two major N—NW-trending faults which define the eastern structural margin of the Emory cauldron. A crude zonation occurs in the district; mines to the south and west have abundant copper, while mines to the east and north have abundant manganese. The Black Colt mine is located in the Mn-rich zone. At the Black Colt the primary mineralization occurs along ESE—WNW-trending fissure veins with related replacement deposits in the Fusselman Dolomite. Pods of massive sulfide, containing pyrite—alabandite—sphalerite—galena—minor acanthite—chalcopyrite (oldest—youngest) occur in a barren quartz vein. Pyrite—sphalerite—galena (oldest—youngest) occur in a rhodochrosite—calcite—quartz gangue in the adjacent replacement deposits. Two types of sphalerite have been distinguished, a dark, marmatitic sphalerite with abundant chalcopyrite blebs and a brown, resinous sphalerite lacking the chalcopyrite. Fluid-inclusion homogenization temperatures for the brown sphalerite range from 307 to 332°C, while the quartz temperatures range from 187 to 351°C. Limited sulfur-isotope analyses suggest disequilibrium during deposition.

Selected conversion factors*

TO CONVERT	MULTIPLY BY	TO OBTAIN
Length		
inches, in	2.540	centimeters, cm
feet, ft	3.048×10^{-1}	meters, m
yards, yds	9.144×10^{-1}	m
statute miles, mi	1.609	kilometers, km
fathoms	1.829	m
angstroms, Å	1.0×10^{-8}	cm
Å	1.0×10^{-4}	micrometers, μm
Area		
in^2	6.452	cm^2
ft^2	9.29×10^{-2}	m^2
yds^2	8.361×10^{-1}	m^2
mi^2	2.590	km^2
acres	4.047×10^{3}	m^2
acres	4.047×10^{-1}	hectares, ha
Volume (wet and dry)		
in^3	1.639×10^{1}	cm^3
ft^3	2.832×10^{-2}	m^3
yds^3	7.646×10^{-1}	m^3
fluid ounces	2.957×10^{-2}	liters, l *or* L
quarts	9.463×10^{-1}	l
U.S. gallons, gal	3.785	l
U.S. gal	3.785×10^{-3}	m^3
acre-ft	1.234×10^{3}	m^3
barrels (oil), bbl	1.589×10^{-1}	m^3
Weight, mass		
ounces avoirdupois, avdp	2.8349×10^{1}	grams, gr
troy ounces, oz	3.1103×10^{1}	gr
pounds, lb	4.536×10^{-1}	kilograms, kg
long tons	1.016	metric tons, mt
short tons	9.078×10^{-1}	mt
oz mt^{-1}	3.43×10^{1}	parts per million, ppm
Velocity		
ft sec^{-1} (= ft/sec)	3.048×10^{-1}	m sec^{-1} (= m/sec)
mi hr^{-1}	1.6093	km hr^{-1}
mi hr^{-1}	4.470×10^{-1}	m sec^{-1}

TO CONVERT	MULTIPLY BY	TO OBTAIN
Pressure, stress		
lb in^{-2} (= lb/in^2), psi	7.03×10^{-2}	kg cm^{-2} (= kg/cm^2)
lb in^{-2}	6.804×10^{-2}	atmospheres, atm
lb in^{-2}	6.895×10^{3}	newtons (N)/m^2, N m^{-2}
atm	1.0333	kg cm^{-2}
atm	7.6×10^{2}	mm of Hg (at 0° C)
inches of Hg (at 0° C)	3.453×10^{-2}	kg cm^{-2}
bars, b	1.020	kg cm^{-2}
b	1.0×10^{6}	dynes cm^{-2}
b	9.869×10^{-1}	atm
b	1.0×10^{-1}	megapascals, MPa
Density		
lb in^{-3} (= lb/in^3)	2.768×10^{7}	gr cm^{-3} (= gr/cm^3)
Viscosity		
poises	1.0	gr cm^{-1} sec^{-1} *or* dynes cm^{-2}
Discharge		
U.S. gal min^{-1}, gpm	6.308×10^{-2}	l sec^{-1}
gpm	6.308×10^{-5}	m^3 sec^{-1}
ft^3 sec^{-1}	2.832×10^{-2}	m^3 sec^{-1}
Hydraulic conductivity		
U.S. gal day^{-1} ft^{-2}	4.720×10^{-7}	m sec^{-1}
Permeability		
darcies	9.870×10^{-13}	m^2
Transmissivity		
U.S. gal day^{-1} ft^{-1}	1.438×10^{-7}	m^2 sec^{-1}
U.S. gal min^{-1} ft^{-1}	2.072×10^{-1}	l sec^{-1} m^{-1}
Magnetic field intensity		
gausses	1.0×10^{5}	gammas
Energy, heat		
British thermal units, BTU	2.52×10^{-1}	calories, cal
BTU	1.0758×10^{2}	kilogram-meters, kgm
BTU lb^{-1}	5.56×10^{-1}	cal kg^{-1}
Temperature		
°C + 273	1.0	°K (Kelvin)
°C + 17.78	1.8	°F (Fahrenheit)
°F − 32	5/9	°C (Celsius)

Divide by the factor number to reverse conversions.
Exponents: for example 4.047×10^{3} (see acres) = 4,047; 9.29×10^{-2} (see ft^2) = 0.0929.

Editor: Jiri Zidek
Drafter: James C. Brannan

Type faces: Text in 10 pt. Palatino, leaded one point
References in 8 pt. Palatino, leaded one point
Display heads in 18 pt. Palatino medium

Presswork: Miehle Single Color Offset
Harris Single Color Offset

Binding: Saddlestitched with softbound cover

Paper: Cover on 12 pt. Kivar
Text on 70-lb white matte

Ink: Cover—PMS 320
Text—Black

Quantity: 900